

**Alma Mater Studiorum – Università di Bologna**

**Dottorato Di Ricerca In Ingegneria Dei Materiali**

Ciclo XXIV

Settore Concorsuale di afferenza: 09/D1

Settore Scientifico disciplinare: ING-IND/22

**NEW ECO-FRIENDLY POLYESTERS FROM  
RENEWABLE RESOURCES**

Presentata da: **Simone Sullalti**

**Coordinatore Dottorato**

**Prof.Ing. Giorgio Timellini**

**Relatore**

**Prof.ssa Annamaria Celli**

**Correlatori**

**Chiar.mo Prof. Corrado Berti  
Dott.ssa Paola Marchese**

**Esame finale anno 2012**



# Table of Contents

<b>CHAPTER 1 : INTRODUCTION.....</b>	<b>7</b>
<b>1.1. BIOPOLYMERS.....</b>	<b>7</b>
<b>1.2. EMERGING BIOPOLYMERS.....</b>	<b>13</b>
1.2.1. POLY(ALKYLENE DICARBOXYLATE)S .....	13
1.2.2. POLYESTERS CONTAINING 1,4-CYCLOHEXYLENE UNITS .....	15
1.2.2.1. POLY(BUTYLENE-1,4-CYCLOHEXANEDICARBOXYLATE) .....	18
1.2.2.2. POLY(1,4-CYCLOHEXYLENEDIMETHYLENE 1,4-CYCLOHEXANEDICARBOXYLATE) .....	19
<b>1.3. AIM OF THE PROJECT.....</b>	<b>20</b>
<b>CHAPTER 2 : EXPERIMENTAL PART .....</b>	<b>23</b>
<b>2.1. MATERIALS .....</b>	<b>23</b>
<b>2.2. SMALL SCALE POLYMERIZATION PLANT.....</b>	<b>24</b>
<b>2.3 BRABENDER MIXER.....</b>	<b>25</b>
<b>2.4. CHARACTERIZATION.....</b>	<b>26</b>
2.4.1. <sup>1</sup> H NMR .....	26
2.4.2. GEL PERMEATION CHROMATOGRAPHY (GPC) .....	27
2.4.3. THERMOGRAVIMETRIC ANALYSIS (TGA) .....	27
2.4.4. DIFFERENTIAL SCANNING CALORIMETRY (DSC) .....	28
2.4.5. DYNAMIC MECHANICAL THERMAL ANALYSIS (DMTA).....	29
2.4.6. RHEOLOGY .....	31
2.4.7. TENSILE TESTING .....	32
2.4.8. WIDE ANGLE X-RAY SCATTERING (WAXS) .....	35
2.4.9. FOURIER TRANSFORMATION INFRARED SPECTROSCOPY (FTIR) .....	36
2.4.10. UV-VIS SPECTROSCOPY .....	37
2.4.11. SCANNING ELECTRON MICROSCOPE (SEM) .....	38
2.4.12. ACCELERATED PHOTOAGEING .....	39
2.4.13. BIODEGRADATION .....	41
<b>CHAPTER 3 : RESULTS AND DISCUSSIONS .....</b>	<b>43</b>

<b>3.1. ECO-FRIENDLY ALIPHATIC POLYESTERS CONTAINING 1,4-CYCLOHEXANE DICARBOXYLATE UNITS.....</b>	<b>43</b>
3.1.1. INTRODUCTION .....	43
3.1.2. SYNTHESIS.....	43
3.1.3. MOLECULAR CHARACTERIZATION .....	45
3.1.4. TGA ANALYSIS.....	46
3.1.5. DSC ANALYSIS .....	47
3.1.6. DMTA ANALYSIS .....	49
3.1.7. TENSILE PROPERTIES .....	50
3.1.8. CONCLUSIONS .....	51
<b>3.2. ECO-FRIENDLY ALIPHATIC COPOLYESTERS CONTAINING 1,4-CYCLOHEXANE DICARBOXYLATE UNITS .....</b>	<b>52</b>
3.2.1. INTRODUCTION .....	52
3.2.2. SYNTHESIS.....	52
3.2.3. MOLECULAR CHARACTERIZATION OF (X-Y)-CO-PBCHD COPOLYESTERS .....	54
3.2.4. TGA ANALYSIS.....	55
3.2.5. DSC ANALYSIS .....	57
3.2.6. DMTA ANALYSIS .....	64
3.2.7. PHOTODEGRADATION ANALYSIS.....	69
3.2.8. CONCLUSIONS.....	73
<b>3.3 FULLY ALIPHATIC OR ALIPHATIC/AROMATIC COPOLYESTERS CONTAINING <math>\Omega</math>-HYDROXY FATTY ACIDS.....</b>	<b>74</b>
3.3.1. INTRODUCTION .....	74
3.3.2. SYNTHESIS.....	75
3.3.3. MOLECULAR CHARACTERIZATION OF THE COPOLYESTERS .....	77
3.3.4. DSC ANALYSIS .....	85
3.3.5. DMTA ANALYSIS .....	90
3.3.6. TENSILE TESTS.....	93
3.3.7. CONCLUSIONS.....	94
<b>3.4. TiO<sub>2</sub> COMPOSITES BASED ON ALIPHATIC POLYESTERS.....</b>	<b>95</b>
3.4.1. INTRODUCTION.....	95
3.4.2. MATERIALS .....	96

3.4.3. SAMPLE PREPARATION.....	97
3.4.4. THERMAL PROPERTIES .....	98
3.4.5. PHOTODEGRADATION OF VIRGIN MATRIXES (PBCHD <sub>100</sub> AND PCCD <sub>97</sub> ) .....	98
3.4.6. PHOTODEGRADATION OF COMPOSITES .....	101
3.4.7. SEM ANALYSIS.....	104
3.4.8. CONCLUSIONS.....	105
<b>3.5. ALIPHATIC POLYESTERS CONTAINING GLYCEROL .....</b>	<b>106</b>
3.5.1. INTRODUCTION.....	106
3.5.2. SYNTHESIS.....	106
3.5.3. MOLECULAR CHARACTERIZATION.....	107
3.5.4. THERMAL CHARACTERIZATION .....	110
3.5.5. DMTA ANALYSIS .....	112
3.5.6. PHOTOSTABILITY.....	113
3.5.7. PHOTODEGRADATION .....	113
3.5.8. BIODEGRADATION .....	118
3.5.9. CONCLUSIONS .....	118
<b>CHAPTER 4 : CONCLUSIONS .....</b>	<b>121</b>
<b>CHAPTER 5 : REFERENCES.....</b>	<b>125</b>
<b>COMPLETE LIST OF PUBLICATIONS.....</b>	<b>133</b>



# Chapter 1 : Introduction

## 1.1. Biopolymers

The term “biopolymer” is not uniformly defined in the literature. European Bioplastics (<http://en.european-bioplastics.org/>) indicates that “bio” in biopolymer can either refer to “biodegradable” or “biobased” (Lee, 2003). Biobased means that a significant proportion of the carbon in the biopolymer comes from renewable raw materials, measured according to ASTM D6866-10. As the greatest potential for market penetration comes from biobased polymers, in this document we use biopolymer as biobased polymer. Environmental degradability is here considered an added value, that is anyway a target objective in the building of new macromolecular structures.

Biopolymers are abundant in nature, i.e. wood, leaves, fruits, seeds, all contain biopolymers: therefore, these natural polymers have been around for a very long time and always constituted one of the essential ingredients of sustainability, first and foremost as food, but also as shelter, clothing and source of energy. These renewable resources have also played an increasingly important role as materials for humanity through their exploitation in a progressively more elaborated fashion. The ever improving technologies associated with papermaking, textile and wood processing, vegetable oils, starch and gelatin utilization, the manufacture of adhesives, etc. represent clear examples of the progressive sophistication with which man has made good use of these natural polymers throughout the millennia. The progress of chemistry, associated with the industrial revolution, created a new scope for the preparation of novel polymeric materials based on renewable resources, first through the chemical modification of natural polymers from the mid-nineteenth century: the first artificial biopolymers, esters of cellulose, were invented in the 1860s and, since then, other new macromolecules derived from natural resources have been developed. Later, these processes were complemented by approaches based on the controlled polymerization of a variety of natural monomers and oligomers, including terpenes, polyphenols and rosins. A further development called upon chemical technologies which transformed renewable resources to produce novel monomeric species like furfuryl alcohol.

However, many of the inventions related to biopolymers made in the 1930s and 1940s remained at laboratory stage and were never used for commercial products. The main reason was the discovery of crude oil and its large-scale industrial use for the synthetic polymers since the 1950s. For over 50 years the world production of polymers has grown continuously: the petrochemical boom of the second half of the last century produced a diversification in the structures available through industrial organic chemistry. The availability of a growing number of cheap chemicals, suitable for the production of macromolecular materials, gave birth to ‘the plastic age’, in which we

still live today, with of course greatly enhanced quantitative and qualitative features. Polymers production increased from 1.5 million tonnes in 1950 to 230 million tonnes in 2009. The growth rate is about 9% a year on average, nevertheless the global financial crisis started around 2008. Indeed, for the plastic product segment, the economic recovery begun in mid 2009 continued in 2011.

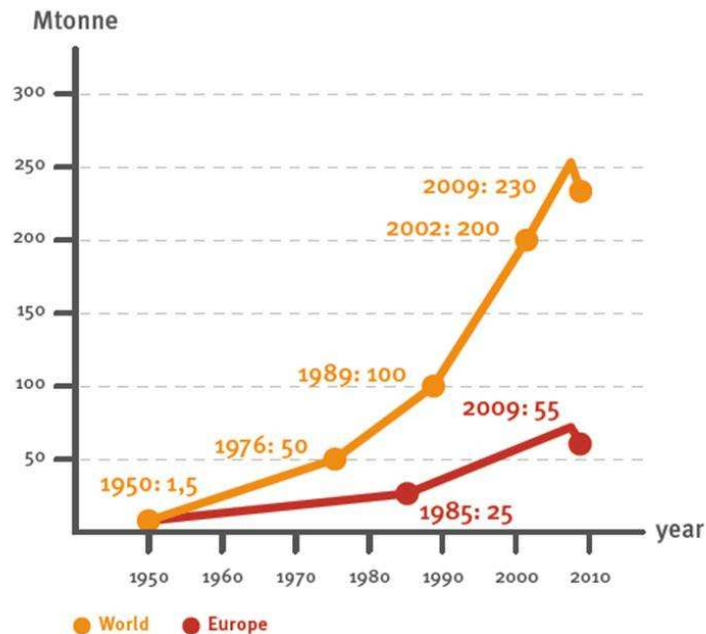


**Figure 1.1 World Plastics Production 1950-2009 (PlasticsEurope Market Research Group)**

This prodigious scientific and technical upsurge went to the detriment of any substantial progress in the realm of polymers from renewable resources. In other words, although these materials never ceased to exist, very modest investments were devoted to their development, compared with the astronomical sums invested in petrochemistry. In 2009 plastics demand in Europe reached 45 million tonnes and packaging represents 40.1% of the overall demand, followed by building and construction (20.4%), automotive (7%), electrical and electronic equipment (5.6%). Other applications include different segments like medical, biomedical, agriculture, machinery engineering etc. Within such a framework, biopolymers actually take up a very limited portion of the worldwide productions of all plastics, approximately only 0.3% by the end of 2007 (Shen, 2009).

The widespread production and application of petroleum-based plastics were due to many favourable factors: easy availability of raw materials (oil, coal and natural gas), development of chemical processes with high yields and low costs, easy processability of the final materials, excellent mechanical and thermal properties (plastics have overtaken aluminium and glass in terms of quantities used), stability, durability (due to the lack of biodegradability) of the manufactured products (Muller, 2006).

Indeed, polymer production in Europe is dominated by a wide variety of petroleum-based synthetic polymers: there are five high-volume plastics families; polyethylene, including low density, linear low density and high density, polypropylene (PP), polyvinylchloride (PVC), polystyrene (PS) and polyethylene terephthalate (PET). The most widely used plastics are polyolefins (PE and PP) which account for approximately 50% of all plastics demand in Europe, followed by PVC (11%) and PET (8%). Biobased versions of some of these are beginning to be produced. The environmental credentials of some of these biopolymers come from either CO<sub>2</sub> capture and/or their building blocks are derived from renewable sugar rather than non-renewable oil. For instance, the production of bio-PE was 200,000 metric tons in 2010, 28% of the biopolymers production capacity. Biobased PP route captures 2.3 tonnes of CO<sub>2</sub> per tonne of polymer produced whereas petrochemical PP emits 1.8 tonnes of CO<sub>2</sub> per tonne of polymer produced. The production of biobased ethylene also opens up the possibility to produce bio-vinyl chloride in the short term, thus implying that within 10 years a significant part of the world's most dominant thermoplastic materials (polyolefins and PVC) could be biobased (Haveren, 2008).

Today's environmental problems, climate changes, limited fossil fuel resources and their price fluctuations (with an overall tendency to rise), associated industrial activities (often ecologically unsound) are the strong drivers for governments, companies and scientists to find alternatives to the petro-based polymers. Therefore, bio-based plastics, which may contribute by reducing the dependence on fossil fuels and the related environmental impacts, are experiencing a renaissance (Gandini, 2011).

Many old processes are being revisited, many new polymers from renewable feedstocks are being developed. Therefore, the market of the emerging bio-based polymers is experiencing rapid growth, even if data on the market for bioplastics are highly variable. A comprehensive market survey of bioplastics (Ceresana Research, 2009) estimated that in the years 2000 to 2008, worldwide consumption of biodegradable plastics based on starch, sugar, and cellulose -so far the three most important raw materials- increased by 600%. According to a survey by Shen (2009), from 2003 to the end of 2007, the global annual growth rate was 38%. In Europe the annual growth rate was as high as 48% in the same period. According to company announcements, the worldwide capacity of bio-based plastics will increase from 0.36 Mt in 2007 to 2.33 Mt in 2013 and to 3.45 Mt in 2020.

The maximum technical substitution potential of bio-based polymers replacing their petrochemical counterparts is estimated at 270 Mt, or 90% of the total polymers that were consumed in 2007 worldwide. Certainly this substitution will not occur in the short to medium term. The main reasons are:

- economic barriers (especially production costs and capital availability),
- technical challenges in scaling-up,
- the short term availability of bio-based feedstocks,
- the need for the plastics conversion sector to adapt to the new plastics.

Nevertheless, from a technical point of view, there are very large opportunities for the replacement of petrochemical by bio-based polymers (Shen, 2009).

As alternatives to the conventional thermoplastics, the bio-based polymers currently produced that found consolidated or potential applications are presented in Figure 1.2 together with their production capacity in metric tons and % with respect to other biopolymers production in 2010.

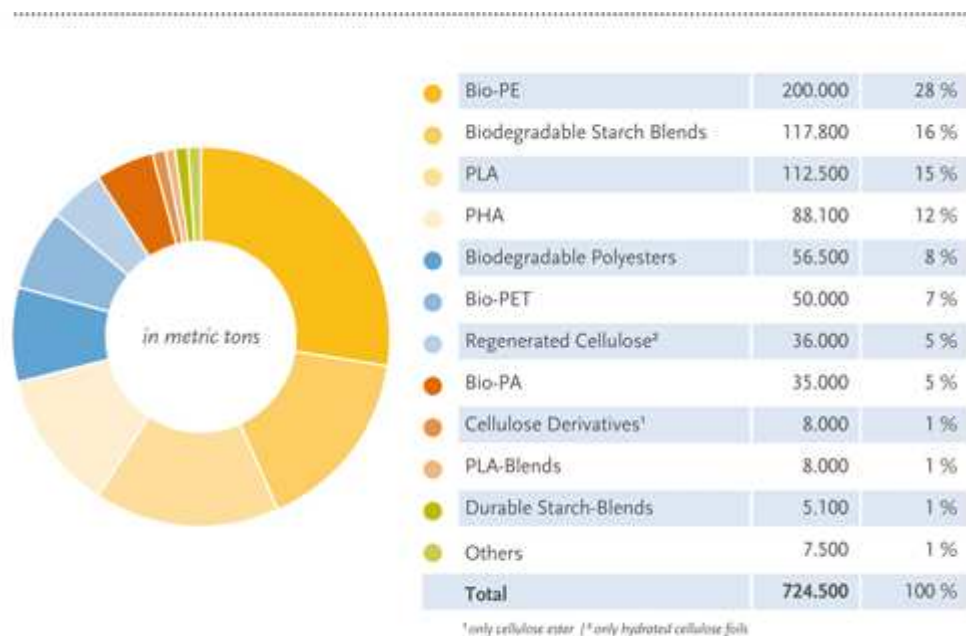


**Figure 1.2 Biopolymers production capacity 2010 by type (European Bioplastics, <http://en.european-bioplastics.org/>)**

Some of them are the recent biobased versions of conventional plastics and are classified bio-based because one monomer (for example, 1,4-butanediol, 1,3-propanediol and 1,2-ethanediol) is now obtained from renewable resources. However, regardless of the route applied to produce these traditional polymers, their molecular structure makes them highly resistant to the biological agents and harmful materials due to their high volume in the waste stream. This is the case of PET, PTT, PBT and copolymers (PEIT).

By considering the class of polyesters, aliphatic chains have the advantage to be potentially environmental degradable. These polymers can conveniently be divided into four categories, depending on the synthesis (Averous, 2004):

- 1) polyesters from biomass, particularly from agro-resources;
- 2) polyesters from microbial production;

- 3) synthetic polyesters obtained from monomers derived from agro-resources;
- 4) synthetic polyesters obtained from petrochemical monomers.

Poly(lactic acid) (PLA) belongs to the first or third category, depending on its biological or chemical synthesis, and has one of the highest potentials among biopolyesters, due to its availability and low price (Auras, 2004). As long as the basic monomers (lactic acid) are produced from renewable resources (carbohydrates) by fermentation, PLA complies with the rising worldwide concept of sustainable development and is classified as an environmentally friendly material. PLA is considered both as biodegradable (adapted for short-term packaging) and as biocompatible in contact with living tissues (for biomedical applications such as implants, sutures, drug encapsulation, etc.). It is one of the few polymers in which the stereochemical structure can easily be modified by polymerizing a controlled mixture of L and D isomers to yield high molecular weight and amorphous or semi-crystalline polymers. PLA can be degraded by abiotic degradation (simple hydrolysis of the ester bond without requiring the presence of enzymes to catalyze it). During the biodegradation process, and only in a second step, the enzymes degrade the residual oligomers till final mineralization (biotic degradation).

Polyhydroxyalkanoates (PHA) are versatile polyesters produced by many bacterial species as carbon and energetic intracellular reserves and they belong to the second family of biopolyesters.; they are potential substitutes of some petroleum-based polymers (e.g. polypropylene) since they exhibit very similar physical-chemical properties. The composition of PHAs depends on the producing microorganism, as well as on media composition and cultivation conditions (López-Cuellar, 2011). Thus, by choosing the appropriate microorganism, carbon source, cosubstrate and culture conditions, a variety of homopolymers, copolymers, ter-polyesters, etc., can be obtained with different physical-chemical properties (Gorenflo, 2001; Keenan, 2006). In the fourth category of biopolyesters, according to their chemical structures, poly- $\epsilon$ -caprolactones, polyesteramides, poly(alkylene dicarboxylate)s and their related copolymers, and aromatic copolyesters are present. Some poly(alkylene dicarboxylate)s are commercially available: for example, polybutylene succinate/adipate copolyester is produced by Showa Highpolymer (Japan) under the Bionolle trademark.

All the totally aliphatic polyesters of the four categories generally combine excellent properties, such as environmental degradability and biocompatibility, with sometimes poor physical properties and sometimes high costs. For example, polyhydroxybutyrate (PHB), the most studied PHA, is very expensive, it has low resistance to thermal degradation and it is brittle (Kopinke, 1996). However some studies show that the incorporation of hydroxyvalerate or other longer units decrease the crystallinity, and the melting and glass transition temperatures, making the polymers more flexible

and elastomeric (Chan, 2006; Keenan, 2006). Poly- $\epsilon$ -caprolactone (PCL) has a very low melting peak temperature (about 60°C) and a high rate of hydrolysis during processing. Therefore, modifications of aliphatic polyesters have recently attracted considerable attention.

In particular, the introduction of aromatic units, often based on terephthalic acid, gives higher melting temperatures and improved physical-mechanical performances, though a decrement in degradation rate is observed (Muller, 1998). Poly(butylene terephthalate-co-butylene adipate) (PBTA), for example, is commercialized by BASF with the trade name of ECOFLEX. It has a melting temperature of 120°C, good mechanical properties and excellent thermal stability (Herrera, 2002). As regards its biodegradation, Witt concluded that there is no indication of environmental risk when it is involved in the composting process (Witt, 2001). Moreover, polymer blending is also a simple and economic way to modify the physical properties and to extend the application field of aliphatic polyesters (Yang, 2009).

Given all these efforts to improve the physical performances of aliphatic polyesters, even though the biodegradation rate can be strongly reduced (Muller, 2001; Zhao, 2006; Lee, 2000), there is clearly a great interest in developing novel biomaterials.

Among the emerging bio-based polymers, an important role is also covered by polymers obtained by enzymatic catalysis. Enzymes are increasingly used to perform a range of chemical reactions. These catalysts from nature are sustainable, selective and efficient, and offer a variety of benefits such as environmentally friendly manufacturing processes, reduced use of solvents, lower energy requirement and high atom efficiency. Enzyme catalyzed polymerization has been shown to afford cleaner products under milder conditions than traditional polymerization (Kobayashi, 1995; Linko, 1996). In vitro enzyme-catalyzed synthesis of polyesters has several marked benefits over conventional chemical polymerization (Kobayashi, 2009): a) high selectivity with the consequent advantage of reducing the incidence of tedious and expensive protection/deprotection strategies (Shen, 1999; Kumar, 2002); b) moderate reaction conditions (Kim, 2001); c) no need for a strict exclusion of air and/or moisture; d) non-toxic nature of the catalysts; e) easy separation and reuse of the biocatalyst when immobilized enzymes are employed.

The concept and industrial feasibility were shown by Baxenden Chemicals (UK) who developed a bio-process that uses lipase B from the yeast *Candida antarctica* (CALB) to catalyse polyester formation at a much lower temperature (60°C) than the temperature used by conventional methods (Webb, 2004). The unique processes operated at lower temperatures than those required for conventional polymerization reactions, resulting in a more energy efficient synthesis. In addition, the polyester process did not require the use of organotin or other organometallic catalysts. However, this kind of production was interrupted and up to now no other examples of successful

application of enzymatic synthesis of polyesters at industrial scale has been reported, but the technical limitations of the methodology have been extensively analyzed and discussed (Korupp, 2010).

## 1.2. Emerging Biopolymers

### 1.2.1. Poly(alkylene dicarboxylate)s

The group of poly(alkylene dicarboxylate)s is characterized by aliphatic polyesters derived from diols and dicarboxylic acids that are described by the formula



and are generally referred to polyesters x-y, where the number of the carbon atom in both diols and dicarboxylic acid are indicated.

They are obtainable from renewable sources and offer the opportunity for easy recovery of the monomers in addition to a high biocompatibility and biodegradability. They are characterized by high thermal stability and they crystallize from the melt at very high crystallization rates, similar to PE (Berti, 2007)

Different studies have been made on the properties of poly(alkylene dicarboxylate)s: depending on the number of methylene groups, important differences in crystalline structure and morphology have been observed. Indeed, in literature it is reported that the length of the aliphatic chain is a key parameter in determining structural and thermal properties (Barbiroli, 2003; Celli, 2007; Berti, 2007).

In these papers the authors synthesized different series of poly(alkylene dicarboxylate)s starting from different diols and carboxylic acids.

For example, Figure 1.3 (Berti, 2007) shows the  $T_{cc}$  and  $T_m$  data for some poly(alkylene dicarboxylate)s

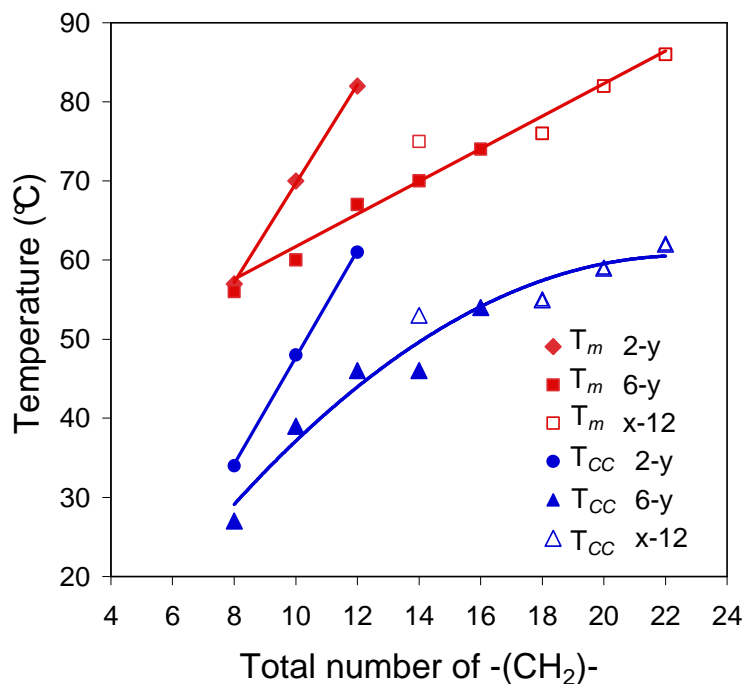


**Figure 1.3 Crystallization temperatures from the melt ( $T_{cc}$ ) and melting temperatures ( $T_m$ ) as a function of the total number of  $-(CH_2)-$  groups in poly(alkylene dicarboxylate)s (Berti, 2007)**

In polymers with a high melting point, above the  $T_m$  of PE (for example, in polyamides),  $T_m$  decreases as the methylene number increases. On the other hand, in polymers with low  $T_m$ , below the  $T_m$  of PE, (for example, in aliphatic polyesters with sequence length of six to ten  $-(CH_2)-$  groups)  $T_m$  increases with the lengthening of the aliphatic chain (Wunderlich 1980). For poly(alkylene dicarboxylate)s, the increment of  $T_m$  by increasing  $-(CH_2)-$  number can be justified by considering that the ester functionalities present along the chain are defects in the polyethylene backbone. As the distance between two ester groups increases, the number of defects decreases and more perfect crystals can be formed: by consequence the structure, in terms of both molecular conformation and intermolecular packing, tends to that of PE, and  $T_m$  increases.

Figure 1.4 (Berti 2007) describes the crystallization rate ( $1/t_{1/2}$ ) as a function of the undercooling  $\Delta T = (T_m^\circ - T_c)$  for some poly(alkylene dicarboxylate)s, for PE and for some common aromatic polyesters such as PET, PTT, and PBT.

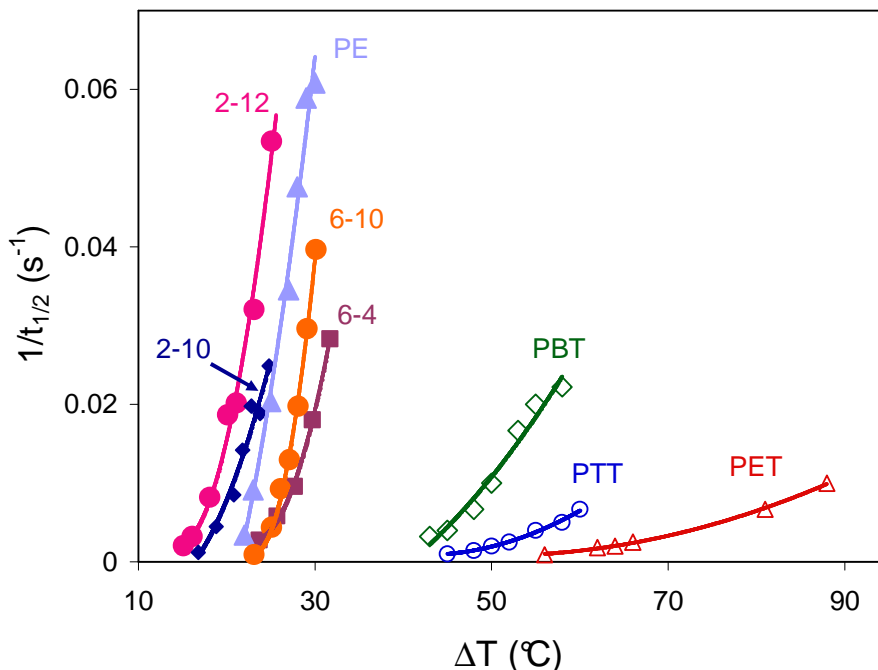


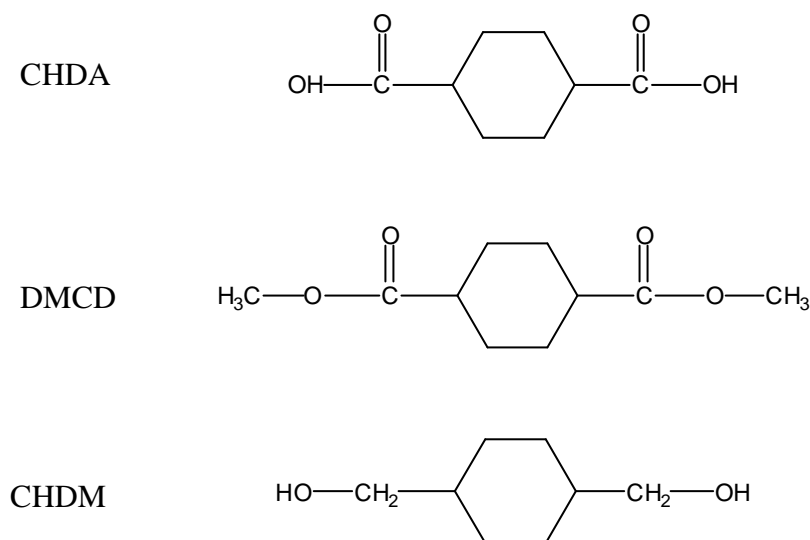
**Figure 1.4 Crystallization rate as a function of the undercooling for some poly(alkylene dicarboxylate)s, aromatic polyesters and PE (Berti, 2007)**

All the poly(alkylene dicarboxylate)s are very fast crystallizing polymers, with a crystallization rate comparable, and sometimes higher, than that of polyethylene. On the other hand, the aromatic polyesters have a significantly slower crystallization rate. Another key difference is that, by increasing the  $-(CH_2)-$  number, from PET to PBT, the chain becomes more flexible and the crystallization process more rapid. For poly(alkylene dicarboxylate)s the increment of chain flexibility with increasing number of methylene units does not play a major part in determining the crystallization rate: indeed, this figure shows that the 2-y series crystallizes more rapidly than the 6-y series, in spite of the shorter polymethylene sequences present in the samples derived from ethanediol.

### 1.2.2. Polyesters containing 1,4-cyclohexylene units

Another group of very interesting polymers is that of polyesters containing 1,4-cyclohexylene units. The monomers that are commercially available are 1,4-cyclohexane dicarboxylic acid (CHDA), dimethyl-1,4-cyclohexane dicarboxylate (DMCD), and 1,4-cyclohexane dimethanol (CHDM) (see Scheme 1.1):

**Scheme 1.1: Molecular structures of cyclic monomers.**



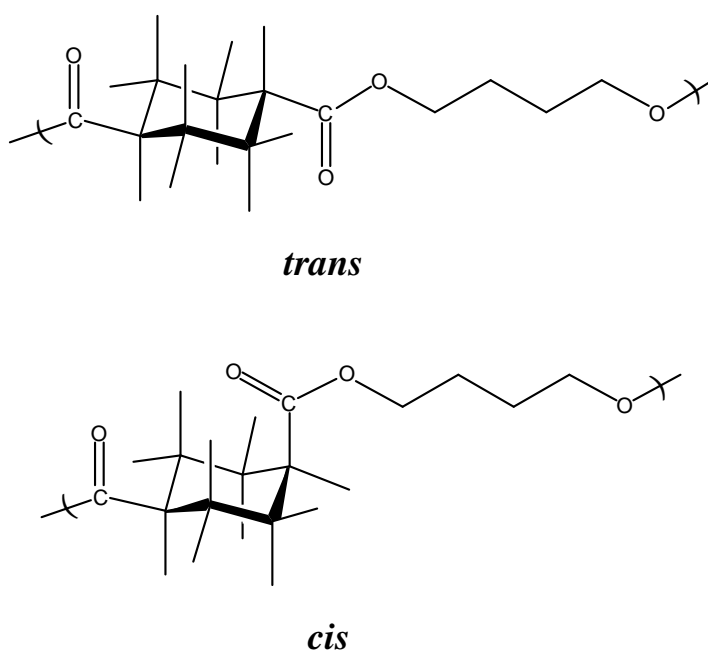
The introduction of cycloaliphatic units to the main chain of the polymer can be a way to increase the rigidity of the macromolecular chains. In literature (Liu and Turner) describe the preparation of a systematic series of random copolyesters using different cycloaliphatic diesters, which are, for the Authors, the most suitable monomers to achieve high  $T_g$  values, up to 115°C. Moreover, conformational transitions of cyclohexylene rings in the backbone originate secondary relaxations in dynamical mechanical spectrum, which contribute to improve the performances of the materials.

The synthesis and properties of polyesters and copolyesters containing these units were studied at the beginning of the eighties by Eastman Chemical Company, interested to develop materials with excellent tensile strength, stiffness and impact properties as well as materials to be used as improved hot melt adhesives.

Today the use of the monomers described in Scheme 1.1 to prepare fully aliphatic polyesters present further advantages. Although CHDA, DMCD, and CHDM are now obtained from petroleum resources, however, they can be prepared from bio-based terephthalic acid, starting from limonene and other terpenes (Berti, 2010). Therefore, polymers derived, for example, from DMCD and a diol obtainable from biomass (as 1,4-butanediol, which can be prepared, for example, from succinic acid (Bechthold, 2008) can be considered fully sustainable materials. Moreover, the presence of the 1,4-cyclohexylene units along a macromolecule does not hinder the attack of microorganisms in some homopolymers and copolymers (Berti, 2009). Therefore, the polyesters containing the 1,4-cyclohexylene units can be considered biodegradable materials and are very promising, environmentally friendly polyesters.

The 1,4-cyclohexylene unit shows another remarkable peculiarity: it can have two possible configurations, *cis* and *trans*, as described in Scheme 1.2 by the monomeric unit of poly(butylenes cyclohexanedicarboxylate, PBCHD). It results that the isomeric ratio of the cycloaliphatic residues along the chains is the key factor which determines the phase behaviour of the materials (Berti, 2008 A; Berti 2008 B;).

**Scheme 1.2: Trans and cis configurations of the monomeric unit in poly(butylene-1,4-cyclohexanedicarboxylate)**



On the market, only two DMCD monomers are available, characterized by 100 and 22 mol% of *trans* isomer respectively. In order to obtain the desired stereochemistry in the final polymer an adequate physical mixture of these two components is used.

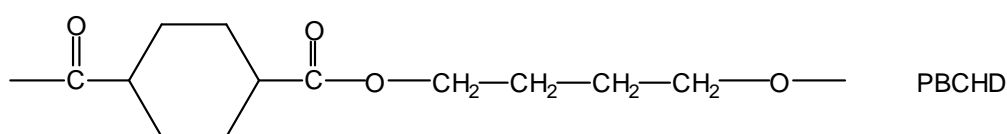
Isomerization reactions, which can change the initial *cis/trans* content towards the thermodynamically stable 34/66 mol%, could take place: they are favored when the synthesis or thermal treatments are carried out at temperatures higher than 260°C and for longer than 1 h, and in the presence of acid groups. Indeed, the use of 1,4-cyclohexane dicarboxylic acid (CHDA) as monomer gives rise to a 5-7% degree of isomerisation, indicating a catalytic effect of the carboxylic acid towards isomerisation (Colonna, 2011). These are the reasons why all the syntheses are preferred to be conducted by starting from DMCD (and not CHDA), and the temperatures do not exceed 220-240°C. Therefore, during the syntheses from DMCD, isomerisation is virtually absent. CHDM is unable to isomerise in the experimental conditions used in literature. The *cis/trans* isomeric ratio in polymers can be evaluated by <sup>1</sup>H NMR analysis.

In this thesis two polymers belonging to this group have been extensively used: poly(butylene-1,4-cyclohexanedicarboxylate) (PBCHD), and poly(1,4-cyclohexylenedimethylene 1,4-cyclohexanedicarboxylate) (PCCD). They are both obtained by a two stage polycondensation reaction.

### 1.2.2.1. Poly(butylene-1,4-cyclohexanedicarboxylate)

In literature (Berti, 2008 A) the polyesters prepared from DMCD and 1,4-butanediol are named with the code PBCHD-xx, (Scheme 1.3) where xx indicates the trans configuration percentage of the aliphatic rings, derived from DMCD.

**Scheme 1.3 Molecular structure of the repeating units of poly(butylene-1,4-cyclohexanedicarboxylate) (PBCHD)**



As already reported before, the cis/trans ratio of the aliphatic ring strongly influence the solid-state behaviour and produce a wide variety of properties.

Table 1.1 collects the properties of PBCHD samples with different cis/trans ratio.

Only some PBCHD samples are able to crystallize, in particular PBCHD-70, -80, -90, and -100, i.e. only the samples with a trans content  $\geq 70\%$ . For these samples,  $T_{CC}$  (crystallization temperature from the melt) and  $\Delta H_{CC}$  (enthalpy of crystallization) have a notable increment as the trans content increases. On the other hand, it is significant that the PBCHD-50 and PBCHD-20, with the lowest percentages of trans stereoisomer, are not able to rearrange towards an ordered state at all: they have the characteristics of completely amorphous materials.

**Table 1.1 Molecular and thermal properties of PBCHD samples compared with those of a PBT specimen (Berti, 2008 A)**

Sample	<i>trans</i> % <sup>a)</sup> in DMCD units of the polymer	$M_w \cdot 10^{-3}$ <sup>b)</sup>	$M_w/M_n$ <sup>b)</sup>	$T_{CC}$ <sup>c)</sup> °C	$\Delta H_{CC}$ <sup>c)</sup> J·g <sup>-1</sup>	$T_g$ <sup>d)</sup> °C	$T_m$ <sup>d)</sup> °C	$\Delta H_m$ <sup>d)</sup> J·g <sup>-1</sup>
PBCHD-20	24	57.0	2.2	-	-	-12	-	-
PBCHD-50	52	88.6	2.8	-	-	-7	-	-
PBCHD-70	72	77.6	2.3	79	34	-2	122	22
PBCHD-80	80	78.4	2.3	106	37	1	132-141	27
PBCHD-90	91	54.9	2.3	130	45	6	150-158	37
PBCHD-100	100	73.4	2.5	149	48	10	165-171	47
PBT	-	47.7	2.4	189	48	42	224	43

<sup>(a)</sup> Calculated by <sup>1</sup>H NMR, <sup>(b)</sup> Measured by GPC in CHCl<sub>3</sub>, <sup>(c)</sup> Measured in DSC during the cooling scan at 10°C·min<sup>-1</sup>, <sup>(d)</sup> Measured in DSC during the 2<sup>nd</sup> heating scan at 10°C·min<sup>-1</sup>.

This behaviour is related to the fact that the aliphatic rings in trans configuration favour crystallizability because in this configuration the polymeric chain assumes a “stretched” form and a high symmetry. These are conditions favourable to the chain packing. On the other hand, the cis isomer introduces kinks into the chain, which hinder the formation of stable crystals. Making a comparison between PBCHD and its aromatic counterpart PBT (the only difference in chemical structures is connected to the substitution of the 1,4-cyclohexylene group with the terephthalate unit) it is clear that  $T_g$ ,  $T_C$  and  $T_m$  have lower values in PBCHD than in PBT. The reason is that the cyclohexyl groups are conformationally more mobile than the rigid phenyl ring.

Another important observation is that the substitution of the aromatic ring with an aliphatic ring improves the thermal stability of the materials (Berti, 2008 A)

#### 1.2.2.2. Poly(1,4-cyclohexylenedimethylene 1,4-cyclohexanedicarboxylate)

The polyesters derived from DMCD and CHDM are indicated with the code PCCD-D<sub>xx</sub>-E<sub>yy</sub> (Scheme 1.4), where xx indicates the percentage of C<sub>6</sub> rings deriving from CHDM (D) in trans configuration and yy the percentage of C<sub>6</sub> rings deriving from DMCD (E) in trans configuration. The PCCD samples considered in literature (Berti, 2008 B), and used in this work, are all prepared from CHDM containing 66 mol % of trans isomer.

**Scheme 1.4 Molecular structure of the repeating units of Poly(1,4-cyclohexylenedimethylene 1,4-cyclohexanedicarboxylate) (PCCD)**

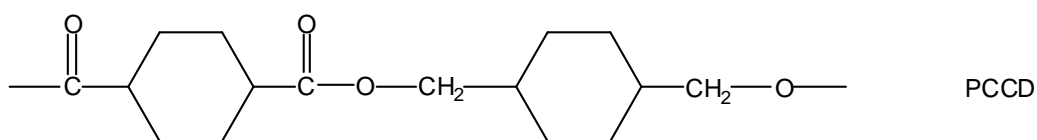


Table 1.2 shows the molecular and thermal data of all PCCD samples with different cis/trans ratio deriving from DMCD monomer.

**Table 1.2 Molecular and thermal properties of PCCD samples (Berti, 2008 B)**

Sample	<i>trans</i> % <sup>a)</sup> in DMCD units of the polymer	$M_w \cdot 10^{-3}$ <sup>b)</sup>	$M_w/M_n$ <sup>b)</sup>	$T_{CC}$ <sup>c)</sup> °C	$\Delta H_{CC}$ <sup>c)</sup> J·g <sup>-1</sup>	$T_g$ <sup>d)</sup> °C	$T_{ch}$ <sup>d)</sup> °C	$\Delta H_{ch}$ <sup>d)</sup> J·g <sup>-1</sup>	$T_m$ <sup>d)</sup> °C	$\Delta H_m$ <sup>d)</sup> J·g <sup>-1</sup>
PCCD-D66-E20	24	43.3	2.2	-	-	38	-	-	-	-
PCCD-D66-E50	52	83.7	2.7	-	-	50	-	-	-	-
PCCD-D66-E70	66	71.7	2.2	-	-	55	142	3	181	4
PCCD-D66-E80	81	75.2	2.2	154	23	60	-	-	200- 205	23
PCCD-D66-E90	91	56.9	2.3	188	29	65	-	-	218- 226	30
PCCD-D66-E100	97	62.0	2.1	204	33	-	-	-	230	34

<sup>(a)</sup>Calculated by <sup>1</sup>H NMR, <sup>(b)</sup> Measured by GPC in CHCl<sub>3</sub>, <sup>(c)</sup> Measured in DSC during the cooling scan at 10°C·min<sup>-1</sup>, <sup>(d)</sup> Measured in DSC during the 2<sup>nd</sup> heating scan at 10°C·min<sup>-1</sup>.

A very similar behaviour to that of PBCHD series has been found in PCCD samples. Even here only the samples with the highest *trans* content can crystallize during the cooling scan from the melt: in particular only D66-E80, D66-E90, and D66-E100. The other samples, with a lower percentage of *trans* stereoisomer, are totally unable to rearrange towards an ordered state.

For *trans* content equal to and higher than about 80% the PCCD is semicrystalline, with crystallization and melting temperatures ( $T_{CC}$  and  $T_m$ ) increasing notably: correspondingly,  $\Delta H_m$  also reaches a high value. Therefore, the stereochemistry of the 1,4-cyclohexylene rings plays a fundamental role in determining the crystallinity and crystallizability of PCCD too.

The thermal stability of PCCD is very high, even higher than PBCHD, and this is due to the fact that the structure of the polymer is characterized by another aliphatic ring instead of the aliphatic sequence: as seen before, the presence of an aliphatic ring contributes to stabilize the material. Indeed the temperature of the maximum degradation rate measured in TGA N<sub>2</sub> flow at 10°C/min for the PBCHD series is around 420°C, the one of PCCD is around 460°C.

### 1.3. Aim of the project

Nowadays the development of sustainable polymers, with convenient properties to substitute the traditional petroleum-based materials, is one of the major issues for material science. The utilization of renewable resources as feedstock for biopolyesters is a challenging target.

The research work described in the present thesis is strictly connected to these urgent necessities and is focused mainly in finding new biopolymers, in particular biopolyesters, which are obtainable from biomass and characterized by a wide range of properties, in order to potentially substitute

polyolefins and aromatic polyesters (for example, poly(ethylene terephthalate)). The research activity starts from some homopolymers already prepared and characterized in the laboratories of the Department of Civil, Environmental and Materials Engineering of the University of Bologna and in Prof. Gross laboratory (NYU University, New York, USA). The work takes advantage of the collaborations with Prof. Gross for the bio-synthesis of new monomers and Prof. Commereuc and Dr. Verney of the Institut de Chimie de Clermont-Ferrand for the photodegradability and biodegradability studies.

In our labs aliphatic polyesters containing 1,4-cyclohexylene ring have been deeply studied. They are an interesting class of materials, as they potentially have some good characteristics typical of biopolymers belonging to aliphatic polyesters group (for example, polyalkylene dicarboxylates and polyhydroxyalkanoates), such as sustainability and biodegradability. Indeed, they are classified as potentially biobased because the starting monomers, 1,4-cyclohexane dicarboxylic acid (CHDA), dimethyl-1,4-cyclohexane dicarboxylate (DMCD), and 1,4-cyclohexane dimethanol (CHDM), are now obtained from non-renewable petrochemical feed-stocks, but alternative routes of synthesis from biomass (Berti, 2010) were successfully tested. Therefore, they can be considered environmentally friendly materials. The homopolymer mainly present in this work is the poly(butylene-1,4-cyclohexanedicarboxylate) (PBCHD), obtained from the polycondensation of 1,4-butanediol and DMCD. PBCHD is not a commercial polymer and has been synthesized in our laboratories with different cis/trans ratio of the 1,4 cyclohexylene units to obtain different properties.

Two other polymers, the poly(1,4-cyclohexylenedimethylene 1,4-cyclohexanedicarboxylate) (PCCD) and the poly(butylene terephthalate) (PBT), can be used as reference materials with respect to the PBCHD properties. PCCD and PBT are commercially available and potentially biobased because they can be obtained following the same synthetic routes for the preparation of DMCD and CHDA from biomass (Berti 2010).

Other interesting homopolymers are biodegradable and fully biobased polyesters: Poly( $\omega$ -hydroxyl tetradecanoic acid) (P14HA), bio-synthesized by Gross from agriculturally fatty acids, and some polyalkylene dicarboxylates, such as those derived from 1,4-butanediol and adipic or 1,4-dodecanedioic acids (4-6, 4-12 polyesters, obtainable from sugars and fatty acids (Burk, 2010, Wenhua, 2010))

Starting from all the above mentioned homopolymers, in order to prepare new polymers it is possible to follow different routes: blending, copolymerization, preparation of composites and nanocomposites, additivation, etc.

In this thesis, only some of these methodologies will be chosen, mainly copolymerization and preparation of composites. Moreover, some macrostructure modification will be carried out by using a polyfunctional monomers (glycerol) and different diols

For the chemical-physics characterization different techniques as  $^1\text{H}$  NMR spectroscopy and gel permeation chromatography (GPC) will be used. Together with these analysis we will perform studies on thermal properties of the new polymers using thermogravimetric analysis (TGA) and differential scanning calorimetry (DSC), on mechanical properties with tensile tests and Dynamic mechanical thermal analysis (DMTA). Moreover, to obtain informations on the nature of crystalline phase we also performed X-ray diffraction analysis.

Biodegradability and photodurability tests using accelerated photoageing will be carried out. FTIR spectroscopy, UV-vis spectroscopy and rheology will be useful techniques to understand the effects of ageing in the polymers.

## Chapter 2 : Experimental part

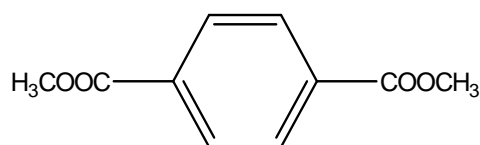
### 2.1. Materials

Chemical structures of monomers used in this study are reported below with their short form. All the products are high purity ones and they have been used as received.

Dimethyl 1,4-cyclohexanedicarboxylate (DMCD)



Dimethyl terephthalate (DMT)



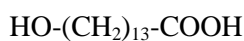
Dimethyl adipate (DMA)



1,12-dodecanedioic acid (DA)



14-hydroxytetradecanoic acid (14HA)



1,2-ethanediol (ED)



1,3-propanediol (P3D)



1,4-Butanediol (BD)



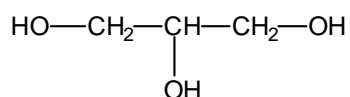
1,5-pentanediol (P5D)



1,8-octanediol (OD)



Glycerol (GL)



Titanium dioxide ( $\text{TiO}_2$ )



Titanium tetrabutoxide (TBT)



C-94

## 2.2. Small scale polymerization plant

Polymers and copolymers that are described in this work are synthesized with a two-stage polycondensation process using titanium tetrabutoxide ( $\text{Ti}(\text{OBu})_4$ ) and C94 as catalysts.

Synthesis are conducted in a small scale: the monomers, around 60 grams total, are placed in the reaction system together with the catalyst and raised to a temperature above the melting point.

Figure 2.1 shows the structure of the polymerization plant:

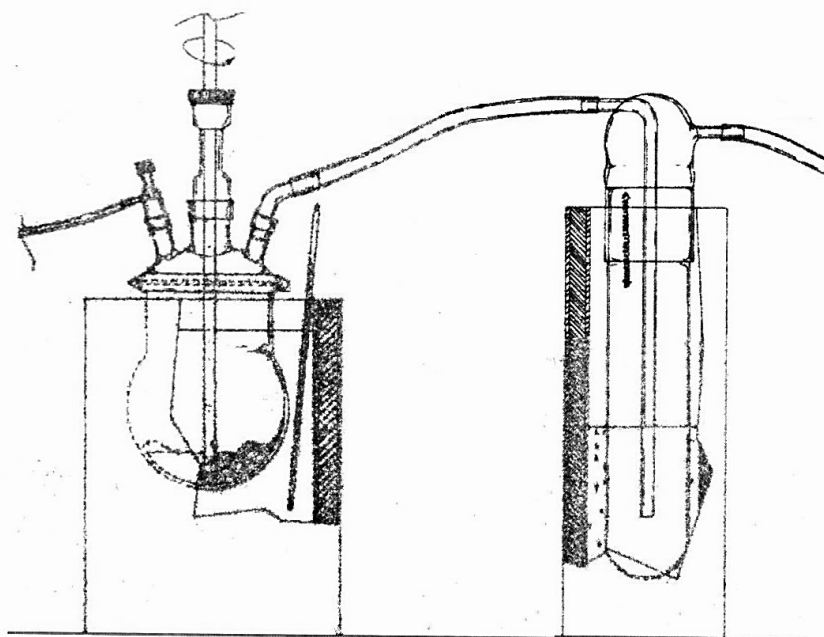


**Figure 2.1 Small scale polymerization plant**

The system is characterized by a round bottom wide-neck glass reactor (250 ml capacity). The reactor was closed with a three-necked flat flange lid equipped with a mechanical stirrer and a torque meter which gives an indication of the viscosity of the reaction melt. The reactor was immersed into a silicone oil bath preheated to 200°C.

During the first stage direct esterification (or transesterification) occurs with continuous removal of methanol (or water) in order to shift the equilibrium towards the products.

This stage was conducted at atmospheric pressure under nitrogen atmosphere and the mixture was allowed to react for 90 min under stirring.

In the second stage the real polymerization reaction takes place: it was started by gradually reducing the pressure to 0.3 mbar with a vacuum pump in order to remove low molecular weight species, while the temperature was raised to the a final value between 220°C and 250°C. These conditions were reached within 60 min, using a linear gradient of temperature and pressure, and

maintained until the viscosity had raised and reached a constant value. The glycol was always used with an excess of about 100% in order to have, at the end of the first stage, oligomers with –OH functional groups that react better than the COOH terminal groups in the second stage.

### 2.3 Brabender Mixer

The composites studied in this work were prepared in a Brabender Mixer (Plasti-Corder PL2000). This apparatus consists of a mixing chamber shaped like a figure eight with a spiral-lobed rotor in each chamber that revolves in opposite directions.

In a chamber, the rotors rotate in order to effect a shearing action on the material mostly by shearing it against the wall. This is illustrated conceptually in Figure 2.2:

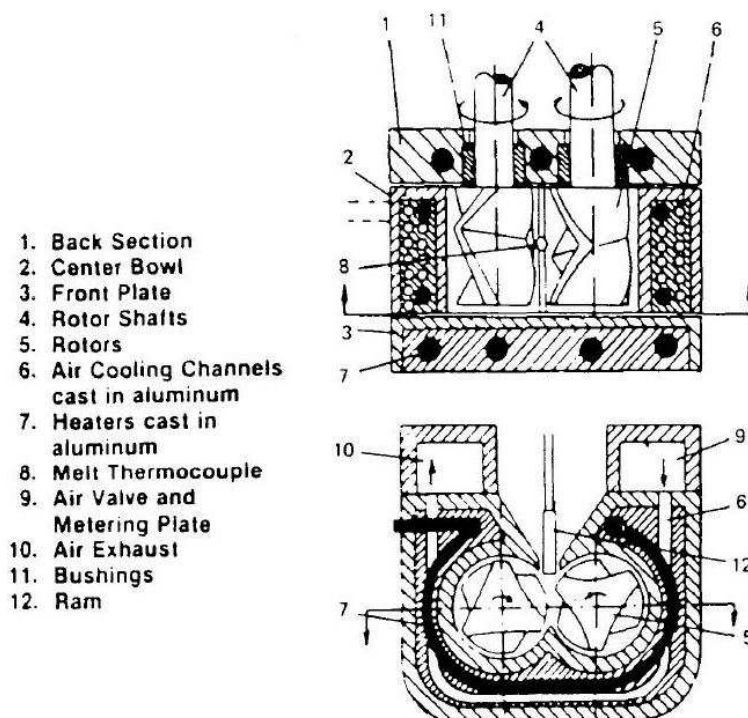


**Figure 2.2 Brabender mixer scheme (Cheremisinoff 1996)**

The rotors have chevrons (helical projections) which perform additional mixing functions by churning the material and moving it back and forth through the mixing chamber. The mixture is fed through a vertical chute with a ram. The lower face of the ram is part of the mixing chamber. There is usually a small clearance between the rotors, in these clearances dispersing mixing takes place. The shape of the rotors and the motion of the ram during operations ensure that all particles undergo high intensive shearing flow in the clearances.

The PL-2000 Plasti-Corder is equipped with a highly sensitive torque measuring load cell, and an heavy duty drive system. It provides for temperature control of up to six heating zones, and pressure monitoring by up to four pressure transducers.

## 2.4. Characterization

### 2.4.1. <sup>1</sup>H NMR

Nuclear Magnetic Resonance (NMR) is a research technique that exploits the magnetic properties of certain atomic nuclei to determine physical and chemical properties of atoms or the molecules in which they are contained. It relies on the principle that the atom nuclei of some elements, under an external magnetic field, orientate in the direction of the imposed field.

Generally, every atomic nucleus has a specific spin number (I), for example  $I=0, 1/2, 1, 3/2, \dots$ , that depends on mass and atomic number.

Nuclei with an odd mass or odd atomic number have "nuclear spin" (in a similar fashion to the spin of electrons). This includes <sup>1</sup>H and <sup>13</sup>C (but not <sup>12</sup>C). The spins of nuclei are sufficiently different that NMR experiments can be sensitive for only one particular isotope of one particular element. Since a nucleus is a charged particle in motion, it will develop a magnetic field. <sup>1</sup>H and <sup>13</sup>C have nuclear spins of 1/2 and so they behave in a similar fashion to a simple, tiny bar magnet. In the absence of a magnetic field, these are randomly oriented but when a field is applied they line up parallel to the applied field, either spin aligned ("up" state") or spin opposed ("down" state") corresponding to an energetic level of  $\pm\mu H_0$  (where  $H_0$  is the intensity of the external magnetic field).

This energy separation or "gap" between the two quantum states is proportional to the strength of the external magnetic field, increasing as the field strength is increased. In a large population of nuclei in thermal equilibrium, slightly more than half will reside in the "up" (lower energy) state, and slightly less than half will reside in the "down" (higher energy) state. As in all forms of spectroscopy, it is possible for a nucleus in the lower energy state to absorb a photon of electromagnetic energy and be promoted to the higher energy state. The energy of the photon must exactly match the energy "gap" ( $\Delta E$ ) between the two states, and this energy corresponds to a specific frequency of electromagnetic radiation:

$$\Delta E = h\nu = 2\mu H_0$$

where  $h$  is Planck's constant and  $\nu$  is the resonant frequency.

The resonant frequency is not only a characteristic of the type of nucleus, but also varies slightly depending on the position of that atom within a molecule (the "chemical environment"). This occurs because the bonding electrons create their own small magnetic field which modifies the external magnetic field in the vicinity of the nucleus. This subtle variation, on the order of one part in a million, is called the chemical shift and provides detailed information about the structure of molecules. Different atoms within a molecule can be identified by their chemical shift, based on

molecular symmetry and the predictable effects of nearby electronegative atoms and unsaturated groups.

The chemical shift is measured in parts per million and is designated by the greek letter delta ( $\delta$ ). The resonant frequency for a particular nucleus at a specific position within a molecule is then equal to the fundamental resonant frequency of that isotope times a factor which is slightly greater than 1.0 due to the chemical shift:

$$\text{resonant frequency} = \nu_0 (1.0 + \delta \cdot 10^{-6})$$

In this work  $^1\text{H}$  NMR has been used to verify the structures of synthesized polymers and to determinate their composition. The spectra were recorded at room temperature on samples dissolved in  $\text{CDCl}_3$  using a Varian Mercury 400 spectrometer, the proton frequency being 400 MHz.

### **2.4.2. Gel permeation chromatography (GPC)**

Gel permeation chromatography (GPC), also called size exclusion chromatography and gel filtration, affords a rapid method for the separation of oligomeric and polymeric species.

The separation is based on differences in molecular size in solution. It is of particular importance for research in biological systems and is the method of choice for determining molecular weight distribution of synthetic polymers. The separation medium is a porous solid, such as glass or silica, or a cross-linked gel which contains pores of appropriate dimensions to effect the separation desired.

The liquid mobile phase is usually water or a buffer for biological separations, and an organic solvent that is appropriate for the polymer and is compatible with the column packing for synthetic polymer characterization. Solvent flow may be driven by gravity, or by a high-pressure pump to achieve the desired flow rate through the column. The sample to be separated is introduced at the head of the column. As it progresses through the column, small molecules can enter all pores larger than the molecule, while larger molecules can fit into a smaller number of pores, again only those larger than the molecule. So the separation of different molecular weights occurs.

Molecular weights (expressed in equivalent polystyrene) were determined using a Hewlett Packard Series 1100 liquid chromatography instrument equipped with a PL gel  $5\mu$  Mixed-C column. Chloroform was used as eluent and a calibration plot was constructed with polystyrene standards.

### **2.4.3. Thermogravimetric analysis (TGA)**

Thermogravimetric analysis (TGA) is an analytical technique used to determine a material's thermal stability and its fraction of volatile components by monitoring the weight change that

occurs as the material is heated at a specific heating rate. The measurement is normally carried out in air or in an inert atmosphere, such as Helium, Nitrogen or Argon, and the weight is recorded as a function of increasing temperature.

The maximum temperature is selected so that the specimen weight is stable at the end of the experiment, implying that all chemical reactions are completed. This approach provides different important numerical pieces of information: ash content (residual mass,  $M_{\text{res}}$ ) whose definition is often unambiguous, degradation temperature, that is the temperature of the maximum in the weight loss rate ( $T_d$ ) and the weight loss onset temperature ( $T_{\text{onset}}$ ). The former refers to the temperature of the maximum degradation rate, while the latter refers to the temperature when degradation just begins.

The analysis was performed using a Perkin-Elmer TGA7 thermobalance under nitrogen atmosphere (gas flow 40 ml/min) at  $10^\circ\text{C min}^{-1}$  heating rate from  $50^\circ\text{C}$  to  $900^\circ\text{C}$ .

#### **2.4.4. Differential scanning calorimetry (DSC)**

Differential scanning calorimetry (DSC) is a thermo-analytical technique in which the difference in the amount of heat required to increase the temperature of a sample and reference are measured as a function of temperature. Both the sample and reference are maintained at nearly the same temperature throughout the experiment. Generally, the temperature program for a DSC analysis is designed such that the sample holder temperature increases linearly as a function of time.

The reference sample should have a well-defined heat capacity over the range of temperatures to be scanned. The basic principle underlying this technique is that, when the sample undergoes a physical transformation such as phase transitions, more (or less) heat will need to flow to it than the reference to maintain both at the same temperature. Whether more or less heat must flow to the sample depends on whether the process is exothermic or endothermic. For example, as a solid sample melts to a liquid it will require more heat flowing to the sample to increase its temperature at the same rate as the reference. This is due to the absorption of heat by the sample as it undergoes the endothermic phase transition from solid to liquid. Likewise, as the sample undergoes exothermic processes (such as crystallization) less heat is required to raise the sample temperature.

By observing the difference in heat flow between the sample and reference, differential scanning calorimeters are able to measure the amount of heat absorbed or released during such transitions. DSC may also be used to observe more subtle phase changes, such as glass transitions. DSC is widely used in industrial settings as a quality control instrument due to its applicability in evaluating sample purity and for studying polymer curing.

The calorimetric analysis was carried out by means of a Perkin-Elmer DSC6, calibrated with high purity standards. The measurements were performed under nitrogen flow. In order to cancel the previous thermal history, the samples (ca. 10 mg) were initially heated at 20°C min<sup>-1</sup> to different temperatures, above melting point according to the sample characteristics, kept at high temperature for 1 min and then cooled to -60°C at 10°C min<sup>-1</sup>. After this thermal treatment, the samples were analyzed by heating again above melting point (2<sup>nd</sup> scan). During the cooling scan the crystallization temperature ( $T_{CC}$ ) and the enthalpy of crystallization ( $\Delta H_{CC}$ ) were measured. During the 2<sup>nd</sup> scan the glass transition temperature ( $T_g$ ), the eventual cold crystallization temperature ( $T_{ch}$ ) and enthalpy ( $\Delta H_{ch}$ ), the melting temperature ( $T_m$ ) and the enthalpy of fusion ( $\Delta H_m$ ) were determined.

#### 2.4.5. Dynamic mechanical thermal analysis (DMTA)

Dynamic mechanical properties refer to the response of a material as it is subjected to a periodic force. These properties may be expressed in terms of a dynamic modulus, a dynamic loss modulus, and a mechanical damping term.

For an applied stress varying sinusoidally with time, a viscoelastic material will also respond with a sinusoidal strain for low amplitudes of stress. The sinusoidal variation in time is usually described as a rate specified by the frequency ( $f = \text{Hz}$ ;  $\omega = \text{rad/sec}$ ). The strain of a viscoelastic body is out of phase with the stress applied, by the phase angle,  $\delta$ . This phase lag is due to the excess time necessary for molecular motions and relaxations to occur. Dynamic stress,  $\omega$ , and strain,  $\varepsilon$ , given as:

$$\begin{aligned}\sigma &= \sigma_o \sin(\omega t + \delta) \\ \varepsilon &= \varepsilon_o \sin(\omega t)\end{aligned}$$

where  $\omega$  is the angular frequency. Using this notation, stress can be divided into an “inphase” component ( $\sigma \cos\delta$ ) and an “out-of-phase” component ( $\sigma_o \sin\delta$ ) and rewritten as,

$$\sigma = \sigma_o \sin(\omega t) \cos\delta + \sigma_o \cos(\omega t) \sin\delta$$

Dividing stress by strain to yield a modulus and using the symbols  $E'$  and  $E''$  for the inphase (real) and out-of-phase (imaginary) moduli yields:

$$\begin{aligned}\sigma &= \varepsilon_o E' \sin(\omega t) + \varepsilon_o E'' \cos(\omega t) \\ E' &= \sigma_o / \varepsilon_o \cos\delta & E'' &= \sigma_o / \varepsilon_o \sin\delta \\ \varepsilon &= \varepsilon_o \exp(i\omega t) & \sigma &= \sigma_o \exp(i\omega t + \delta) \\ E^* &= \sigma / \varepsilon = \sigma_o / \varepsilon_o e^{i\delta} = \sigma_o / \varepsilon_o (\cos\delta + i \sin\delta) = E' + i E''\end{aligned}$$

This equation shows that the complex modulus obtained from a dynamic mechanical test consists of “real” and “imaginary” parts. The real part (storage modulus) describes the ability of the

material to store potential energy and release it upon deformation. The imaginary part (loss modulus) is associated with energy dissipation in the form of heat upon deformation.

The phase angle  $\delta$  is given by

$$\tan\delta = E''/E'$$

The storage modulus is often times associated with “stiffness” of a material and is related to the Young’s modulus,  $E$ . The dynamic loss modulus is often associated with “internal friction” and is sensitive to different kinds of molecular motions, relaxation processes, transitions, morphology and other structural heterogeneities.

During measurement of  $E'$ ,  $E''$  and  $\tan\delta$  of a polymer at a chosen oscillatory frequency over a sufficiently wide range of temperature, the effect of the polymer’s glass transition can be clearly observed: the glass transition (called  $\alpha$  transition) temperature  $T_g$ , can be measured accurately by DMTA. The glass transition is detected as a sudden and considerable (several decades) change in the elastic modulus and an attendant peak in the  $\tan\delta$  curve. This underscores the importance of the glass transition as a material property, for it shows clearly the substantial change in rigidity that the material experiences in a short span of temperatures.

Besides  $\alpha$  transition, dynamic mechanical spectroscopy can reveal other secondary transition phenomena, connected to local motions of small entities. Secondary transitions are indicated with  $\beta$  and  $\gamma$  in order of decreasing temperature. Figure 2.3 shows the typical DMTA spectra of both amorphous and semicrystalline polymer:

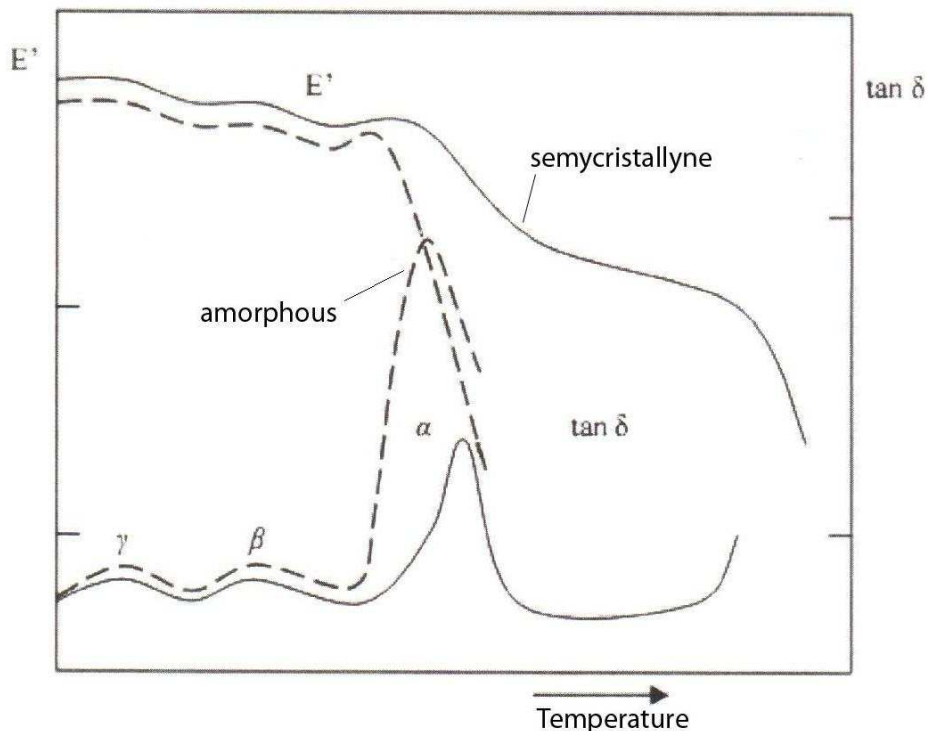


**Figure 2.3 Example of DMTA spectrum**

Specimens for dynamic mechanical measurements were obtained by injection molding in a Mini Max Molder (Custom Scientific Instruments) equipped with a rectangular mold (30 x 8 x 1.6 mm<sup>3</sup>). Dynamic mechanical measurements were performed with a dynamic mechanical thermal analyzer (Rheometrics Scientific, DMTA IV), operated in dual cantilever bending mode, at a frequency of 3 Hz and a heating rate of 3°C·min<sup>-1</sup>, over a temperature range from -150°C to a final temperature below the melting point of the polymer.

#### 2.4.6. Rheology

Rheology is the science of deformation and flow of matter under controlled testing conditions. In dynamic frequency sweeps tests, the polymer is strained sinusoidally and the stress is measured as a function of the frequency. The strain amplitude is kept small enough to evoke only a linear response. The advantage of this test is that it separates the moduli into an elastic one, the dynamic storage modulus ( $G'$ ) and into a viscous one, the dynamic loss modulus ( $G''$ ).

Following the considerations already written in the DMTA chapter we can rewrite the equation of complex modulus for shear state:

$$G^* = G' + iG''$$

From these measurements one can determine fundamental properties such as:

- Zero shear viscosity (which can be related to weight average molecular weight and long chain branching).
- Tan delta
- Plateau modulus (which can indicate the extent and “tightness” of crosslinking).
- Complex viscosity (which can be related to the steady shear viscosity).

Differences in  $G'$  and  $G''$  and hence in the properties mentioned above will be found if there are differences in molecular weight, molecular weight distribution (MWD) or long chain branching.

In particular the zero shear viscosity  $\eta_0$  obeys a power law:

$$\eta_0 \propto M_w^\alpha$$

with  $\alpha$  about 3,4.

The zero shear viscosity  $\eta_0$  can be obtained from the complex viscosity  $\eta^*(\omega)$ :

$$\eta^* = G^*(\omega) / i\omega = \eta' - i\eta''$$

and

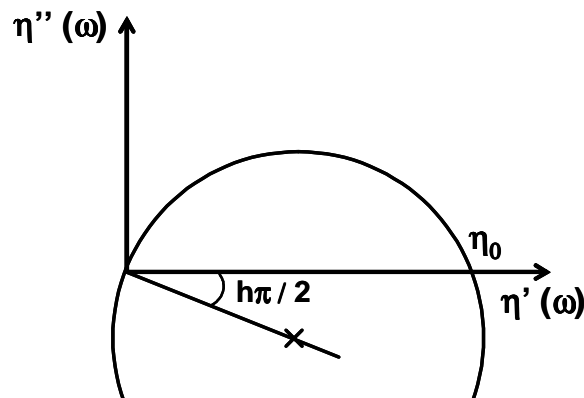
$$|\eta^*|_{\omega \rightarrow 0} = |\eta'|_{\omega \rightarrow 0} = \eta_0$$

An empirical rheological model used to fit dynamic data is the Cole-Cole plot expressed by:

$$\eta^*(\omega) = \eta_0 / [1 + (i \omega \lambda_0)^{1-h}]$$

where  $\lambda_0$  is the average relaxation time and  $h$  is the relaxation-time distribution parameter (Verney, 1989; Vega, 1996; Montfort, 1984).

This model predicts the variation of the viscosity components ( $\eta''$  versus  $\eta'$ ) to be an arc of a circle in the complex plane. From this representation it is easy to determine the distribution parameters:  $\eta_0$  is obtained through the extrapolation of the arc of a circle on the real axis, while the distribution parameter  $h$  is obtained through the measurement of the  $\Phi = h\pi/2$  angle between the real axis and the radius going from the origin of the axis to the centre of the arc of a circle (see Scheme 2.1).



**Scheme 2.1 Cole-Cole- plot**

Rheological experiments were performed in oscillatory shear mode using a rotational controlled strain rheometer (ARES / Rheometric Scientific) equipped with parallel plate geometry, with an 8 mm diameter, while the gap between the plates was about 1 mm. For all cases, the values of the strain amplitude were checked to ensure that all measurements were conducted within the linear viscoelastic region. At different time during the photoageing, a frequency sweep extending from 0.1 to 100  $\text{rad}\cdot\text{s}^{-1}$  was performed. All experiments were carried out at 85°C or 130°C.

#### 2.4.7. Tensile testing

Tensile properties indicate how the material will react to forces being applied in tension. A tensile test is a fundamental mechanical test where a carefully prepared specimen is loaded in a very controlled manner while measuring the applied load and the elongation of the specimen over some distance. Tensile tests are used to determine the modulus of elasticity, elastic limit, elongation,

proportional limit, reduction in area, tensile strength, yield point, yield strength and other tensile properties.

The main product of a tensile test is a load versus elongation curve which is then converted into a stress versus strain curve. Since both the engineering stress and the engineering strain are obtained by dividing the load and elongation by constant values (specimen geometry information), the load-elongation curve will have the same shape as the engineering stress-strain curve. The stress-strain curve relates the applied stress to the resulting strain and each material has its own unique stress-strain curve. A typical engineering stress-strain curve is shown in figure 2.4.

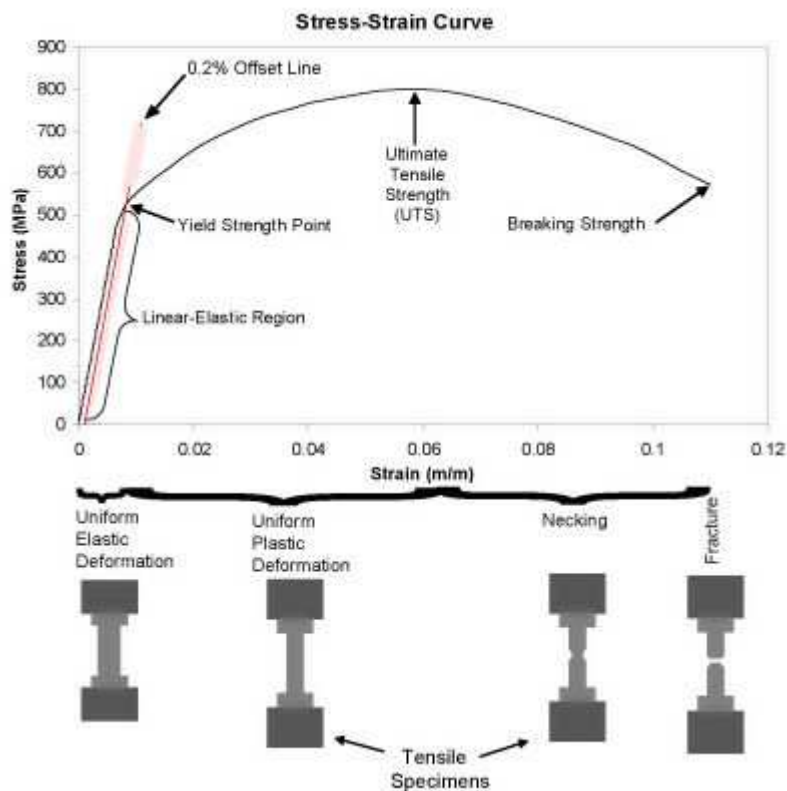


**Figure 2.4 Stress strain curve**

As can be seen in the figure, the stress and strain initially increase with a linear relationship. This is the linear-elastic portion of the curve and it indicates that no plastic deformation has occurred. In this region of the curve, when the stress is reduced, the material will return to its original shape. In this linear region, the line obeys the relationship defined as Hooke's Law. The slope of the line in this region where stress is proportional to strain and is called the modulus of elasticity or Young's modulus. The modulus of elasticity ( $E$ ) defines the properties of a material as it undergoes stress, deforms, and then returns to its original shape after the stress is removed. It is a measure of the stiffness of a given material.

In ductile materials, at some point, the stress-strain curve deviates from the straight-line relationship and Law no longer applies as the strain increases faster than the stress. From this point on in the tensile test, some permanent deformation occurs in the specimen and the material is said to react plastically to any further increase in load or stress. The material will not return to its original, unstressed condition when the load is removed. In brittle materials, little or no plastic deformation occurs and the material fractures near the end of the linear-elastic portion of the curve.

With most materials there is a gradual transition from elastic to plastic behavior, and the exact point at which plastic deformation begins to occur is hard to determine. The yield strength is defined as the stress required to produce a small, amount of plastic deformation. The ultimate tensile strength (UTS) or, more simply, the tensile strength, is the maximum engineering stress level reached in a tension test. The strength of a material is its ability to withstand external forces without breaking. In brittle materials, the UTS will be at the end of the linear-elastic portion of the stress-strain curve or close to the elastic limit. In ductile materials, the UTS will be well outside of the elastic portion into the plastic portion of the stress-strain curve.

The ductility of a material is a measure of the extent to which a material will deform before fracture. The amount of ductility is an important factor when considering forming operations such as rolling and extrusion. It also provides an indication of how visible overload damage to a component might become before the component fractures.

The conventional measures of ductility are the engineering strain at fracture (usually called the elongation ) and the reduction of area at fracture. Both of these properties are obtained by fitting the specimen back together after fracture and measuring the change in length and cross-sectional area. Elongation is the change in axial length divided by the original length of the specimen or portion of the specimen. It is expressed as a percentage.

Dumbbell shaped sample bars with dimensions of 9.0 mm (length) x 3.0 mm (neck width) x 1.0 mm (thickness) were prepared by press-molding at different temperatures (depending on samples  $T_m$ ) and subsequent quenching at ambient temperature. An Instron 5542 tensile testing machine with a 500 N load cell was used. The crosshead speed was 5 mm/min and the test temperature was 25°C. Merlin software was used to collect and analyze tensile results (stress was calculated according to the initial cross-section area). Values of Young's modulus, elongation at yield and break and stress at yield were obtained by averaging the data obtained from  $\geq 5$  samples. Young's modulus was measured as the slope of stress-strain curves at strain below 1%, using the linear least square method. Elongation and stress at break measurements were determined at the (x,y) coordinates after which the slope of the stress-strain curve became negative.

### 2.4.8. Wide Angle X-ray Scattering (WAXS)

Wide angle X-ray scattering (WAXS) is an X-ray diffraction technique that is often used to determine the crystalline structure of polymers.

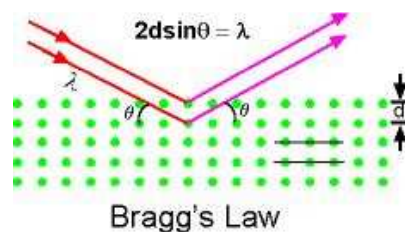
X-rays are electromagnetic radiation with typical photon energies in the range of 100 eV - 100 keV. X-rays are produced generally by x-ray tubes which are the primary x-ray source used in laboratories. They are generated when a focused electron beam accelerated across a high voltage field bombards a stationary or rotating solid target.

The peaks in a x-ray diffraction pattern are directly related to the atomic distances. Let us consider an incident x-ray beam interacting with the atoms arranged in a periodic manner as shown in Scheme 2.2. The atoms, represented as green spheres in the graph, can be viewed as forming different sets of planes in the crystal.

The distance between these planes is called the d-spacing. The intensity of the d-space pattern is directly proportional to the number of electrons (atoms) that are found in the imaginary planes. Every crystalline solid will have a unique pattern of d-spacings (known as the powder pattern), which is a “finger print” for that solid. In fact solids with the same chemical composition but different phases can be identified by their pattern of d-spacing. The condition for a diffraction (peak) to occur can be simply written as

$$2d\sin\theta = n\lambda$$

which is known as the Bragg's law (Scheme 2.2). In this equation,  $\lambda$  is the wavelength of the x-ray,  $\theta$  the scattering angle, and  $n$  an integer representing the order of the diffraction peak.



**Scheme 2.2 Bragg's Law**

According to this method the sample is scanned in a wide angle X-ray goniometer, and the scattering intensity is plotted as a function of the  $2\theta$  angle. X ray diffraction is a non destructive method of characterization of solid materials. When X-rays are directed in solids they will scatter in predictable patterns based upon the internal structure of the solid. The Wide Angle X-ray Scattering (WAXS) data were collected with a X'PertPro diffractometer, equipped with a copper anode ( $K_{\alpha}$  radiation,  $\lambda = 1.5418 \text{ \AA}$ ). The data were collected in the  $2\theta$  range  $5^{\circ}$ - $60^{\circ}$  by means of a X'Celerator detector. The measurements were performed on samples at which the thermal history has been cancelled by thermal treatment in DSC (heating at  $20^{\circ}\text{C min}^{-1}$  to different temperatures, varying from  $100$  to  $190^{\circ}\text{C}$  according to the sample characteristics,  $1$  min of isotherm at this temperature, and then cooling at  $10^{\circ}\text{C min}^{-1}$  to a temperature above the crystallization temperature, varying from  $-20$  to  $30^{\circ}\text{C}$ ).

## 2.4.9. Fourier Transformation Infrared Spectroscopy (FTIR)

Infrared spectroscopy is a technique based on the vibrations of atoms of a molecule. An IR spectrum is commonly obtained by passing IR radiation through a sample and determining what fraction of the incident radiation is absorbed at a particular energy. The energy at which any peak in an absorption spectrum appears corresponds to the frequency of a vibration of a part of a sample molecule. The most useful information that an IR spectrum provides is what functional groups are present in the molecule.

In order to better understand IR, it is useful to compare a vibrating bond to the physical model of a vibrating spring system. The spring system can be described by Hooke's Law:

$$\nu = (1/2\pi c) * \sqrt{(f/\mu)}$$

$\nu$  = frequency

$c$  = speed of light

$f$  = force constant (bond strength)

$\mu$  = reduced mass =  $(m_1 m_2)/(m_1 + m_2)$

Consider a bond and the connected atoms to be a spring with two masses attached. Using the force constant  $k$  (which reflects the stiffness of the spring) and the two masses  $m_1$  and  $m_2$ , then the equation indicates how the frequency,  $\nu$ , of the absorption should change as the properties of the system change. As examples of this look at the positions of C-C ( $1000 \text{ cm}^{-1}$ ), C=C ( $1600 \text{ cm}^{-1}$ ) and C=C ( $2200 \text{ cm}^{-1}$ ), and the positions of C-H ( $3000 \text{ cm}^{-1}$ ) and C-C ( $1000 \text{ cm}^{-1}$ ).

The following diagram reflects some of the trends that can be accounted for using Hooke's Law. It also gives an approximate outline of where specific types of bond stretches may be found.

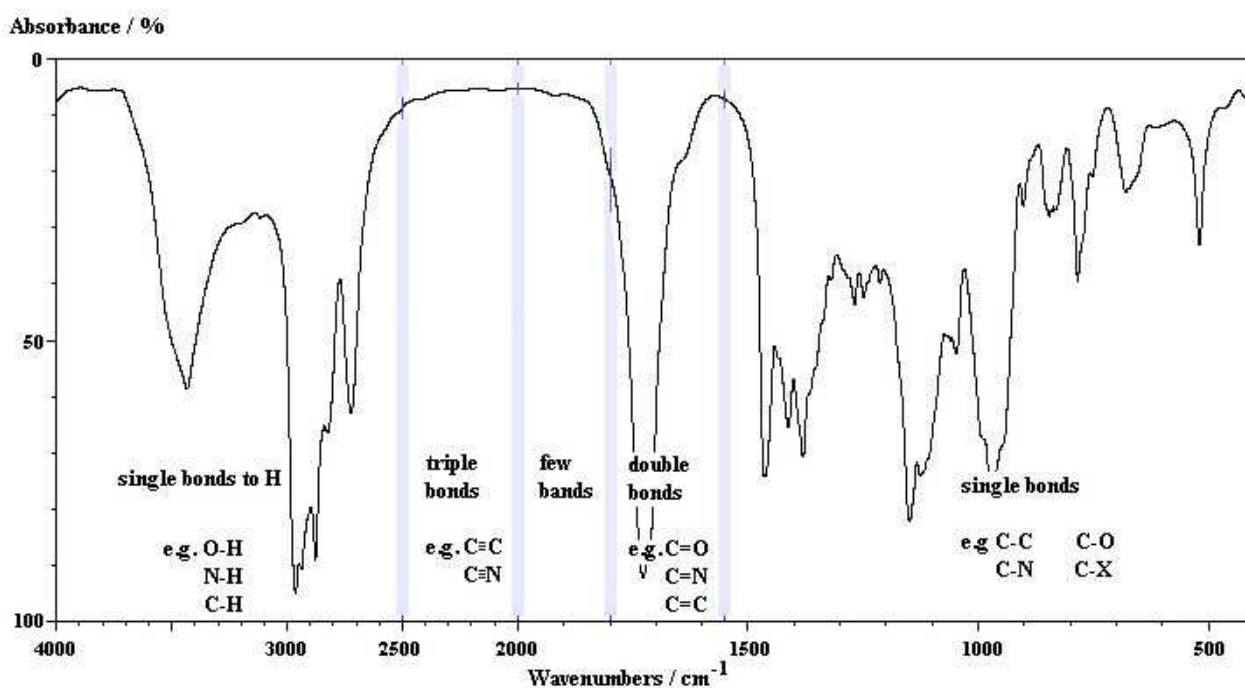


Figure 2.5 IR spectra with typical peaks of functional groups

The most significant advances in IR spectroscopy, however, have come about as a result of the introduction of Fourier transform spectrometers (Othmer, 2005). This type of instrument employs an interferometer and exploits the well-established mathematical process of Fourier transformation. Fourier transformation infrared spectroscopy is based on the idea of the interference of radiation between two beams to yield an interferogram. An interferogram is a signal produced as a function of the change of pathlength between the two beams. The two domains of distance and frequency are interconvertible by the mathematical method of Fourier transformation.

Performing a mathematical Fourier Transform on this signal results in a spectrum identical to that from conventional (dispersive) infrared spectroscopy. FTIR spectrometers are cheaper than conventional spectrometers because building of interferometers is easier than a monochromator. In addition, measurement of a single spectrum is faster for the FTIR technique because the information at all frequencies is collected simultaneously. This allows multiple samples to be collected and averaged together resulting in an improvement in sensitivity.

The instrument is a FT-IR NICOLET 6700 of THERMOFISHER Scientific (OMNIC Software). Wavelength range varies between 4000 e 400  $\text{cm}^{-1}$ , each spectrum is the result of 32 scans with a resolution of 4  $\text{cm}^{-1}$ .

#### **2.4.10. UV-Vis Spectroscopy**

UV-visible spectroscopy can be used to determine many physicochemical characteristics of compounds and thus can provide information as to the identity of a particular compound. Ultraviolet (UV) and visible radiations comprise only a small part of the electromagnetic spectrum, which includes other forms of radiation as radio, infrared (IR), cosmic, and X rays (Agilent, 2003).

Electromagnetic radiation can be considered a combination of alternating electric and magnetic fields that travel through space with a wave motion. Because radiation acts as a wave, it can be classified in terms of either wavelength or frequency, which are related by the following equation:

$$\nu = c / \lambda$$

where  $\nu$  is frequency (in seconds),  $c$  is the speed of light ( $3 \times 10^8 \text{ms}^{-1}$ ), and  $\lambda$  is wavelength (in meters). In UV-visible spectroscopy, wavelength usually is expressed in nanometers.

It follows from the above equations that radiation with shorter wavelength has higher energy. In UV-visible spectroscopy, the low-wavelength UV light has the highest energy.

When radiation interacts with matter, a number of processes can occur, including reflection, scattering, absorbance, fluorescence/phosphorescence (absorption and reemission), and photochemical reaction (absorbance and bond breaking). In general, when measuring UV-visible spectra, we want only absorbance to occur.

In some molecules and atoms, photons of UV and visible light have enough energy to cause transitions between the different electronic energy levels. The wavelength of light absorbed is that having the energy required to move an electron from a lower energy level to a higher energy level.

These transitions should result in very narrow absorbance bands at wavelengths highly characteristic of the difference in energy levels of the absorbing species. However, for molecules, vibrational and rotational energy levels are superimposed on the electronic energy levels. Because many transitions with different energies can occur, the bands are broadened. When light passes through or is reflected from a sample, the amount of light absorbed is the difference between the incident radiation ( $I_0$ ) and the transmitted radiation ( $I$ ). The amount of light absorbed is expressed as either transmittance or absorbance. Transmittance usually is given in terms of a fraction of 1 or as a percentage and is defined as follows:

$$T = I/I_0 \quad \text{or} \quad \% T = (I/I_0) \times 100$$

Absorbance is defined as follows:

$$A = -\log T$$

For most applications, absorbance values are used since the relationship between absorbance and both concentration and path length normally is linear.

#### **2.4.11. Scanning Electron Microscope (SEM)**

A scanning electron microscope (SEM) is a type of electron microscope that images a sample by scanning it with a high-energy beam of electrons in a raster scan pattern. The electrons interact with the atoms that make up the sample producing signals that contain information about the sample's surface topography, composition, and other properties such as electrical conductivity.

The types of signals produced by an SEM include secondary electrons, back-scattered electrons (BSE), characteristic X-rays, light, specimen current and transmitted electrons. Secondary electron detectors are common in all SEMs, but it is rare that a single machine would have detectors for all possible signals. The signals result from interactions of the electron beam with atoms at or near the surface of the sample. In the most common or standard detection mode, the SEM can produce very high-resolution images. Due to the very narrow electron beam, SEM micrographs have a large depth of field yielding a characteristic three-dimensional appearance useful for understanding the surface structure of a sample.

For conventional imaging in SEM, specimens must be electrically conductive, at least at the surface, and electrically grounded to prevent the accumulation of electrostatic charge at the surface. Metal objects require little special preparation for SEM except for cleaning and mounting on a specimen stub. Nonconductive specimens tend to charge when scanned by the electron beam, and

especially in secondary electron imaging mode, this causes scanning faults and other image artifacts. They are therefore usually coated with an ultrathin coating of electrically-conducting material, commonly gold, deposited on the sample either by low vacuum sputter coating or by high vacuum evaporation. Conductive materials in current use for specimen coating include gold, gold/palladium alloy, platinum, osmium, iridium, tungsten, chromium and graphite. Coating prevents the accumulation of static electric charge on the specimen during electron irradiation.

#### **2.4.12. Accelerated Photoageing**

Photodegradation (chains scission and/or crosslinking) occurs by the activation of the polymer macromolecule provided by the absorption of a photon of light by the polymer (Rabek, 1995).

In the case of photoinitiated degradation light is absorbed by photoinitiators, which are photocleaved into free radicals, which further initiate degradation (in non-photochemical processes) of the polymer macromolecules. In photo-thermal degradation both photodegradation and thermal degradation processes occur simultaneously and one of these can accelerate another. Photoageing is usually initiated by solar UV radiation, air and pollutants, whereas water, organic solvents, temperature and mechanical stresses enhance these processes.

During photochemical degradation two distinct processes occur: a series of photochemical reactions, due to the absorption of radiations, that lead to the production of free radicals or to rearrangement of non-radicals; reactions that are independent from light between the obtained radicals.

In semicrystalline polymers, degradation reactions occur generally in the amorphous phase. However, the degradation process can be modified by different physical factors like dimension and distribution of crystalline phases. In polymer systems Photodegradation kinetic depends on the permeability of the oxygen through the material. The oxidation rate decreases decreasing the oxygen diffusion, following the increasing of crystallinity and molecular orientation.

These characteristics determine radicals mobility and reduce termination rate promoting the propagations of chemical reactions that lead to chain scission that is an opposite effects compare to the one caused by the reduction of oxygen mobility. Which of these effects will predominate depends on oxidation conditions.

During photo-oxidative degradation of almost all polymers the following steps can be considered

1. Initiation step: formation of free radicals
2. Propagation step: reaction of free polymer radicals with oxygen, production of polymer oxy- and peroxy-radicals and secondary polymer radicals, resulting in chain scission
3. Termination step: reaction between free radicals leading to crosslinking

Natural ageing gives a lot of informations about curability of stabilized polymers in the different application fields. Nevertheless it also has several disadvantages: it is difficult to compare results from different geographic places even when materials are submitted to solar radiations of the same intensities: temperature and air pollution can vary. Indeed, time is not a reproducible factor, both in short and long period and this limits the prediction of life time of polymers that undergo natural ageing.

For these reasons samples were exposed to UV irradiation at 60°C in an accelerated photo-ageing device based on SEPAP 12-24 device (Service d'Etude du Photovieillissement Accéléré des Polymères) (Penot, 1983; Tidjani, 1995). The polychromatic set up was equipped by a « medium pressure » mercury source filtered by borosilicate envelope (Mazda type MA 400) supplying radiation of wavelengths longer than 300 nm. This source is positioned along the focal axis of a cylinder with elliptical base. Sample films, fixed on aluminum holders, turned around the other focal axis. The inside of the chamber is made of highly reflecting aluminum as shown in Figure. 2.6:



**Figure 2.6 Inside of SEPAP chamber**

The temperature of samples was controlled by a thermocouple connected with a temperature regulator device which controls a fan.

Generally, irradiating a LDPE film for 24h inside this system at 60°C equals to about 960 h (40 days) of solar exposition (Lemaire, 1996).

Photodegradability studies were performed on films (about 100 µm) prepared by compression molding between two teflon sheets at temperature that vary between 100°C and 250°C and P = 200 bar.

### 2.4.13. Biodegradation

Before investigation, the samples were dissolved in chloroform and then precipitated from methanol for the purpose of purification. After being dried thoroughly under vacuum, the purified materials are white powders.

Among the different tests to evaluate the biodegradability, the measurement of the biological breakdown in aerobic liquid medium is of main interest (Pagga, 1997). The international standard of standardization (ISO: “International Standards Organization”) ISO 14852 described the experimental conditions for the tests of biodegradability in aqueous medium (ISO14852, 1999). They are rather easy to carry out and reproducible. The measurements are based on the evaluation of the  $O_2$  consumption and the quantity of  $CO_2$  released during the biological breakdown of the plastic specimen, as in the method of Sturm (Sturm, 1973). The material to be tested is placed in an aqueous mineral nutrient liquid medium inoculated by micro-organisms resulting from activated sludge, suspensions of active ground or compost.

An experimental device has been built based on this respirometric method, based on the measurement of pressure drop. A schematic representation is shown in Figure 2.7:

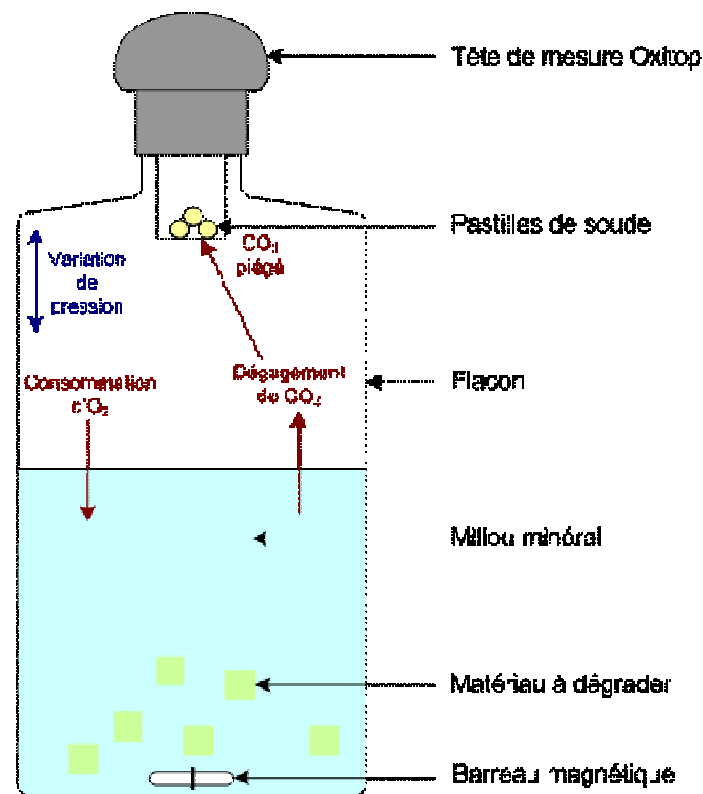


**Figure 2.7 Biodegradation apparatus based on Oxygen consumption**

Since  $CO_2$  is trapped, the decrease of pressure inside the bioreactor is assigned to the  $O_2$  consumption. In our experimental conditions, the colonization medium is a solution containing only inorganic species. This medium of growth was inoculated with a biological *inoculum* (sewage

sludge taken *in situ* from a station of purification of the worn water). In this way, the only source of carbon available is from the tested polymeric film, whether soluble or not, which is submitted to biodegradation. The incubating test is performed at 30°C under continuous shaking over 19 days and aeration ensures that there is sufficient oxygen in the bioreactor at all times. The percentage of biodegradation could be evaluated from the amount of O<sub>2</sub> consumed by the plastic sample compared to the total amount of O<sub>2</sub> which could be theoretically consumed (noted ThO<sub>2</sub>). This parameter corresponding to the whole biodegradation of the sample is calculated by the following equation:

$$\text{ThO}_2 = (44/12) Q_r \cdot m \cdot X_c \quad (\text{in moles})$$

where Q<sub>r</sub> is the theoretical respirometric parameter considered as fixed to 0.7, X<sub>c</sub> is the average carbon in the material considered (%), and m is the mass of the studied sample in g. Hence, a mineralization level T<sub>min</sub> could be determined as the ratio of the measured O<sub>2</sub> consumed and the theoretical consumption value. The calculation is done according to the following equation:

$$T_{\min} = \frac{n}{\text{ThO}_2} \times 100 \quad (\text{in \%})$$

where n is the number of consumed moles.

## Chapter 3 : Results and discussions

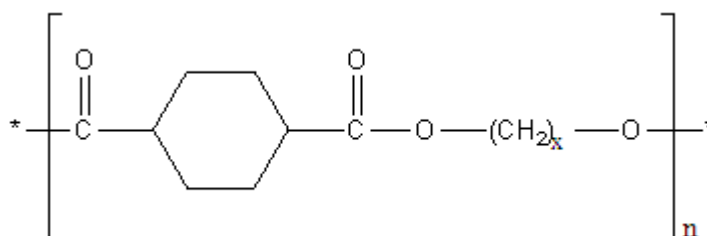
### 3.1. Eco-Friendly Aliphatic Polyesters Containing 1,4-Cyclohexane Dicarboxylate Units

#### 3.1.1. Introduction

Aliphatic polyesters containing 1,4-cyclohexane dicarboxylate unit are very interesting materials: they are potentially biobased (Berti, 2010) and biodegradable (Berti, 2009) ,and their properties can be easily modified by changing the cis/trans ratio in the aliphatic ring.

In this research we have synthesized a new series of polyesters, characterized by the presence of the 1,4-cyclohexane dicarboxylate unit and various length of the methylene sequences by using different diols (Scheme 3.1). Five diols have been used as monomers for polymer synthesis, starting from 1,2-ethanediol to 1,8-octanediol. In order to compare the effect of the chain length on the final properties. Moreover two trans contents of the cyclohexylene units have been tested (100% trans and 50% trans).

**Schema 3.1** General formula of PXCHD, where x can be equal to 2, 3, 4, 5, 8



The solid state properties of these novel materials are investigated in order to study the relationships between chemical structure of aliphatic polyesters and final characteristics. In order to obtain a more complete study, a comparison of these aliphatic polymers with some of their aromatic counterparts (PET, PTT and PBT) has been conducted.

#### 3.1.2. Synthesis

The polyesters were synthesised in a two-stage process starting from DMCD and one of the following diols: 1,2-ethanediol, 1,3-propanediol, 1,4-butanediol, 1,5-pentanediol, 1,8-octanediol. The final percentages of trans isomer in the 1,4-cyclohexane dicarboxylate units (90 and 50%) were obtained by starting from a convenient mixture of the two DMCD monomers, characterized by 22

and 100% of trans isomer. Indeed, previous studies indicated that isomerization reactions do not occur or are very limited during the synthesis mainly by starting from the diester (Colonna, 2011).

The synthesis of the polymer derived from 1,3-propanediol is here described.

DMCD 100% trans (26.15 g, 0.131 mol), DMCD 22% trans (3.85 g, 0.019 mol), 1,3-propanediol (15.96 g, 0.210 mol), and TBT (0.04 g, 0.12 mmol) were placed into a round-bottomed wide-neck glass reactor (250 ml capacity). The reactor was closed with a three-neck flat flange lid equipped with a mechanical stirrer and a torque meter which gives an indication of the viscosity of the reaction melt. The reactor was immersed into a salt bath preheated to 200°C. The first stage was conducted at atmospheric pressure under nitrogen atmosphere and the mixture was allowed to react during 120 minutes under stirring with continuous removal of methanol. The second stage was started to gradually decreasing the pressure to 0.4 mbar while the temperature was raised to the final temperature of 220°C. These conditions were reached within 60 minutes, using a linear gradient of temperature and pressure, and maintained during 180minutes.

The same synthesis conditions were used with 1,5-pentanediol. The synthesis of the polymer derived from 1,4-butanediol is reported in literature (Berti, 2008 A). Using 1,2-ethanediol and 1,8-octanediol the same protocol is followed but in the second stage, the temperature is raised to 250°C.

The polymers are named PXCHD<sub>zz</sub> where X is the number of carbon atoms in the diol and zz is the theoretical trans % of the cycloaliphatic units in the polymers.

The synthesized samples are described in Table 3.1, where their molecular characteristics are reported:

**Table 3.1 Molecular characteristics of the samples**

Sample	<i>trans</i> % of the ring in the polymer <sup>a</sup>	$M_w \times 10^{-3}$ <sup>b</sup>	$M_w/M_n$ <sup>b</sup>
P2CHD <sub>90</sub>	87	85.6	2.5
P3CHD <sub>90</sub>	87	65.6	2.5
P4CHD <sub>90</sub>	91	54.9	2.3
P5CHD <sub>90</sub>	87	72.8	2.2
P8CHD <sub>90</sub>	88	50.7	2.3
P2CHD <sub>50</sub>	53	90.5	2.1
P3CHD <sub>50</sub>	53	62.4	2.4
P4CHD <sub>50</sub>	52	88.6	2.8
P5CHD <sub>50</sub>	49	52.4	2.0
P8CHD <sub>50</sub>	56	91.1	2.6

<sup>a</sup> Calculated by <sup>1</sup>H NMR. <sup>b</sup> Measured by GPC in CHCl<sub>3</sub>.

### 3.1.3. Molecular characterization

Figure 3.1 shows the  $^1\text{H}$  NMR spectra of P8CHD with the proton assignments, as example of the new polymers. For all the samples the spectra were found to be consistent with the expected structures. It is possible to observe the two distinct peaks assigned to the protons in cis and trans configurations, centred at 2.5 and 2.3 ppm, respectively. The ratio of the area of these signals has been used to calculate the trans percentages reported in Table 3.1.

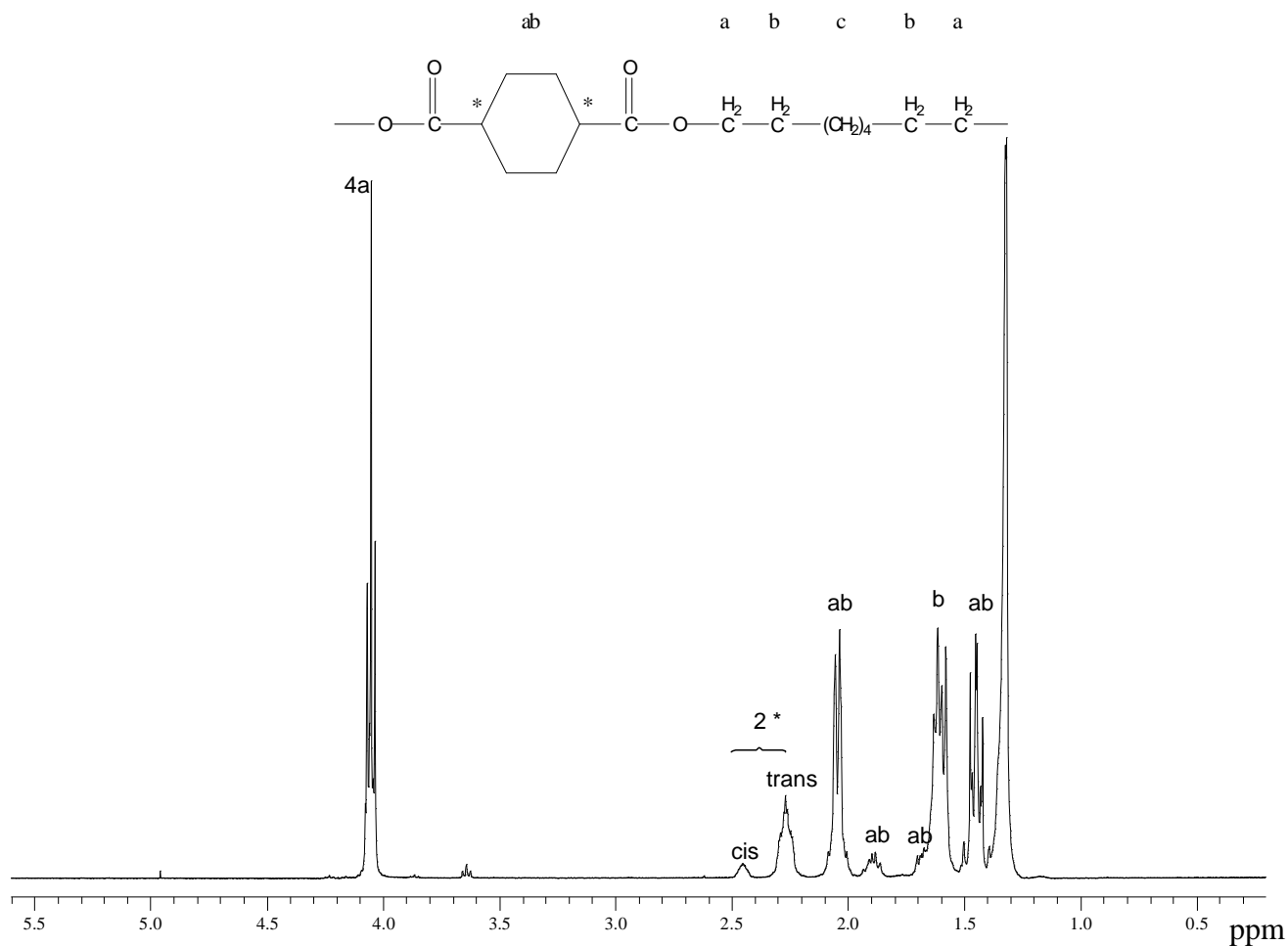


Figure 3.1  $^1\text{H}$  NMR spectrum of P8CHD<sub>90</sub>

The syntheses of the PXCHD samples have been planned in order to prepare two series of samples, characterized by trans percentages of the 1,4-cyclohexylene units equal to 90 and 50 mol%, respectively. From the data of Table 3.1 it is noteworthy that the PXCHD samples are characterized by a trans content very close to that expected. Indeed, it is around 90% and 50 mol% .

Generally the synthesis of the polyesters containing the 1,4-cyclohexylene moieties is not characterized by the presence of isomerisation reactions, if the monomer is the diester (DMCD). Indeed, isomerisation reactions occur when the syntheses are performed starting from the diacid (CHDA), because the isomerisation is catalyzed by acids. However, isomerisation processes may

take place also at high temperatures: the aliphatic C<sub>6</sub> rings tend to assume the most stable configurations and it has been reported that the thermodynamically stable cis/trans ratio in the amorphous and molten states is equal to 34/66 % (Kricheldorf, 1987). Therefore, it is justified why during the syntheses PXCHD<sub>90</sub> tends to slightly decrease its trans % and PXCHD<sub>50</sub> to slightly increase it.

The molecular weight data, calculated by GPC, show that all the samples have significantly high and similar molecular weights, that is they are suitable for comparison in terms of thermal behaviour.

### 3.1.4. TGA analysis

Table 3.2 shows the results obtained from the thermal analysis, by using TGA and DSC analyses.

**Table 3.2 Thermal analysis of all the samples**

Sample	T <sub>D</sub> <sup>a)</sup> °C	T <sub>CC</sub> <sup>b)</sup> °C	ΔH <sub>CC</sub> <sup>b)</sup> J.g <sup>-1</sup>	T <sub>g</sub> <sup>c)</sup> °C	T <sub>C</sub> <sup>c)</sup> °C	ΔH <sub>C</sub> <sup>c)</sup> J.g <sup>-1</sup>	T <sub>m</sub> <sup>c)</sup> °C	ΔH <sub>m</sub> <sup>c)</sup> J.g <sup>-1</sup>
P2CHD <sub>90</sub>	429	-	-	22	-	-	147	4
P3CHD <sub>90</sub>	400	-	-	7	80	28	140	29
P4CHD <sub>90</sub>	405	130	39	0	-	-	149-158	29
P5CHD <sub>90</sub>	404	-	-	-14 <sup>d)</sup>	-	-	42-60 <sup>d)</sup>	26 <sup>d)</sup>
P8CHD <sub>90</sub>	407	67	48	-28	-	-	99	39
P2CHD <sub>50</sub>	426	-	-	14	-	-	-	-
P3CHD <sub>50</sub>	401	-	-	-1	-	-	-	-
P4CHD <sub>50</sub>	405	-	-	-9	-	-	-	-
P5CHD <sub>50</sub>	405	-	-	-22	-	-	-	-
P8CHD <sub>50</sub>	404	-	-	-35	30	9	60	9

<sup>a)</sup>Measured by TGA (heating scan at 10°C min<sup>-1</sup>) <sup>b)</sup>Measured in DSC (cooling scan at 10°C.min<sup>-1</sup>)

<sup>c)</sup>Measured in DSC (2<sup>nd</sup> heating scan at 10°C.min<sup>-1</sup>) <sup>d)</sup>Measured in DSC (1<sup>st</sup> heating scan at 10°C.min<sup>-1</sup>).

Figure 3.2 reports the thermogravimetric curves obtained in nitrogen atmosphere for P4CHD<sub>90</sub> and other common polymers (poly(butylenes adipate), PBA; polylactic acid, PLA and poly(butylene terephthalate), PBT): the weight % is plotted versus temperature and the decrement of the weight represents the degradation process of the polymers.

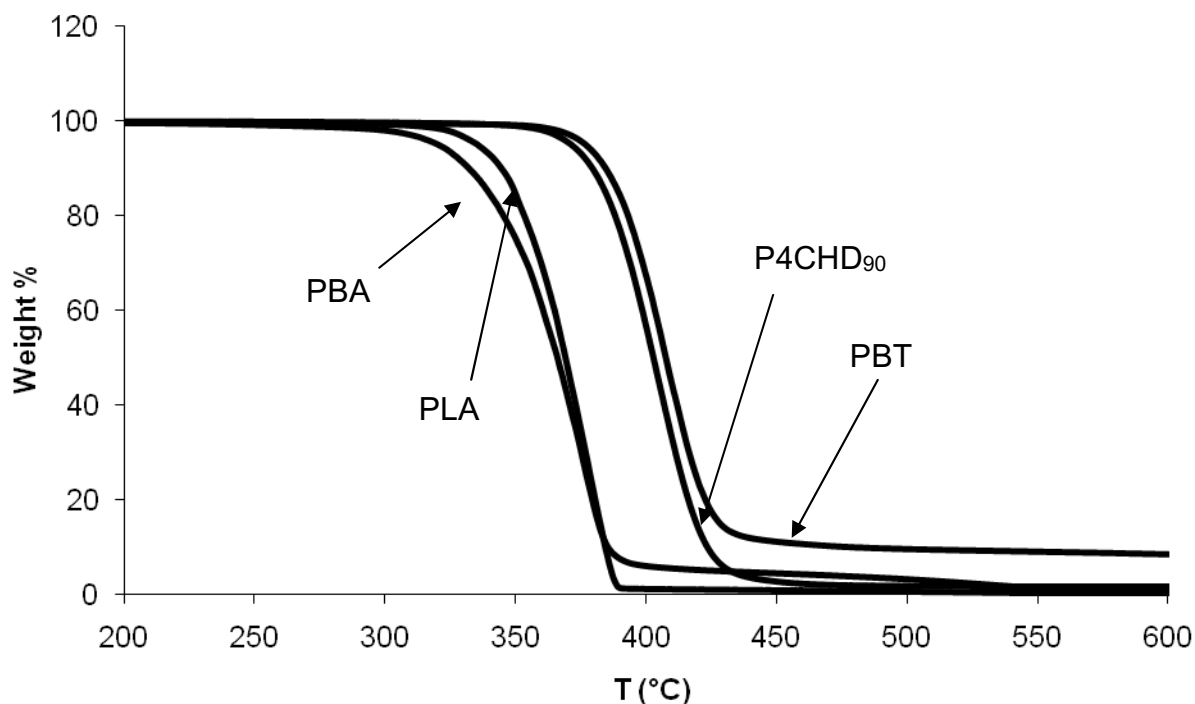


**Figure 3.2 TGA curves of P4CHD<sub>90</sub> and other commercial polymers**

For P4CHD<sub>90</sub> the degradation process begins at above 370°C and it occurs in one step, up to complete weight loss. The temperature of the maximum degradation ( $T_D$ ), reported in Table 3.2, is 435°C.

All novel polyesters are materials with high thermal stability compared to other thermoplastic aliphatic polymers and they almost approach the stability of the aromatic PBT. They all have a similar behaviour: the stereochemistry of the ring and the length of the aliphatic chains do not have an impact on the stability of the polymer.

### 3.1.5. DSC analysis

Concerning the DSC analysis, in Figure 3.3 the curves obtained during the second heating scans are shown. It is notable that the samples containing the 50 mol% of trans isomer are fully amorphous materials. This behaviour is due to the presence of a high percentage of cis isomer, which does not favour the rearrangement towards an ordered state (Berti, 2008 A).

The only exception is represented by P8CHD<sub>50</sub>, which is characterized by a small crystallization process and then melting, with low values of enthalpies (9 J/g). In this case, a longer aliphatic chain, which generally easily crystallizes (see polyethylene), improves a certain degree of reorganization with the formation of crystals.

On the other hand, the samples containing high trans percentage are semi-crystalline materials. In this case, it is interesting to compare the capability of crystallizing for different samples as a function of the length of the aliphatic chain. In particular, it is necessary to have in mind that an even-odd effect can be present: the trend of  $T_g$  and  $T_m$  versus the number  $x$  of  $-(CH_2)-$  units in the monomer can be different for samples with  $x = \text{odd}$  and samples with  $x = \text{even}$  number.

The melting temperatures of P2CHD<sub>90</sub> and P4CHD<sub>90</sub> are similar, but decrease of about 50°C by passing from P4CHD<sub>90</sub> to P8CHD<sub>90</sub>: therefore, an increment of four  $-(CH_2)-$  units in the diol is able to strongly vary the thermal behaviour of the material. Moreover, the melting enthalpy increases from 4 to 39 J/g: longer chains are able to reach a higher crystallinity. Comparing the P3CHD<sub>90</sub> and P5CHD<sub>90</sub> we can observe the same trend: the melting point decreases of almost 90°C but there is no change in melting enthalpy. It has to be underlined that P5CHD<sub>90</sub> crystallizes only in the first heating scan, i.e. it has a very low crystallization rate.

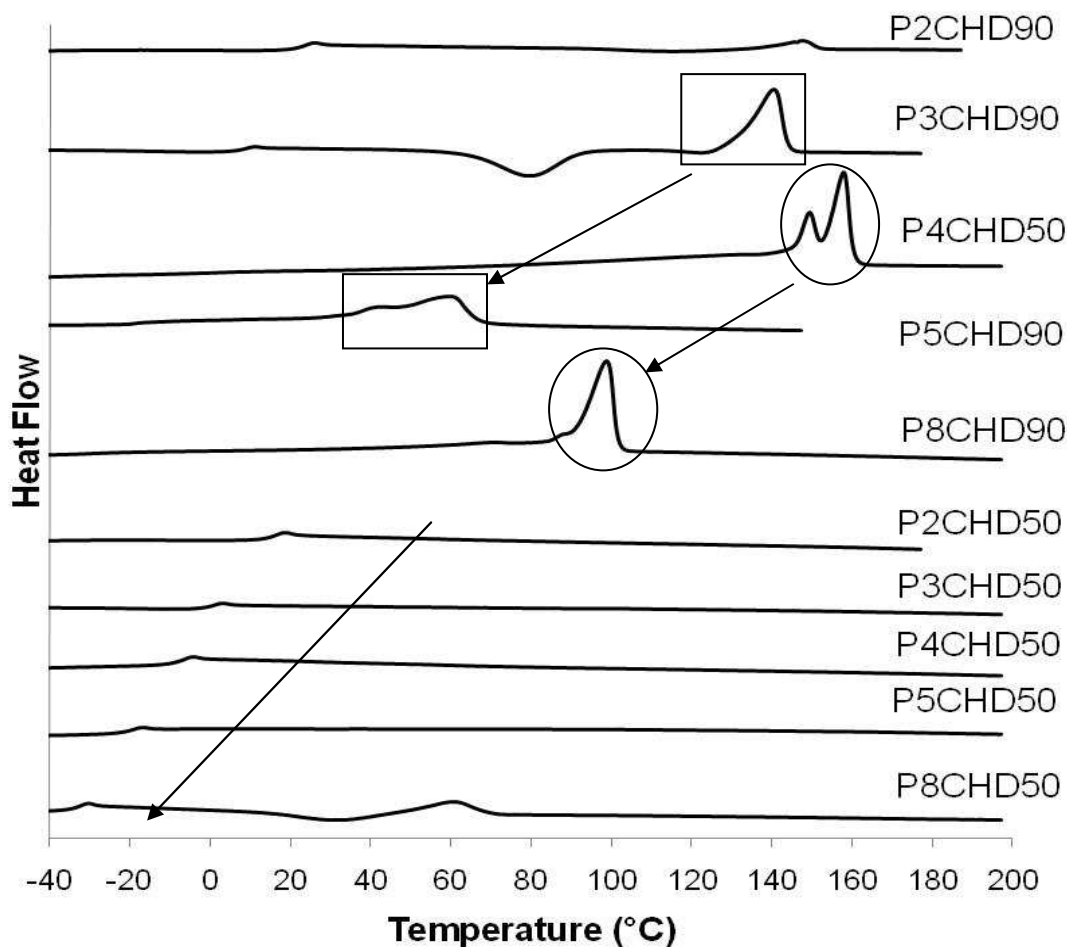


**Figure 3.3 DSC 2nd heating scan**

The comparison between these data and the thermal behaviour of PET (poly(ethylene terephthalate)) and PBT (poly(butylene terephthalate)) can be significant (PET has  $T_m = 252^\circ\text{C}$ ,  $\Delta H_m = 37 \text{ J/g}$  and PBT has  $T_m = 224^\circ\text{C}$ ,  $\Delta H_m = 43 \text{ J/g}$ ). Also for aromatic polyesters a small

increment of the length of the aliphatic chain cause an important decrement of the melting temperature.  $\Delta H_m$  are similar even if the PBT is characterized by a higher crystallization rate. Indeed, the longer aliphatic chain gives a higher flexibility to the chains and, thus, higher capability to rearrange towards an ordered state. Accordingly, the higher flexibility of the chains in PBT cause a lower Tg value with respect to PET. Similar behaviour is observed in our polyesters: both samples with 90% trans and 50% trans show a decrease in the value of Tg while increasing the length of aliphatic chain.

### 3.1.6. DMTA analysis

Figure 3.4 and 3.5 shows the DMTA spectra for all the samples with 90% trans content. For all the materials the main relaxation peak of the dissipation factor,  $\tan \delta$  (Fig. 3.5), can be attributed to the glass transition, according to the DSC data. The intensity of the peaks is proportional to the amorphous content, i.e. higher for P2CHD<sub>90</sub> sample. Correspondently to the glass transition process, the elastic modulus E' is characterized by an important decrement corresponding to a change from the rigid glassy state to the rubbery state.

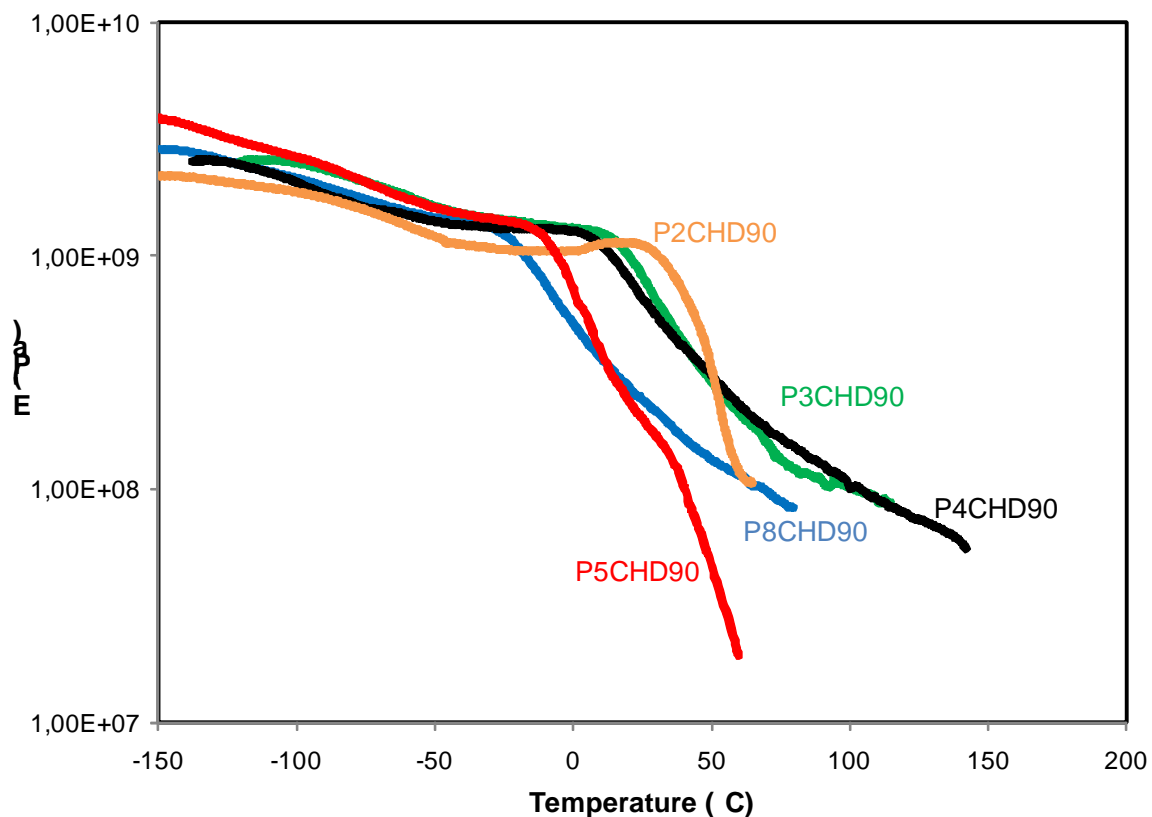


**Figure 3.4 : Elastic modulus vs Temperature for PXCHD<sub>90</sub> samples**

At temperatures lower than  $T_g$ , in the range from  $-150$  to  $0^\circ\text{C}$ , other processes are present: two relaxations for  $\text{P4CHD}_{90}$  and only one for the others. The comprehension of the nature of the chain movements which cause these processes is quite difficult. For  $\text{P4CHD}_{90}$  an interpretation has been hypothesized: the relaxation at the lowest temperature is due to the motions of the  $-(\text{CH}_2)-$ sequences, whereas the other process is due to the motions of the cycloaliphatic units (Berti, 2008 A).

In any case, it is worth remembering that the presence of secondary relaxations, due to the main chain, is beneficial for impact resistance and is often described as a phenomenon which facilitates the macroscopic shear yielding. Therefore, the incorporation of 1,4-cyclohexylene rings, which are able to originate conformational transitions, are particularly advantageous in improving the mechanical properties.

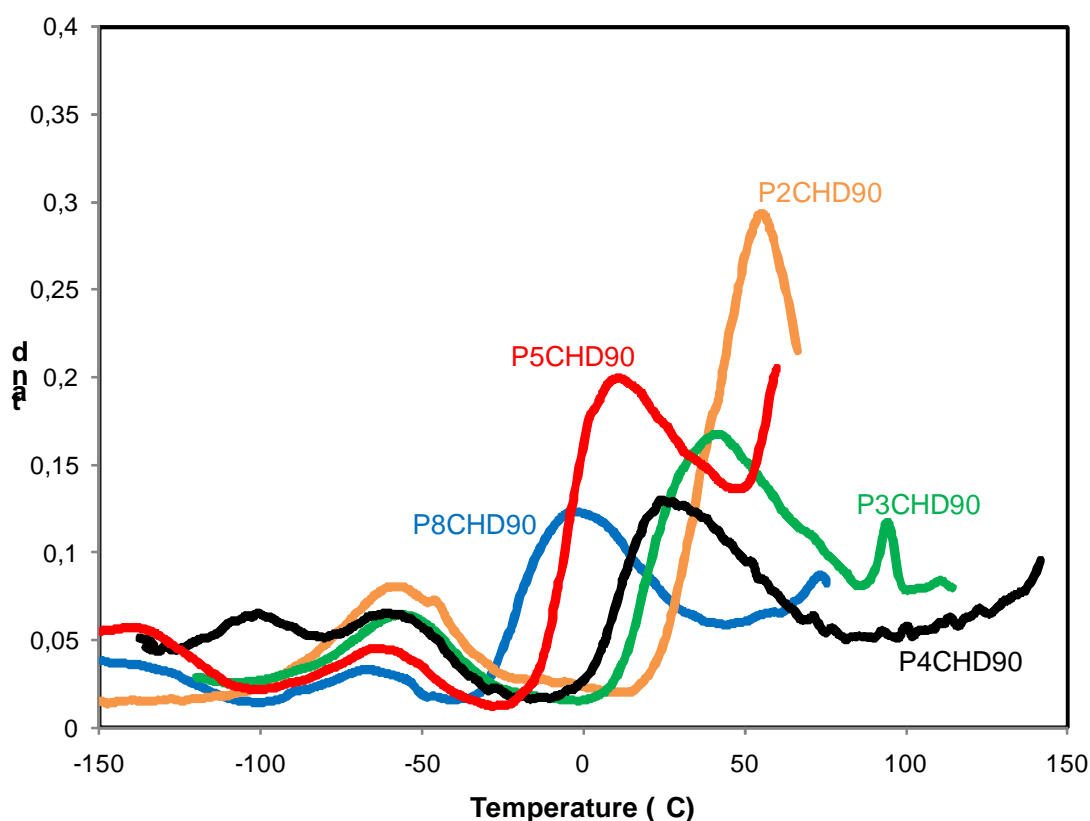


**Figure 3.5 :  $\tan\delta$  curves of  $\text{PXCHD}_{90}$  samples from DMTA analysis**

### 3.1.7. Tensile properties

Tensile tests of some of the novel polyesters have been carried out and the results compared with those of their aromatic analogues. All the data are reported in Table 3.3.

It is possible to see that, substituting the aromatic ring with the aliphatic one, the properties change dramatically: the modulus is lower in aliphatic samples, while the elongation at break

increases. In particular, P2CHD<sub>90</sub> is a material with a very high ductility, while PET, due to the presence of the aromatic ring has a very high modulus and a brittle behaviour.

In aliphatic polyesters the trans content influences the mechanical properties of the materials: the samples with a high content of trans stereoisomer have high modulus because this conformation is less flexible and more symmetrical than the cis one and the symmetrical units tend to increment chain packing and crystal perfection. On the other hand the samples with low content of trans stereoisomer are all very ductile materials with very low modulus but high elongation at break. P2CHD has a ductile behaviour even with a high percentage of trans isomer, because of its low crystallinity that permits a high elongation. All these results are in agreement with the DSC results.

**Table 3.3 Tensile test results**

Sample	Young's Modulus (Mpa)	Elongation at break, %	Stress at break (MPa)	Stress at yield (MPa)	Strain at yield %
P2CHD <sub>90</sub>	2.6±0.5	1118.3±67.7	3.3±0.5	--	--
P3CHD <sub>90</sub>	330.7±110.7	42.0±15.0	9.4±1.3	17.6±1.7	14.5±2.1
P4CHD <sub>90</sub>	464.1±47.0	344.7±48.7	25.4±2.8	28.9±2.3	28.8±0.8
P2CHD <sub>50</sub>	0.6±0.1	1284*	0.2±0.0	0.3±0.0	132.9±1.6
P3CHD <sub>50</sub>	25.8±11.8	31.3±12.5	4.3±1.6	--	--
P4CHD <sub>50</sub>	157.7±15.4	494.3±52.1	10.6±0.6	10.3±0.7	23.2±1.5
PET	1055.9±226.1	3.0±1.0	28.3±12.4	--	--
PTT	941.6±84.8	5.4±0.9	41.8±5.0	--	--
PBT	950.3±104.2	271.9±70.7	37.6±2.5	48.3±1.5	15.0±1.1

\* no breakage

### 3.1.8. Conclusions

Novel polyesters have been successfully prepared by using DMCD and different aliphatic diols as monomers. The new materials are interesting because potentially derived from natural resources and potentially biodegradable (Berti, 2010). Moreover their properties can be modified by varying the cis/trans ratio of the 1,4-cyclohexylene unit and the length of the -CH<sub>2</sub>- sequences in the diol. Interesting correlations between chemical structure and properties have been obtained.

All the thermal transitions (T<sub>g</sub>, T<sub>cc</sub>, and T<sub>m</sub>) can be varied by changing the repeating units derived from diols.

A very wide range of mechanical properties going from ductile materials to high modulus materials can be achieved.

## 3.2. Eco-Friendly Aliphatic Copolyesters Containing 1,4-Cyclohexane Dicarboxylate Units

Part of this research has already been published: Berti, A. Celli, P. Marchese, E. Marianucci, S. Sullalti, G. Barbiroli, “Environmentally Friendly Copolyesters Containing 1,4-Cyclohexane Dicarboxylate Units, 1-Relationship Between Chemical Structure and Thermal Properties”, *Macromol. Chem. Phys.*, **2010**, 211, 1559-1571

### 3.2.1. Introduction

Copolymerization is a simple and economic way to modify the physical properties and to extend the application field of aliphatic polyesters (Yang, 2009). Nowadays this approach can be very helpful in developing novel biomaterials.

Recently, in literature, a modification of a poly(alkylene dicarboxylate), the poly(butylene dodecanoate) (4-12), by copolymerization and introduction of a fully aliphatic unit, containing the 1,4-cyclohexane dicarboxylate group has been proposed (Berti, 2009). The presence of an aliphatic ring enables the material to have good thermal and mechanical properties and to maintain the biodegradation rate. Since these results were highly significant we considered to study more in depth this family of novel copolymers, especially in terms of their physical properties which can be easily modulated by changing the chemical structure.

In this section the properties of the (x-y)-*co*-PBCHD copolymers are discussed, mainly for some novel materials derived from poly(butylene adipate) (4-6) and PBCHD: the copolymers derived from adipic ester and 1,4-butanediol are really interesting because of the easy availability and low cost of the monomers.

### 3.2.2. Synthesis

The synthesis of the 4-12 homopolymer is described in literature (Barbiroli, 2003) and the synthesis of the 4-6 homopolymer is analogous, with the substitution of 1,12-dodecanedioic acid (DA) with dimethyl adipate (DMA).

The PBCHD samples used in the present work are described by Berti et al. (Berti, 2008 A). PBCHD samples are indicated with the code PBCHD<sub>zz</sub>, where zz indicates the theoretical trans % of the cycloaliphatic units in the polymers. The real trans percentages are shown in Table 3.4, together with other molecular characteristics of the samples.

**Table 3.4 Molecular characteristics of the samples**

Sample	(4-y)/PBCHD molar ratio <sup>a</sup>	<i>trans</i> % of the ring in the polymer <sup>a</sup>	$M_w \times 10^{-3}$ <sup>b</sup>	$M_w/M_n$ <sup>b</sup>
4-6	-	-	90.0	2.5
4-12	-	-	78.6	2.5
PBCHD <sub>100</sub>	-	100	73.4	2.5
PBCHD <sub>90</sub>	-	91	54.9	2.3
PBCHD <sub>70</sub>	-	72	77.6	2.3
PBCHD <sub>50</sub>	-	52	88.6	2.8
(4-6)- <i>co</i> -PBCHD <sub>100</sub> -70/30	64/36	100	95.4	2.1
(4-6)- <i>co</i> -PBCHD <sub>100</sub> -50/50	47/53	100	73.6	2.3
(4-6)- <i>co</i> -PBCHD <sub>100</sub> -30/70	24/76	100	97.4	2.2
(4-6)- <i>co</i> -PBCHD <sub>90</sub> -70/30	65/35	88	84.9	2.0
(4-6)- <i>co</i> -PBCHD <sub>90</sub> -50/50	47/53	87	87.8	2.2
(4-6)- <i>co</i> -PBCHD <sub>90</sub> -30/70	24/76	90	99.4	2.4
(4-6)- <i>co</i> -PBCHD <sub>70</sub> -70/30	65/35	70	86.3	2.0
(4-6)- <i>co</i> -PBCHD <sub>70</sub> -50/50	47/53	68	88.5	2.3
(4-6)- <i>co</i> -PBCHD <sub>70</sub> -30/70	24/76	72	95.3	2.4
(4-6)- <i>co</i> -PBCHD <sub>50</sub> -70/30	65/35	53	76.4	2.1
(4-6)- <i>co</i> -PBCHD <sub>50</sub> -50/50	46/54	56	65.1	2.1
(4-6)- <i>co</i> -PBCHD <sub>50</sub> -30/70	24/76	56	128.3	2.2
(4-12)- <i>co</i> -PBCHD <sub>90</sub> -70/30	74/26	92	122.6	2.2
(4-12)- <i>co</i> -PBCHD <sub>90</sub> -50/50	53/47	92	82.5	2.2
(4-12)- <i>co</i> -PBCHD <sub>90</sub> -30/70	31/69	92	78.0	2.4

<sup>a</sup> Calculated by <sup>1</sup>H NMR. <sup>b</sup> Measured by GPC in CHCl<sub>3</sub>.

The copolymers derived from BD, DMA, and DMCD are named (4-6)-*co*-PBCHD<sub>zz</sub>-a/b, where a/b is the feed molar ratio of the DMA/DMCD. Their synthesis is here described, in particular for the (4-6)-*co*-PBCHD<sub>90</sub>-50/50 sample.

DMA ( 16.20 g, 0.093 mol), DMCD 100% *trans* ( 16.22 g, 0.081 mol), DMCD 22% *trans* ( 2.40 g, 0.012 mol), BD ( 20.12 g, 0.223 mol), TBT ( 0.02 g, 0.047 mmol) were placed into a round bottom wide-neck glass reactor (250 ml capacity). The reactor was closed with a three-necked flat flange lid equipped with a mechanical stirrer and a torque meter which gives an indication of the viscosity of the reaction melt. The reactor was immersed into a salt bath preheated to 200°C. The first stage was conducted at atmospheric pressure under nitrogen atmosphere and the mixture was allowed to react for 90 min under stirring with continuous removal of water. The second stage was started by gradually reducing the pressure to 0.2 mbar while the temperature was raised to the final value of 220°C. These conditions were reached within 90 min, using a linear gradient of temperature and pressure, and maintained for 120 min.

The feed DMA/DMCD molar ratios used are 30/70, 50/50, and 70/30 in order to obtain copolyesters with different compositions. The final molar composition of the copolymers is reported in Table 3.4.

The synthesis of the copolymers derived from BD, DA, and CHDA is described in literature (Berti, 2009) and here they are named (4-12)-*co*-PBCHD<sub>zz</sub>-*c/d*, where *c/d* is the feed molar ratio of DA/CHDA. Also in this case the final molar composition of the copolymers is reported in Table 3.4.

For (4-6)-*co*-PBCHD, samples with four different *trans* % of the PBCHD units have been prepared (100, 90, 70 and 50 mol%) by starting from a suitable amount of the 100 mol% and 22 mol% of DMCD. For (4-12)-*co*-PBCHD only samples with 90 mol% *trans* have been considered.

### 3.2.3. Molecular characterization of (x-y)-*co*-PBCHD copolyesters

The chemical structure was analyzed by <sup>1</sup>H NMR spectroscopy. As an example, Figure 3.6 depicts the <sup>1</sup>H NMR spectrum for (4-6)-*co*-PBCHD<sub>90-50/50</sub> copolymer and the signal assignments have been highlighted. For all the samples the spectra confirm the expected structures.

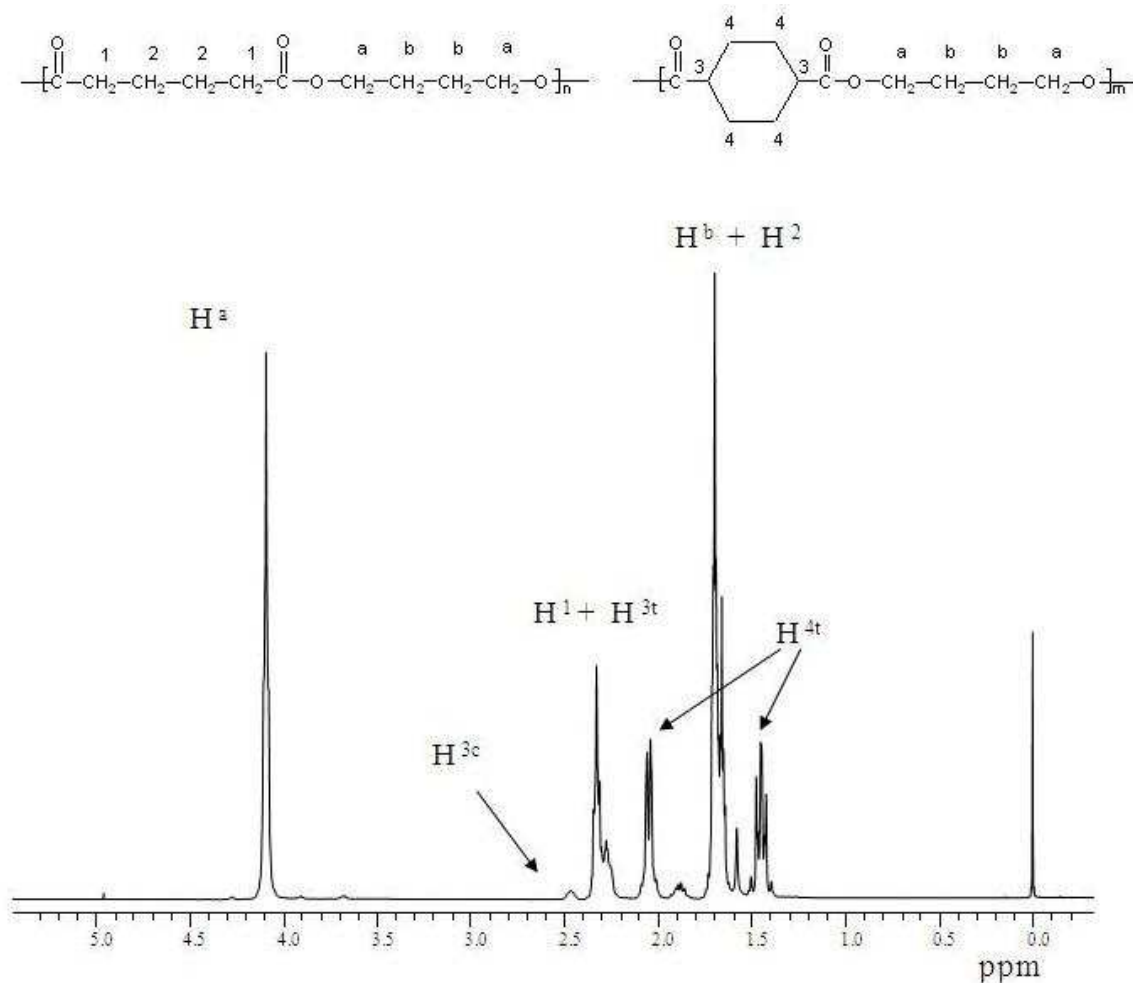


Figure 3.6 <sup>1</sup>H NMR spectrum of (4-6)-*co*-PBCHD<sub>90-50/50</sub> copolymer

The composition of the copolyesters was calculated by considering four different signals: 1) at 1.45 and 2.05 ppm, due to the eight  $H^{4t}$  protons in trans configuration of the DMCD; 2) at 2.28 and 2.33 ppm, due to the protons of the cycloaliphatic ring in trans configuration ( $H^{3t}$ ) and to the protons of DMA in  $\alpha$  position with respect to the carbonyl group ( $H^1$ ); 3) at 2.44 ppm due to the protons of the cycloaliphatic ring in cis configuration ( $H^{3c}$ ). In particular, from the addition of the area of the signals at 1.45 and 2.05 ppm the contribution of a single proton in trans configuration of DMCD has been evaluated; this value was then used to calculate the contribution of a single proton of DMA ( $H^1$ ) by using the signals at 2.28 and 2.33 ppm. From the ratio of the contributions of the protons in DMA and in (cis + trans) DMCD the molar composition has been obtained. The resulting data are reported in Table 3.4. Since the (4-12)-*co*-PBCHD series were already synthesized materials the calculation have already been made in literature (Berti, 2009).

As a result, the copolyesters differentiate for molar composition and for trans mol-% of the PBCHD units. In particular, the trans content varies from 50 to 100 mol%, as in the case of the corresponding homopolymers. As for the (4-12)-*co*-PBCHD samples, also in this case it was not possible to evaluate the degree of randomness and the average length of the sequences from the  $^1H$  NMR analysis. However, since we observed no differences in the reactivity of BD with respect to the two esters during the synthesis of the two homopolymers (4-6 and PBCHD), we hypothesize that the copolyesters have a random distribution of the sequences along the chain, as already demonstrated for aliphatic-aromatic (4-12)-*co*-PBT samples (Berti, 2008 C).

The molecular weights of all the samples are very high.

### 3.2.4. TGA analysis

Figure 3.7 shows the thermogravimetric curves of some samples and Table 3.5 reports the temperature of the maximum degradation rate ( $T_D$ ) of all the specimens, measured under nitrogen atmosphere by TGA.

**Table 3.5 Thermal results of all the samples**

Sample	$T_D^a$ (°C)	$T_{CC}^b$ (°C)	$T_g^c$ (°C)	$\Delta H_{CC}^b$ (J g <sup>-1</sup> )	$T_c^c$ (°C)	$\Delta H_c^c$ (J g <sup>-1</sup> )	$T_m^c$ (°C)	$\Delta H_m^c$ (J g <sup>-1</sup> )
4-6	376	32	-58	67	-	-	52 and 57	70
4-12	425	53	-	90	-	-	75	89
PBCHD <sub>100</sub>	421	149	10	48	-	-	165 and 171	49
PBCHD <sub>90</sub>	421	130	5	44	-	-	150 and 158	40
PBCHD <sub>70</sub>	418	79	-2	34	-	-	122	32
PBCHD <sub>50</sub>	421	-	-7	-	-	-	-	-
(4-6)- <i>co</i> -PBCHD <sub>100</sub> -70/30	428	14	-49	28	-	-	53	24
(4-6)- <i>co</i> -PBCHD <sub>100</sub> -50/50	440	66	-43	33	-	-	94	32
(4-6)- <i>co</i> -PBCHD <sub>100</sub> -30/70	437	97	-23	41	-	-	125 and 134	40

(4-6)- <i>co</i> -PBCHD <sub>90-70/30</sub>	428	2	-49	30	-	-	43	27
(4-6)- <i>co</i> -PBCHD <sub>90-50/50</sub>	457	41	-40	25	-	-	80	26
(4-6)- <i>co</i> -PBCHD <sub>90-30/70</sub>	444	74	-25	29	-	-	119	27
(4-6)- <i>co</i> -PBCHD <sub>70-70/30</sub>	389	-20	-50	4	-9	19	30	23
(4-6)- <i>co</i> -PBCHD <sub>70-50/50</sub>	441	-	-40	-	19	14	56	16
(4-6)- <i>co</i> -PBCHD <sub>70-30/70</sub>	444	27	-25	16	21	5	86	22
(4-6)- <i>co</i> -PBCHD <sub>50-70/30</sub>	393	-	-52	-	-2	5	18	6
(4-6)- <i>co</i> -PBCHD <sub>50-50/50</sub>	426	-	-41	-	-	-	-	-
(4-6)- <i>co</i> -PBCHD <sub>50-30/70</sub>	427	-	-26	-	-	-	-	-
(4-12)- <i>co</i> -PBCHD <sub>90-70/30</sub>	424	34	-44	52	-	-	55	51
(4-12)- <i>co</i> -PBCHD <sub>90-50/50</sub>	421	38	-42	33	-	-	40 and 73	40
(4-12)- <i>co</i> -PBCHD <sub>90-30/70</sub>	422	84	-39	37	-	-	112	37

<sup>a</sup> Measured by TGA (heating scan at 10°C/min), <sup>b</sup> Measured by DSC (cooling scan at 10°C/min),  
<sup>c</sup> Measured by DSC (2<sup>nd</sup> heating scan at 10°C/min)

It is interesting to observe that the stability of PBCHD is slightly higher than the one of PBT. This result indicates that the substitution of the aromatic ring with an aliphatic ring could improve the thermal stability of the materials.

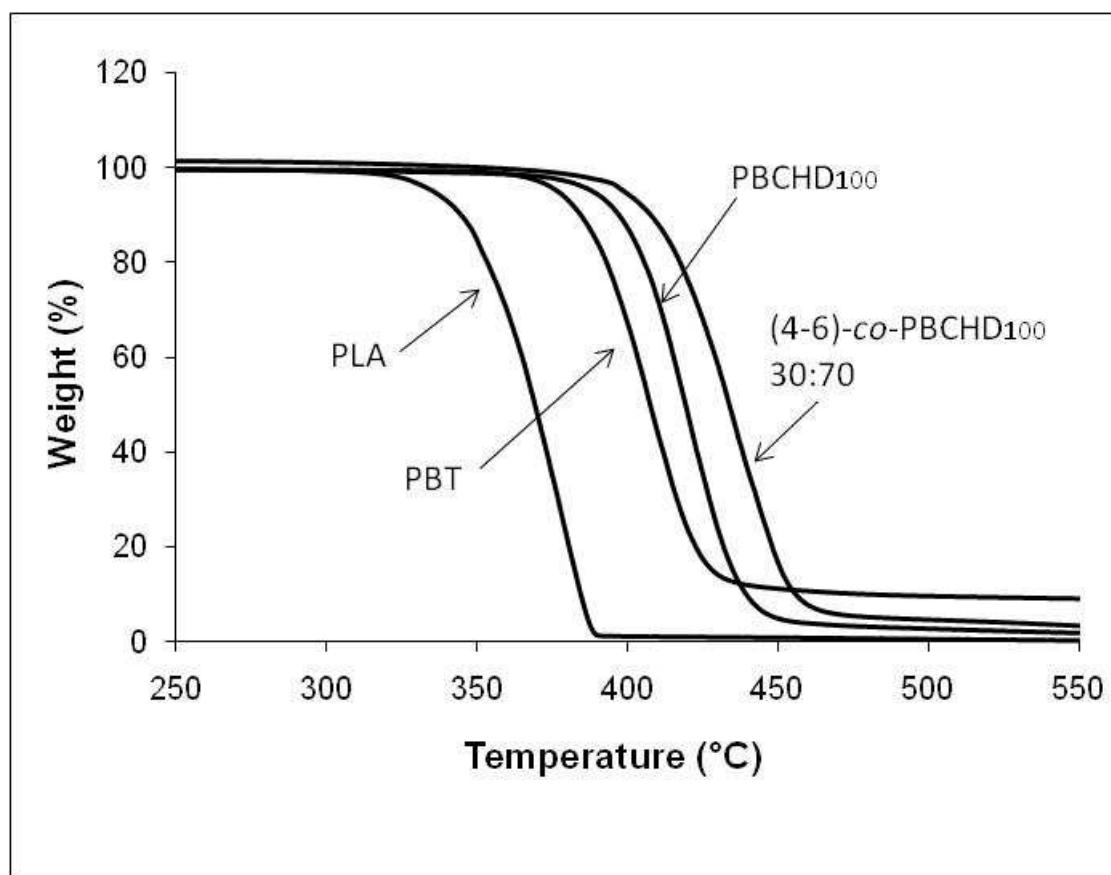


**Figure 3.7 TGA curves in nitrogen atmosphere of PBCHD<sub>100</sub>, (4-6)-*co*-PBCHD<sub>100-30/70</sub>, and a commercial PBT.**

(4-6)-*co*-PBCHD copolymers, like the (4-12)-*co*-PBCHD samples, are characterized by a slightly higher thermal stability than the PBCHD, as evident in Figure 3.7 for the (4-6)-*co*-PBCHD<sub>100-30/70</sub> specimen. Other aliphatic polyesters, instead, have lower thermal stability. Polylactic acid (PLA),

for example, begins to lose weight at about 300°C and shows a degradation curve shifted at lower temperatures. Poly(R)-3-hydroxybutyrate (PHB) begins to lose weight at about 250°C and a similar behavior is typical of poly-ε-caprolactone too (Aoyagi, 2002; Scandola, 1990).

These results are significant considering that the thermal stability is an important property for possible future applications of the novel materials.

### 3.2.5. DSC analysis

#### *Effect of the molar composition of copolyesters*

In order to underline the effect of the molar composition on the properties of the copolymers we focus mainly on the (4-6)-*co*-PBCHD<sub>90</sub> series. Figure 3.8 shows the crystallization curves (curves a) and the 2<sup>nd</sup> heating scans (curves b) of these copolymers with different composition. From curves a) it is evident that the two homopolymers, particularly the 4-6, have very narrow and intense exothermic peaks.

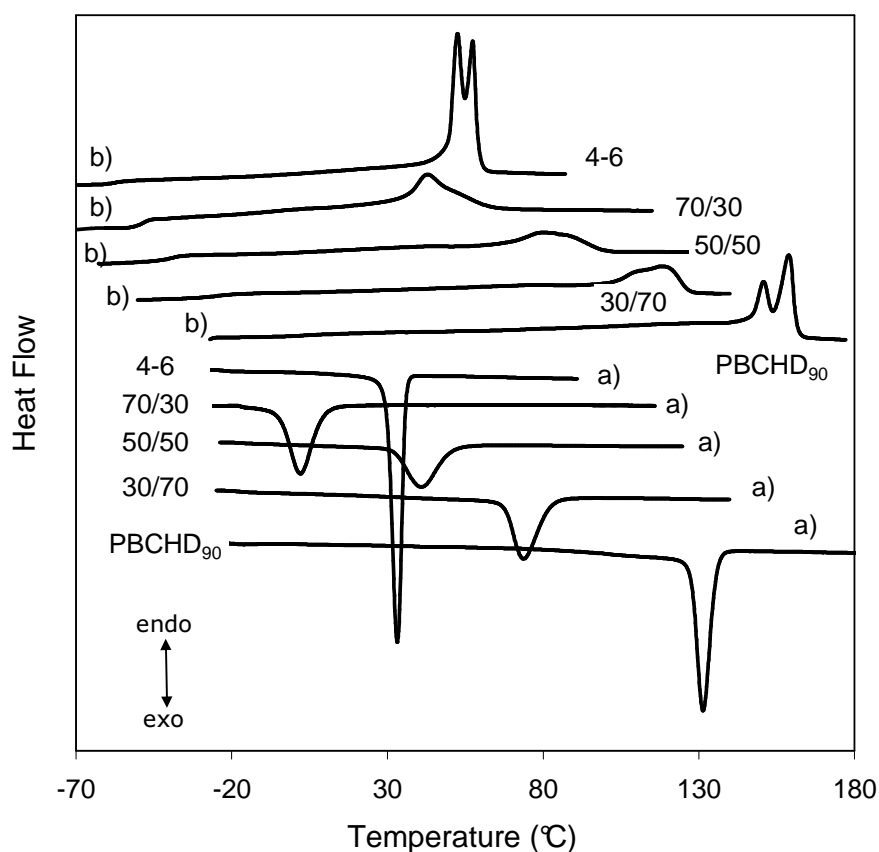


**Figure 3.8 DSC curves of the cooling scan (a) and the second heating scan (b) for (4-6)-*co*-PBCHD<sub>90</sub> samples.**

For PBCHD<sub>90</sub> the high percentage of the trans isomer of the 1,4-cyclohexylene units allows the polymer to crystallize and to reach a relatively high level of crystallinity. The copolymers show the

ability to crystallize too, although a continuous decrement in crystallization temperature with the decrement of the PBCHD unit content is evident. Also the crystallization enthalpy tends to be reduced with respect to the homopolymers, as reported in Table 3.5.

Both 4-6 and PBCHD<sub>90</sub> samples show complex melting peaks, which generally are discussed in terms of melting-recrystallization-remelting processes (Berti, 2008 A; Celli, 2007, Gan, 2004). On the other hand, the copolymers show broader melting processes, with lower intensities, compared to the homopolymers. The melting temperatures of copolymers increase in a continuous way from 4-6 to PBCHD, with the increment of the PBCHD unit content.

To better understand the crystallization and melting behavior of the copolymers, Figure 3.9 shows the WAXD spectra performed at room temperature. 4-6 shows the X-ray profile typical of the crystalline  $\alpha$ -form, which is the thermodynamically most stable phase of the polymer (Gan, 2004; Pan, 2009). This is in agreement with the fact that  $\alpha$ -form shows a double melting peak due to a fusion-recrystallization process. For PBCHD four main diffraction peaks may be seen.

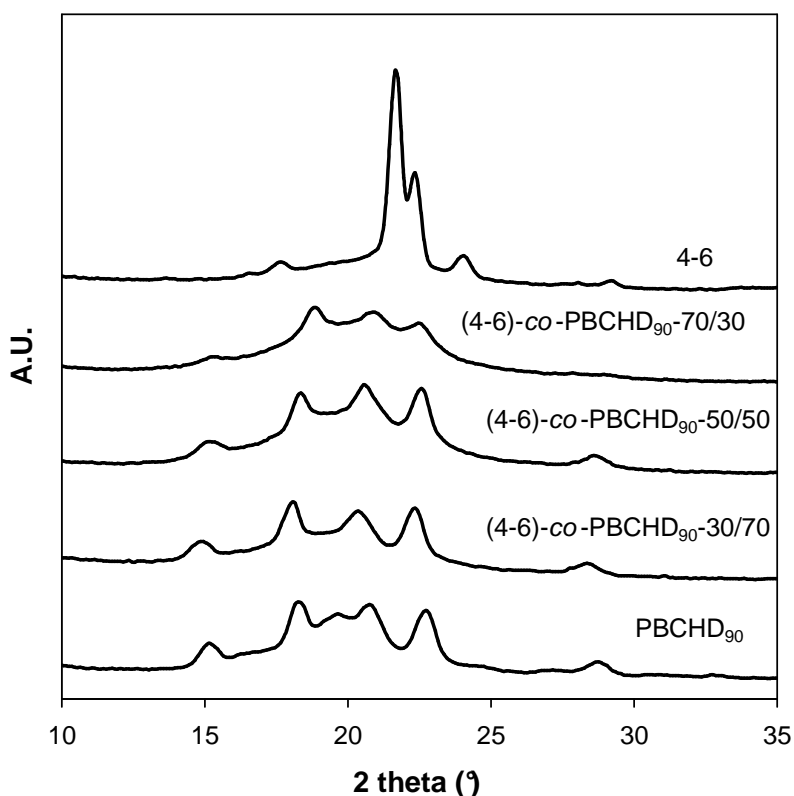


**Figure 3.9** X-ray diffraction patterns of (4-6)-co-PBCHD<sub>90</sub> samples.

WAXD patterns appear to be characterized by relatively intense diffraction peaks over the whole compositional range, confirming the presence of a crystalline phase for all the (4-6)-co-PBCHD samples. On the basis of the profile shapes, it can be deduced that all the materials (70/30, 50/50, and 30/70 copolymers) are characterized by the presence of the PBCHD crystalline phase.

Anyway, in order to verify the possible presence of the 4-6 crystalline phase in copolymers, the enthalpies of crystallization have been evaluated: indeed, they are more significant than the enthalpies of melting, because the crystallization does not show multiple, broad processes. The  $\Delta H_{CC}$  data, normalized with respect to the PBCHD content, are quite in agreement with the  $\Delta H_{CC}$  experimental values for the 30/70 and 50/50 copolymers. This is an indication that probably for these compositions the only crystalline phase present is that of PBCHD units. For 70/30 sample, instead, the  $\Delta H_{CC}$  value, normalized with respect to the PBCHD content, is about 15 J/g, significantly lower than the value of 30 J/g reported in Table 3.5. Therefore, although the X-ray spectrum does not give a clear indication, for 70/30 copolymer the presence of 4-6 crystals cannot be excluded, even if the PBCHD crystals are dominant.

In any case, it is clear that in copolymers the crystallization of 4-6 units is hindered. This behavior can be justified by considering the low crystallization rate of poly(alkylene dicarboxylate)s characterized by short aliphatic sequences (Celli, 2007). During the cooling from the melt, the competition between crystallization rates of PBCHD and 4-6 crystals favors the growth of the PBCHD crystalline phase, which is more or less perfect, depending on the copolymer composition. The PBCHD crystals dominate in the whole range of compositions and, thus, the 4-6 units tend to remain in the amorphous state.

On the other hand, by considering the series of (4-6)-*co*-PBCHD<sub>50</sub> copolyesters, the PBCHD phase cannot crystallize, due to its trans content being too low (Berti, 2008 A). Indeed, the PBCHD<sub>50</sub> homopolymer is a fully amorphous material. As reported in Table 3.4, (4-6)-*co*-PBCHD<sub>50</sub>-30/70 and (4-6)-*co*-PBCHD<sub>50</sub>-50/50 do not show any crystallization and melting process, indicating that the 4-6 sequences are not long enough to favor the crystallization process and the PBCHD units act as defects and strongly inhibit the formation of the 4-6 crystalline phase. The (4-6)-*co*-PBCHD<sub>50</sub>-70/30, instead, shows an exothermic phenomenon at about -2°C and a melting process at 18°C with a  $\Delta H_m = 6 \text{ J g}^{-1}$ , during the 2<sup>nd</sup> heating scan. In this case, the 4-6 sequences can form a crystal phase, but the degree of crystallinity reached is really low. Therefore, it is confirmed that in copolyesters the presence of rigid PBCHD units makes the crystallization of 4-6 units extremely difficult.

As regards the non-crystalline phase, in all the copolymer series only a single glass transition process is observed, indicating the presence of a single, homogeneous amorphous phase. The  $T_g$  values, reported in Table 3.4, tend to increase with the increment of the PBCHD units, accordingly to the fact that the cycloaliphatic ring has a more rigid structure than the -(CH<sub>2</sub>)- sequences.

### Effect of the $-(CH_2)-$ sequence length

To understand the effect of the length of the aliphatic chain in the poly(alkylene dicarboxylate) moieties on the thermal behavior, (4-6)-*co*-PBCHD<sub>90</sub> and (4-12)-*co*-PBCHD<sub>90</sub> copolymers are compared. Figure 3.10 collects some DSC curves obtained during the cooling from the melt for the two series of copolymers and parent homopolymers. This figure highlights that the crystallization process is present in all the samples, but with some important differences.

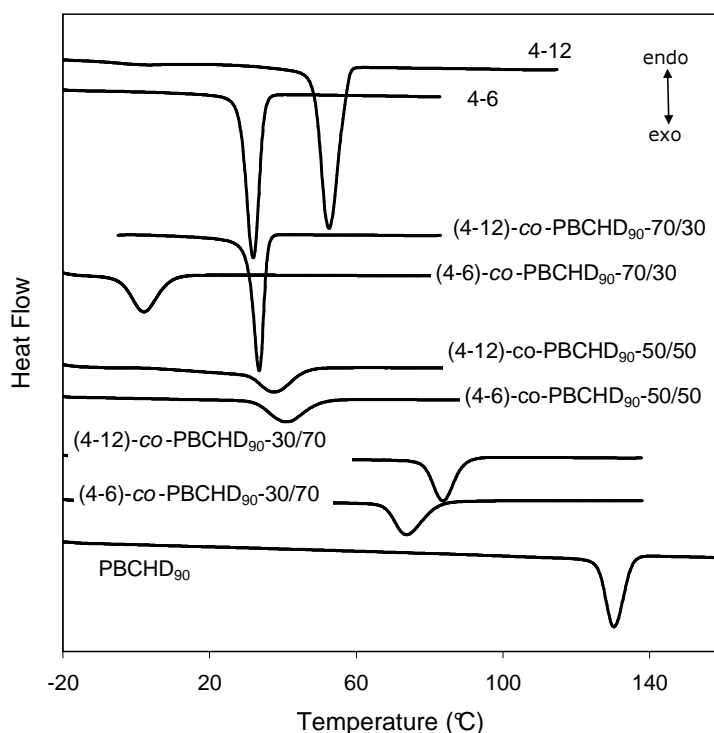


**Figure 3.10** DSC curves of the cooling scan for (4-6) and (4-12)-*co*-PBCHD<sub>90</sub> samples.

Firstly, both 4-6 and 4-12 homopolymers have very intense and sharp crystallization peaks, although the crystallization enthalpies are much higher in 4-12 than in 4-6 ( $\Delta H_{CC} = 90$  and  $67 \text{ J g}^{-1}$ , respectively): this behavior can be attributed to the higher flexibility of the 4-12 than 4-6 units, which promotes the crystallizability of the samples.

In 70/30 copolyesters, the exothermic peaks differentiate considerably as regards the shape of the peak, temperature and intensity. Indeed, in (4-12)-*co*-PBCHD<sub>90</sub>-70/30 sample the crystallization process maintains the characteristics observed for 4-12 homopolymer, i.e. narrow and intense peak, even if the  $T_{CC}$  is  $20^\circ\text{C}$  lower. In (4-6)-*co*-PBCHD<sub>90</sub>-70/30, instead, the crystallization peak is broad and with low intensity.

This difference is not evident for the other copolymer compositions. For the other samples, indeed, the aliphatic chain length does not affect the shape of the calorimetric curves to any great degree and influences only the  $T_{cc}$  values, according to the copolymer composition.

Correspondingly, the melting processes, shown in Figure 3.11 for the two copolymer series, highlights the different behavior of the 70/30 samples.

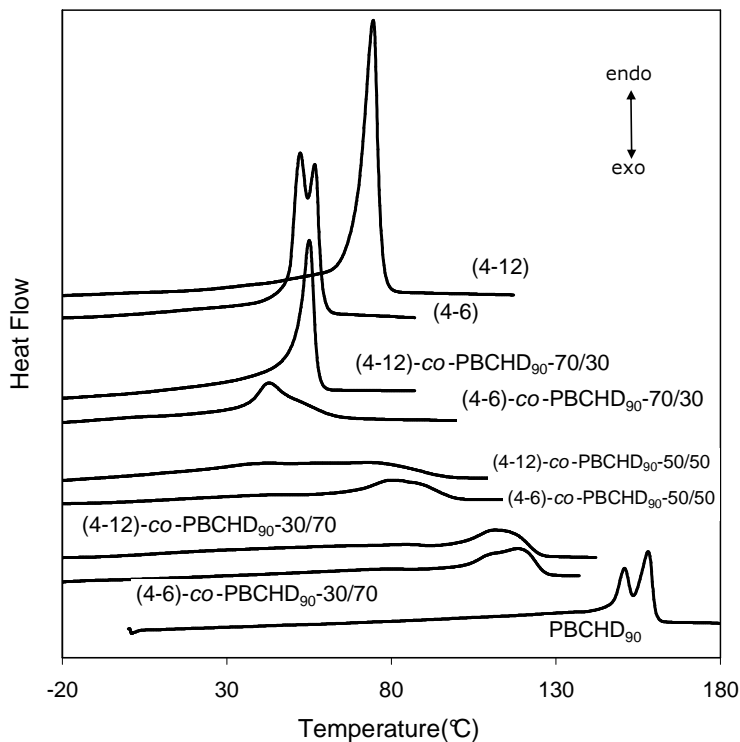


**Figure 3.11 DSC curves of the second heating scan for (4-6) and (4-12)-co-PBCHD<sub>90</sub> samples.**

(4-12)-co-PBCHD<sub>90</sub>-70/30 presents a relatively intense and sharp endothermic peak, whereas (4-6)-co-PBCHD<sub>90</sub>-70/30 is characterized by a very broad melting process. This difference is not evident for the other copolymer composition.

The X-ray diffraction analysis (see Figure 3.12) enables understanding of the thermal behavior of the 4-12 based copolyesters.

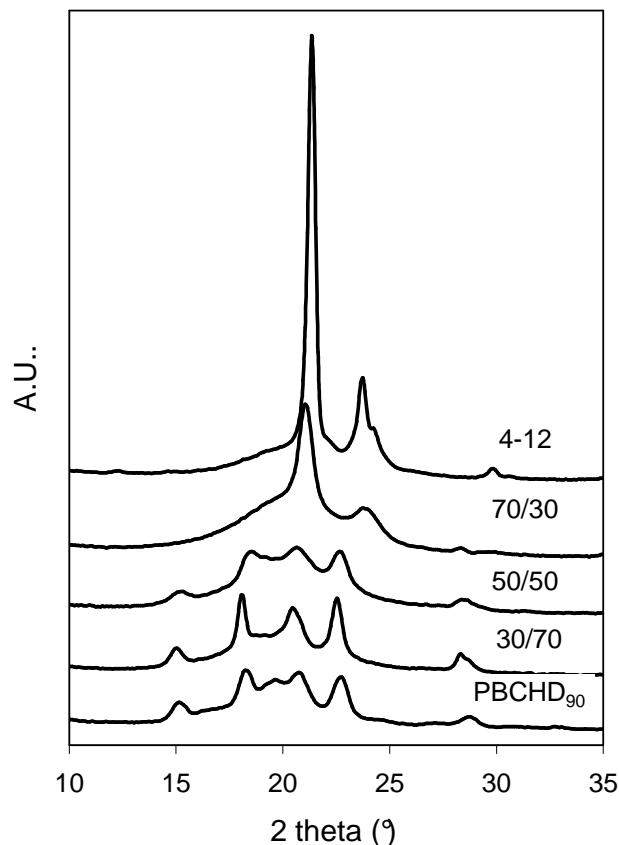


**Figure 3.12** X-ray diffraction patterns of (4-12)-co-PBCHD<sub>90</sub> samples.

In this case, the crystalline phase of the 4-12 homopolymer is present also in the 70/30 copolymer. This means that the 4-12 units are able to crystallize even in the presence of the PBCHD units. This behavior differs from that observed for the 4-6 based copolymers, where the 4-6 crystallization is always extremely difficult, even if it is not completely excluded for the 70/30 sample (Figure 3.9). This difference can be attributed to the faster crystallization rate of poly(alkylene dicarboxylate)s with long  $-(CH_2)-$  sequences, thanks to the higher flexibility of the chain (Celli, 2007). Therefore, the crystallization curves for 70/30 copolymers in Figure 3.10 and the melting peaks in Figure 3.11 refer to two different crystalline phase: the 4-12 crystalline phase for (4-12)-co-PBCHD<sub>90</sub> copolymer and the PBCHD crystalline phase for (4-6)-co-PBCHD<sub>90</sub> copolymer.

For the other compositions, instead, the calorimetric curves always refer to the PBCHD phase, in both the copolymer series, even if in the (4-12)-co-PBCHD<sub>90</sub>-50/50 sample the coexistence of two crystalline phases is probable (Berti, 2009).

### ***Effect of the trans content of the PBCHD units***

Finally, the thermal behavior of the (x-y)-co-PBCHD copolyesters may be strongly influenced by the cis/trans ratio of the aliphatic ring in the PBCHD units. Figure 3.13 reports some examples of DSC curves (cooling and heating scans), obtained on (4-6)-co-PBCHD-30/70 samples, with trans percentage varying from 100 to 50 mol-%. In this case, the copolymers at high percentage of PBCHD units are taken in account, because the effect of the stereochemistry of the cycloaliphatic ring is more evident.

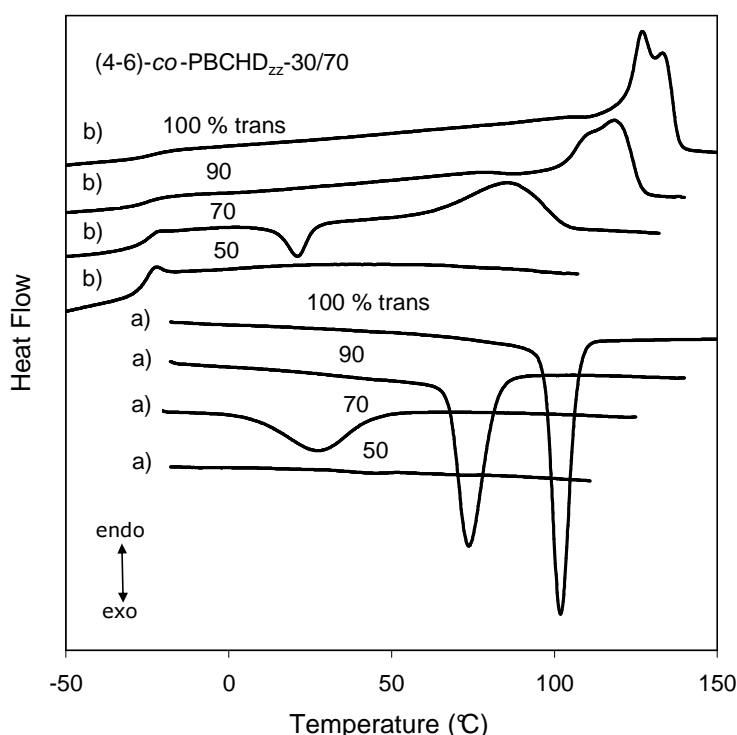


**Figure 3.13** DSC curves of the cooling scan (a) and the second heating scan (b) for (4-6)-co-PBCHD<sub>zz</sub> 30/70 samples.

The copolymer containing PBCHD units with 50 mol-% of trans isomer is a fully amorphous material, which is not able to crystallize either during the cooling scan from the melt or during the subsequent heating scan. By increasing the trans content to 70 mol-%, the copolymer gains the capacity to organize itself into a more ordered structure, partially during the cooling scan and partially during the heating scan. Samples at high trans contents (90 and 100 mol-%) crystallize with narrow peaks, reaching level of crystallinity similar to that of the homopolymer, although  $T_{CC}$  values are significantly lower ( $T_{CC}=97^{\circ}\text{C}$  for (4-6)-co-PBCHD<sub>100</sub>-30/70 and  $149^{\circ}\text{C}$  for PBCHD<sub>100</sub>). Correspondently, the  $T_m$  values also increase with the trans content, as evident from an analysis of all the data of Table 3.5.

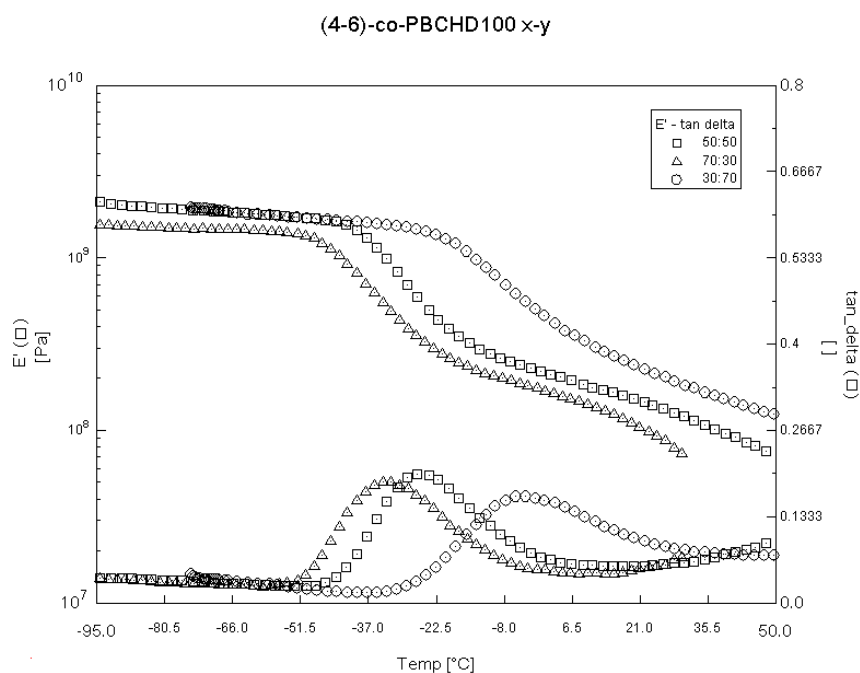
Different observations can be made for the  $T_g$  values. Indeed, if the  $T_g$  data of PBCHD samples are compared as a function of the trans content, it is evident that  $T_g$  decreases with the decrement of the trans content, due to the low flexibility of the 1,4-cyclohexylene ring in trans configuration. From PBCHD<sub>100</sub> to PBCHD<sub>50</sub>  $T_g$  varies from 10 to -7°C. For the (4-6)-*co*-PBCHD copolymers, instead, this trend is not observed. For example, all the (4-6)-*co*-PBCHD-70/30 samples have experimental  $T_g$  values of about -50°C, independently of the fact that the trans content varies from 100 to 50 mol-%. All the (4-6)-*co*-PBCHD-50/50 copolymers have  $T_g$  values of about -40°C and all the (4-6)-*co*-PBCHD-30/70 copolymers have  $T_g$  values of about -25°C. In this case, the effect of the stereoregularity of the aliphatic ring on the chain flexibility seems to be absent.

The presence of a PBCHD crystalline phase creates a more rigid matrix and originates an amorphous phase whose composition is not perfectly correspondent to the theoretical one, but richer in 4-6 units. The 4-6 units can lead to a greater flexibility of the chain and, thus, to lower  $T_g$  data. Therefore, opposite effects are present: the trans isomer and the crystalline phase increase the rigidity of the system and cause an increment of  $T_g$ , whereas the 4-6 units, which are preferentially in the amorphous state, induces a decrement of  $T_g$ . As a result, the final  $T_g$  value could be a constant.

### 3.2.6. DMTA analysis

#### *Effect of the molar composition of copolyesters*

Figure 3.14 collects the DMTA spectra of the (4-6)-*co*-PBCHD samples by comparing specimens with different compositions and the same trans content



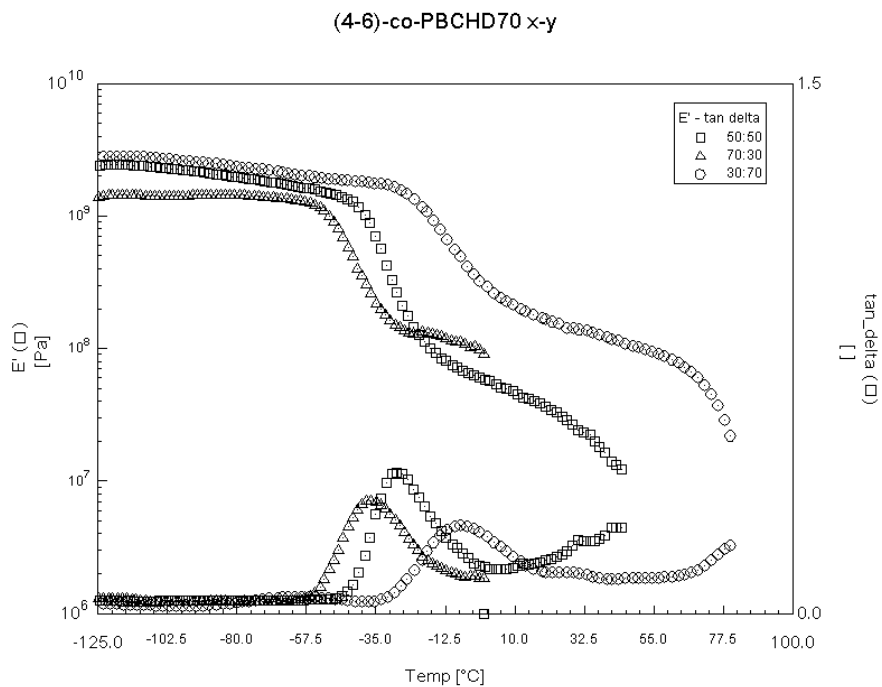
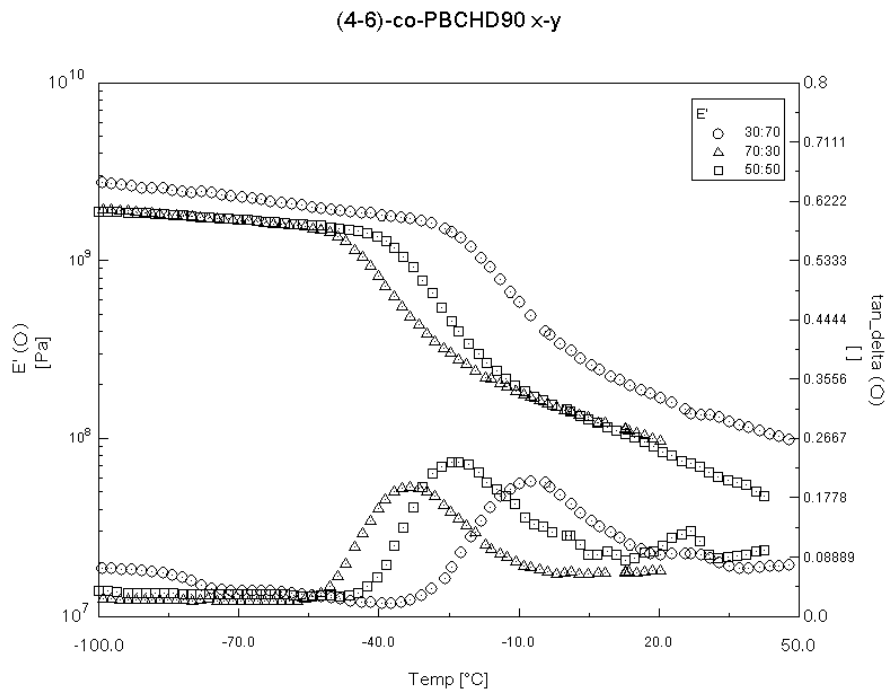


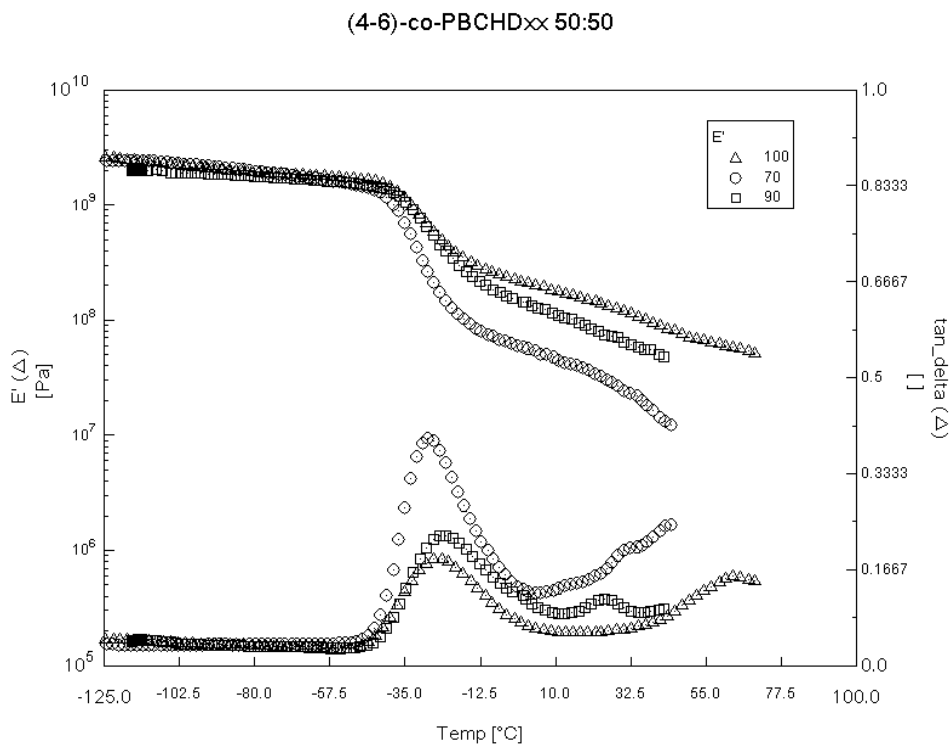
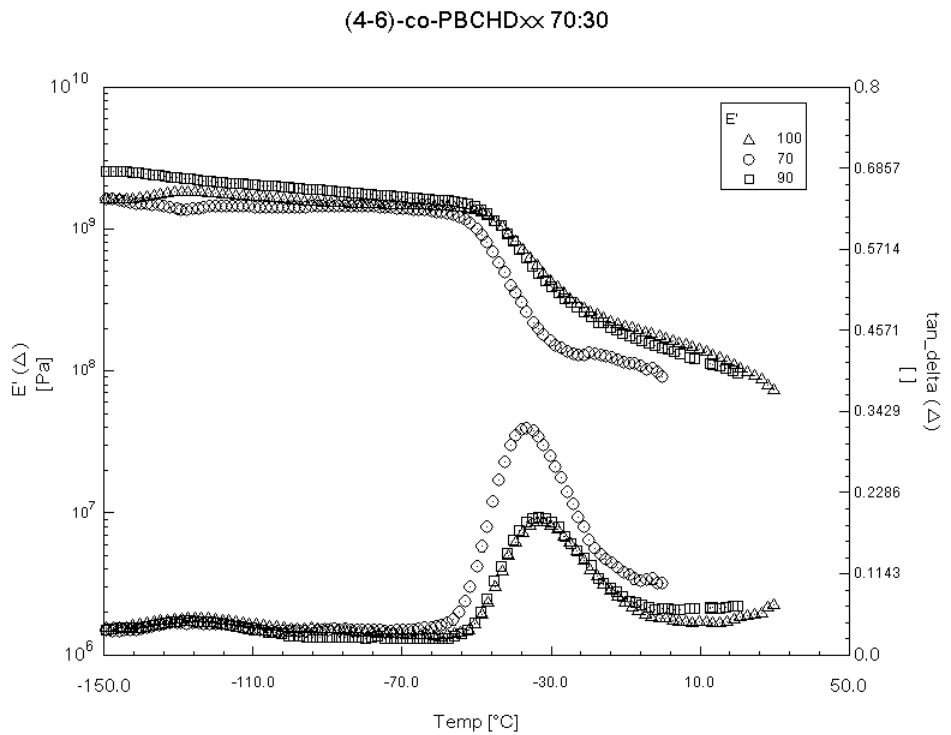
**Figure 3.14 DMTA curves of copolymers with different composition**

Copolymers with PBCHD unit with a trans content of 50% have not been tested because of difficulties in processing the materials.

In each graphs it is notable that the behavior of the elastic modulus and tan delta is a function of copolymer composition. The copolymers with the highest content of PBCHD units have high Tg values that decrease by adding 4-6 units. The elastic modulus values tend to decrease by increasing the content of the 4-6 homopolymer. This trends are due to the higher rigidity of PBCHD units, due to the presence of the aliphatic ring, in comparison to the 4-6 units, that show a ductile behavior.

### Effect of the trans content of the PBCHD units

Figure 3.15 compare the DMTA curves of elastic modulus and tan delta of copolymer having the same composition but different trans content:



(4-6)-co-PBCHD<sub>xx</sub> 30:70

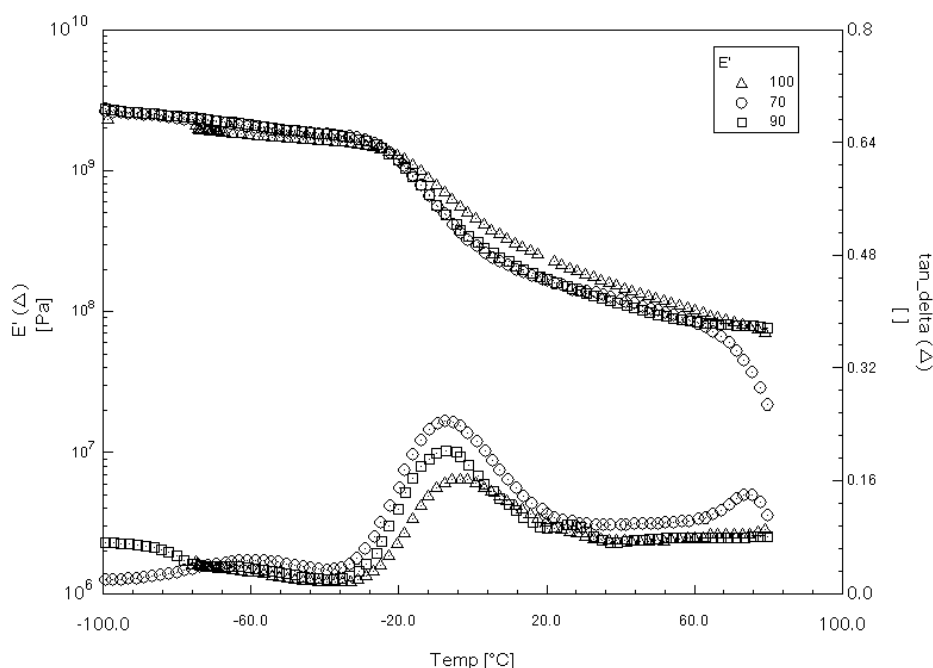


**Figure 3.15 DMTA curves of copolymers with different trans content**

It is notable that the decrement of the trans content from 100 to 90 mol% doesn't consistently affect the mechanical properties: both the elastic modulus and the tan delta curves of the samples with the same composition are almost overlapped.

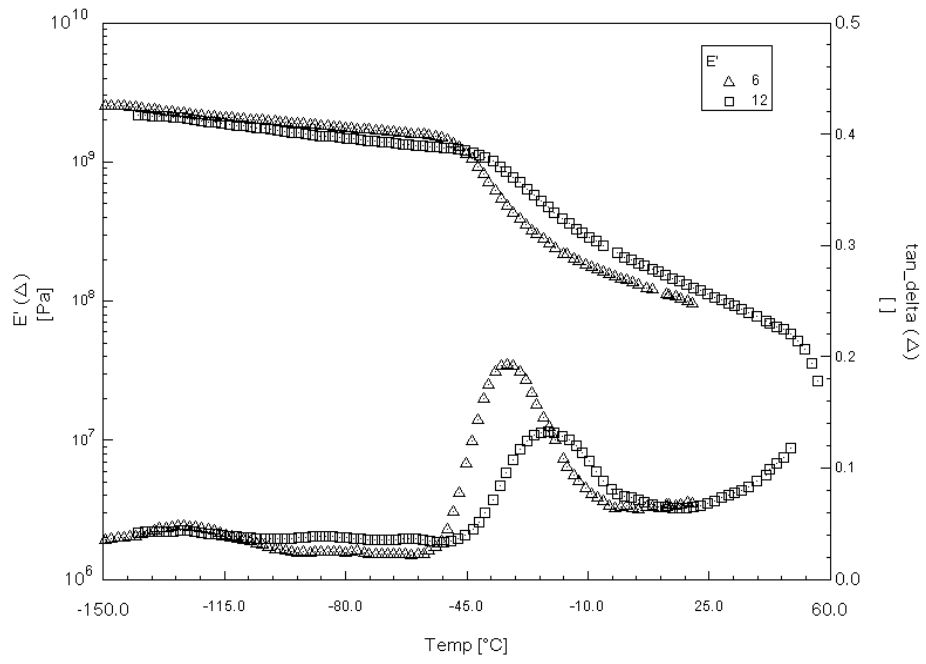
In the copolymers with a trans content of 70% some changes in the DMTA curves have been founded: the peak of tan delta is more intense than the others, due to the higher amorphous content. Indeed, as seen for thermal behavior, higher content of cis stereoisomer leads to lower crystallinity because of its low symmetry. Corresponding, also the modulus ( $E'$ ) decreases more rapidly than the other copolymers at  $T_g$ .

Therefore, as seen for thermal analysis, even the mechanical properties is influenced by the cis/trans ratio of the aliphatic ring in the PBCHD unit.

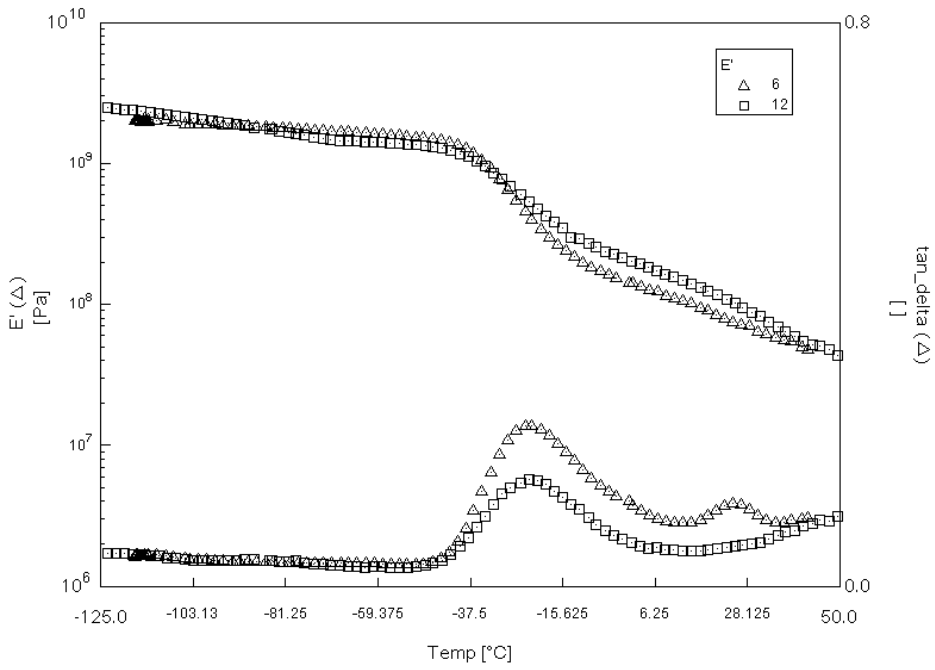
***Effect of the  $-(CH_2)$ - sequence length***

The last parameter that can influence the mechanical properties of the synthesized polymers is the length of the aliphatic chain. In figure 3.16 the DMTA spectra of the (4-6)-co-PBCHD<sub>90</sub> and (4-12)-co-PBCHD<sub>90</sub> are compared at the same composition.

(4-x)-co-PBCHD90 70:30



(4-x)-co-PBCHD90 50:50



(4-x)-co-PBCHD90 30:70

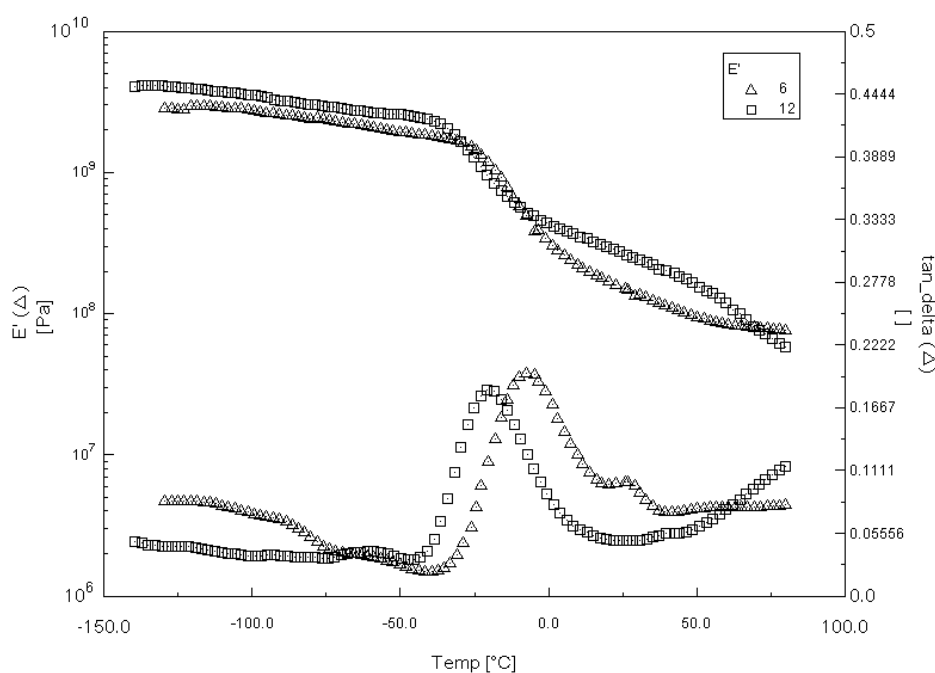


**Figure 3.16 Comparison of DMTA curves of 4-6 and 4-12 copolymers**

According to the DSC, the 4-6 copolymers are always characterized by a relaxation peak of tan delta with a higher intensity than that of 4-12 copolymers. This behavior is due to the low crystallinity of 4-6 samples

### 3.2.7. Photodegradation analysis

For the aliphatic polyesters the study of the photostability, i.e. the resistance to UV irradiation, can be interesting for outdoor applications. The relationship between chemical structures and evolution of molecular properties of the synthesized (co)polyesters through photoageing has been evaluated by using rheology: indeed, the evolution of the rheological material properties (dynamic viscoelastic properties) directly reflects changes in molecular parameters. Hence, dynamic oscillatory measurements were carried out upon UV irradiation of considered (co)polyesters. A modification of the viscoelastic properties of every material is highlighted, indicating a molecular structure evolution from the start of the photo ageing.

For this study three homopolymers and some copolymers have been analyzed. All the samples are not purified (tq) except for the (4-6)-co-PBCHD<sub>90</sub> 30/70 (pu). After purification the copolymer shows a slightly higher viscosity than the not purified one: this is due to the disappearance of the low molecular species that give fluidity to the melt after purification.

Figure 3.17 shows the evolution of complex viscosity components of all the samples before accelerated photoageing:

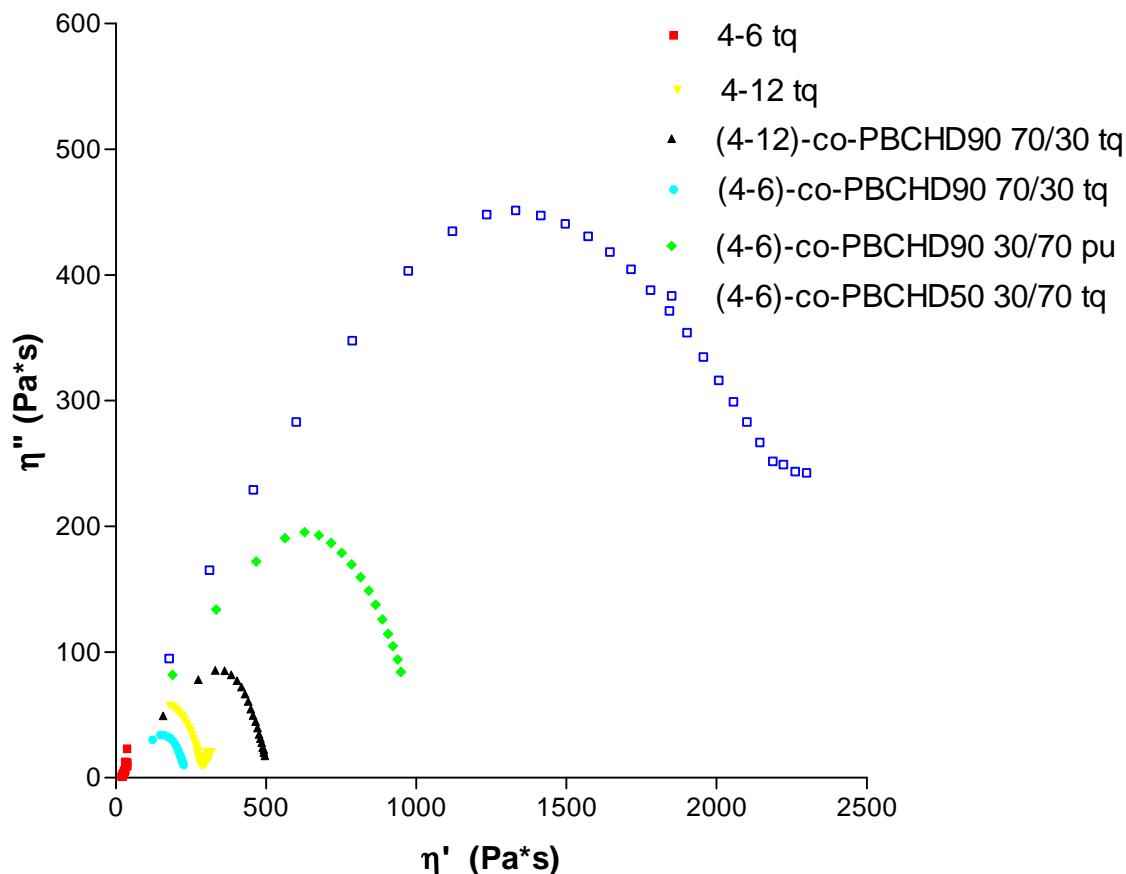


**Figure 3.17 Cole-Cole plots of all the samples before photoageing**

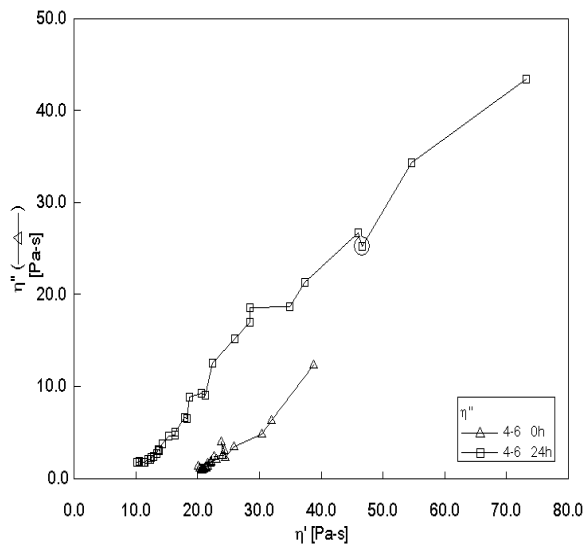
Almost all the samples, at initial time show a Cole-Cole plot that looks like a standard circle. For (4-6)-*co*-PBCHD<sub>50</sub> 30/70, it could be noticed a slight deviation at lower frequencies (higher  $\eta'$ ) exhibiting a double distribution of the molecular weights due to very long macromolecular chains.

The Cole-Cole curve could be considered as the convolution of a standard arc of circle (corresponding to not crosslinked phase) and a straight-line (ascribed to a network).

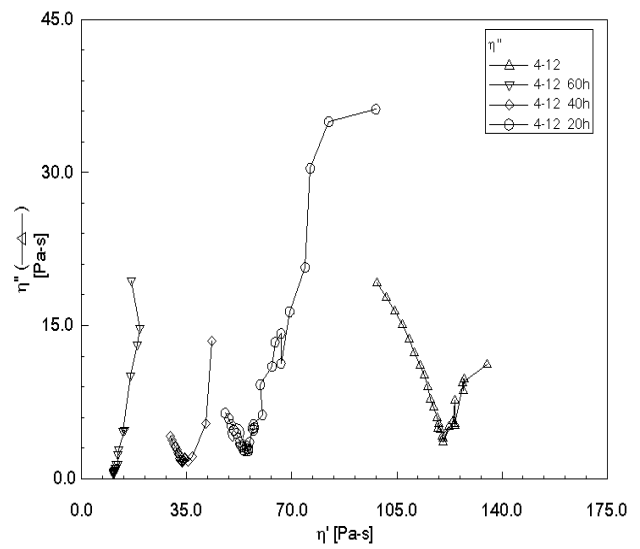
The effect of the length of the aliphatic chain is clear: long  $-(CH_2)-$  sequences show a higher viscosity: this is true both for the homopolymer and the copolymers.

Even the *cis/trans* ratio of the aliphatic ring in the PBCHD units influences the viscosity of the sample: the copolymer with low *trans* percentage ((4-6)-*co*-PBCHD<sub>50</sub> 30/70) has a very high viscosity probably due to the presence of kinks along the chain, whereas the *trans* isomer has a stretched form.

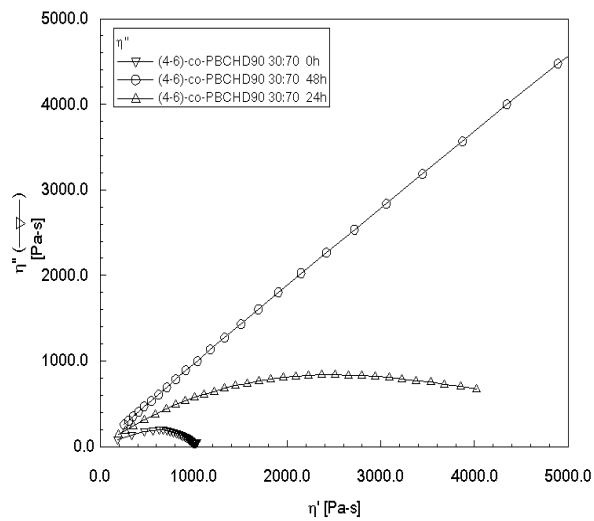
Figure 3.18 shows the evolution of Cole-Cole plots of all the samples analyzed through accelerated photoageing at 60°C for different times



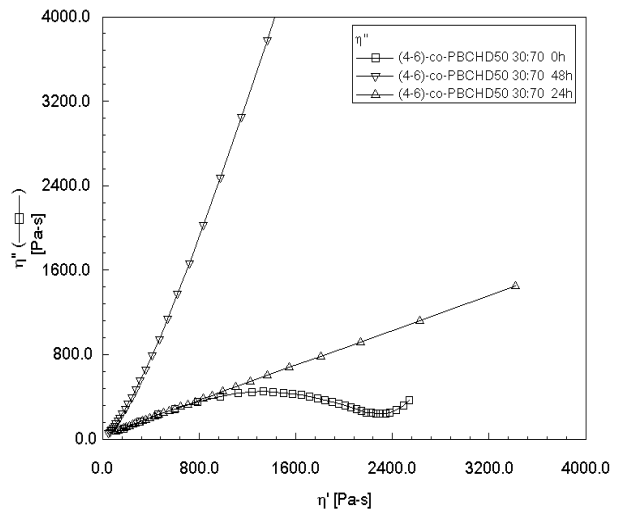
a)



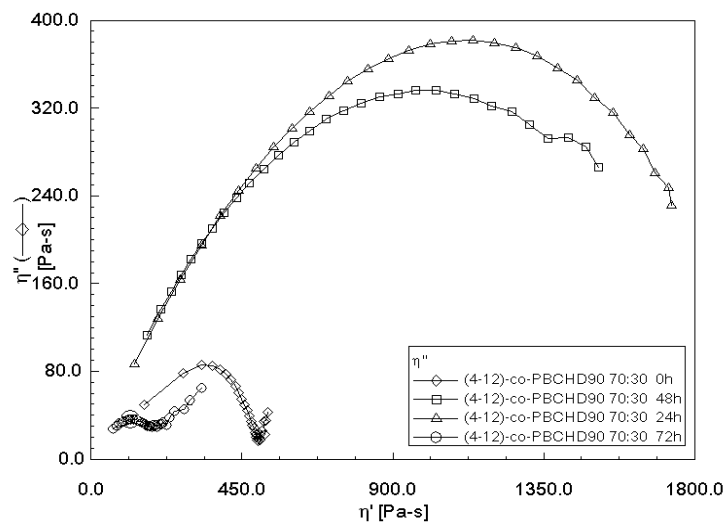
b)



c)



d)



e)

**Figure 3.18 Cole-Cole plots of all the samples after accelerated photoaging at 60°C for different times**

Curves of 4-6 homopolymer (a) clearly put in evidence double phases as photoageing proceeds: one is described as a standard Cole-Cole plot (to better see this phase we should have started from lower frequency). It is worth nothing that the zero shear viscosity  $\eta_0$  has a strong decrement as a consequence of UV exposure. Thus, mass-average molecular weight decreasing points out that scission reactions prevail in this phase. Elsewhere, a second phase is characterized by a strong deviation of the Cole-Cole curve leading to a linear relationship between  $\eta'$  and  $\eta''$ . It is a typical feature of a crosslinked system (Winter, 1989).

Hence, the photodegradation of 4-6 homopolymer exhibits a dual process under our experimental conditions: chain scissions and chain recombinations simultaneously occur, leading to two phases, a crosslinked one and another not crosslinked. Same considerations can be made for 4-12 homopolymer (see Figure 3.18 b).

For (4-6)-*co*-PBCHD<sub>90</sub> 30/70 (Figure 3.18 c) and (4-6)-*co*-PBCHD<sub>50</sub> 30/70 (Figure 3.18 d), after UV exposure Cole-Cole curves are typically those of a tridimensional network polymer system and could be drawn as a line with a very high slope. In this case, UV radiation promotes chain recombination: the formation of a very complex molecular structure occurs in the starting material. This behavior is close to that of all the homopolymers PBCHD<sub>xx</sub> (Commereuc, 2010), and this is in accordance with the thermal considerations: in (4-6) copolymers, the PBCHD unit is present with the highest percentage and this influences their photodegradation properties.

(4-12)-*co*-PBCHD<sub>90</sub> 70:30 (Fig. 3.18 e), instead, shows a double behavior: at the beginning the viscosity increases and the Cole-Cole plot is similar to those of all the copolymers analyzed before, following the PBCHD behavior (chain recombination). After 48h of photodegradation, instead, the viscosity decreases reaching, at 72h, a lower value than that of the non-irradiated sample. The PBCHD unit increase the viscosity (recombination mechanism) at the beginning of UV irradiation, but at longer times the 4-12 units controls the photodegradation action (chain scission).

Table 3.6 collects all the results of the photoageing experiments, in terms of mechanisms of photodegradation.

**Table 3.6 Mechanisms of photodegradation for the different samples**

Sample	Mechanism
4-6, 4-12	chain scission / recombination
PBCHD <sub>90</sub> , PBCHD <sub>50</sub>	Chain recombination
(4-6)- <i>co</i> -PBCHD <sub>90</sub> 30/70 (4-6)- <i>co</i> -PBCHD <sub>50</sub> 30/70	Chain recombination
(4-12)- <i>co</i> -PBCHD <sub>90</sub> 70:30	1) chain recombination 2) chain scission

It is evident that during UV exposure the scission and recombination reactions compete and one of them can be predominant. The evolution of the molecular structure is important and can strongly modify other properties, such as mechanical behavior and biodegradation. Therefore, this kind of study can be very useful for outdoor applications.

### 3.2.8. Conclusions

In this work focus has been made on novel, fully aliphatic, random copolyesters, named (4-6)-*co*-PBCHD, prepared by copolymerization between 1,4-butanediol (BD) and different molar ratio of dimethyl adipate (DMA) and 1,4-cyclohexane dicarboxylate (DMCD). Their thermal behavior has been studied by examining three variables: the molar composition of the copolyesters, the length of the aliphatic  $-(CH_2)-$  chain in the comonomeric unit, the cis/trans ratio of the 1,4-cyclohexilene units in DMCD.

The behavior of the (4-6)-*co*-PBCHD copolymers has been compared with that of the related homopolymers and that of similar copolyesters, named (4-12)-*co*-PBCHD and obtained from BD and different molar ratio of 1,12-dodecanedioc acid (DA) and 1,4-cyclohexanedicarboxylic acid (CHDA).

The effect of the molar composition of the copolyesters on the thermal properties is connected to the capacity of co-units to crystallize. In the (4-6)-*co*-PBCHD copolyesters the PBCHD crystalline phase dominates for all the composition. The rigid PBCHD units tend to prevent the crystallization of the 4-6 units, probably due to the fact that these latter units have very slow crystallization rate. On the other hand, in the (4-12)-*co*-PBCHD copolyesters there is competition between the crystallization of the 4-12 and PBCHD units. This behavior is due to the fact that the 4-12 units, characterized by longer  $-(CH_2)-$  sequences, have faster crystallization rates with respect to the 4-6 units. Therefore, in 70/30 specimens the 4-12 units crystallize, in 50/50 samples two crystalline phases can coexist, and in 30/70 copolymer only the PBCHD crystal phase is present. Indeed this phenomena is confirmed also by photodurability tests: the (4-12)-*co*-PBCHD<sub>90</sub> 70/30 is the only copolymers that shows a double behavior of chain recombination after short times of UV exposure due to the PBCHD unit and chain scissions after longer times due to the influence of 4-12 unit. In the (4-6)-*co*-PBCHD copolymer, the 4-6 unit has no effect and the samples show only the recombination behavior typical of the PBCHD unit.

The amorphous phase composition depends on the fact that some chain segments can separate from the homogeneous melt because of crystallization. As a consequence of this separation, the amorphous phase is found to be richer in the non-crystallizable component. This is particularly true for the semicrystalline (4-6)-*co*-PBCHD series, where the amorphous phase is rich in 4-6 units. On

the other hand, the fully amorphous samples (for example, the (4-6)-*co*-PBCHD<sub>50</sub> samples) have a single, homogeneous amorphous phase.

The trans content of the PBCHD units is found to have a significant influence on the thermal behavior of the copolymers. Indeed, at low trans content (50 mol%), homopolymer and copolyesters are in the fully amorphous state. By increasing the trans content, up to 100 mol-%, the copolyesters reach significantly high melting temperatures (about 125-134°C) and high melting enthalpies. DMTA behavior is also affected by trans content, mainly when it decreases to 70 mol%.

In conclusion, by changing the chemical structure of the copolyesters, based on the three variables described above, it is possible to prepare materials with the desired properties for specific applications. Novel copolyesters are therefore not only characterized by good physical properties and potential biodegradability, but also have the advantage that their properties can easily be modified, according to the requests for future applications.

### **3.3 Fully Aliphatic or Aliphatic/Aromatic Copolyesters Containing $\omega$ -Hydroxy Fatty Acids**

#### **3.3.1. Introduction**

Because of today's environmental problems, in order to substitute traditional petro-based polymers, biopolymers have to feature adequate physical properties, must be processed by environmental friendly approaches and are to be cost-competitive on the market. Notable efforts of researchers are devoted to found novel routes to prepare monomers and polymers derived from renewable resources and characterized by a good balance of performances and costs.

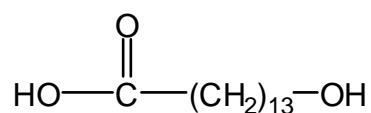
As alternative to the conventional thermoplastics, very attractive bio-polymers are the polyethylene (PE)-like polyesters, characterized by long methylene sequences separated by ester groups, that can notably improve the environmental degradability of the materials (Iwata, 1999; Mochizuki, 1999).

Vegetable oils offer a very attractive potential in regard to their availability and sustainability for the preparation of building blocks for PE-like polyesters (Biermann, 2011). However, the chemical conversions, up to now proposed to transform fatty acids and their derivatives to bifunctional monomers for polyesters, are often very difficult and expensive, for example by metathesis (Meier, 2009; Rybak, 2008; Trzaskowski, 2011), thiol-ene reactions (Turunc, 2011;

Desroches, 2011), methoxycarbonylation (Quinzler, 2010), ozonolysis and reduction (Petrovic, 2010).

Recently, Gross and coworkers prepared a new monomer, the  $\omega$ -hydroxytetradecanoic acid (14HA) (Scheme 3.2), by following a biotechnological way, a fermentation process starting from an engineered *Candida tropicalis* strain (Lu, 2010). To develop the strain 16 genes encoding 6 cytochrome P450s, 4 fatty alc. oxidases, and 6 alc. dehydrogenases from the *C. tropicalis* genome were identified and eliminated. By starting from the 14HA the synthesis of the novel Poly( $\omega$ -hydroxyl tetradecanoic acid) (P14HA) has been described (Liu, 2011).

### Scheme 3.2 Chemical structure of $\omega$ -hydroxytetradecanoic acid (14HA)



This polymer, in agreement with similar macrostructures, is characterized by a relatively low melting temperature (92°C), very high crystallinity degree, poor mechanical properties.

In order to modify P14HA properties and mainly to improve the performance of this novel polyester, in collaboration with Prof. Gross, novel random copolymers have been synthesized, characterized by tunable properties. They are based on P14HA and PBT or PBCHD units, is described. These new copolymers can be interesting for different reasons: firstly they are potentially fully biobased polyesters. Indeed, all the monomers can be prepared by renewable resources, including the dimethyl terephthalate and dimethyl cyclohexane dicarboxylate (DMCD) (Berti, 2010). Moreover, the materials present properties that can be easily modified, by changing the molecular composition of the copolymers and the cis/trans ratio of the aliphatic ring, in the case of PBCHD.

#### 3.3.2. Synthesis

The synthesis of P14HA homopolymer is described in literature (Liu, 2011). The preparation of the PBCHD samples is reported by Berti et al. (Berti, 2008 A). PBCHD samples are indicated with the code PBCHD<sub>zz</sub>, where zz indicates the theoretical trans % of the cycloaliphatic units in the polymers. The real trans percentages are reported in Table 3.7.

**Table 3.7 Molecular characteristics of the samples**

Sample		<i>Trans % in the polymer<sup>a</sup></i>	$M_w \times 10^{-3}{}^b$	$M_w/M_n{}^b$
<i>Homopolymers</i>				
P14HA		-	78.7	2.8
PBT		-	47.7	2.4
PBCHD <sub>100</sub> (100% trans)		100	73.4	2.5
PBCHD <sub>50</sub> (50% trans)		52	88.6	2.8
<i>Aliphatic aromatic copolymers</i>		<i>Molar ratio 14HA/PBT<sup>a</sup></i>		
P14HA-co-PBT-80/20		78/22	132.6	2.5
P14HA-co-PBT-60/40		62/38	110.5	2.4
P14HA-co-PBT-40/60		41/59	100.0	2.2
P14HA-co-PBT-20/80		21/79	84.1	2.5
ECOFLEX		-	121	2.3
<i>Aliphatic copolymers</i>		<i>Molar ratio 14HA/PBCHD<sup>a</sup></i>		
P14HA-co-PBCHD <sub>100</sub> -80/20		79/21	47.2	2.3
P14HA-co-PBCHD <sub>100</sub> -60/40		57/43	156.0	2.8
P14HA-co-PBCHD <sub>100</sub> -40/60		40/60	105.0	2.9
P14HA-co-PBCHD <sub>100</sub> -20/80		20/80	121.0	2.8
P14HA-co-PBCHD <sub>50</sub> -80/20		79/21	50.7	2.2
P14HA-co-PBCHD <sub>50</sub> -20/80		21/79	86.7	2.5

<sup>a</sup> Calculated by <sup>1</sup>H NMR. <sup>b</sup> Measured by GPC in CHCl<sub>3</sub>.

The synthesis of the copolymers derived from BD, 14HA, and DMCD is here described, in particular for the P14HA-co-PBCHD<sub>100</sub>-60/40 sample.

14HA (27 g, 0,110 mol), DMCD 100% trans (14,6 g, 0,073 mol), BD (23,9 g, 0,265 mol), TBT (0,061 g, 0,179 mmol) were placed into a round bottom wide-neck glass reactor (250 ml capacity). The reactor was closed with a three-necked flat flange lid equipped with a mechanical stirrer and a torque meter which gives an indication of the viscosity of the reaction melt. The reactor was immersed into a salt bath preheated to 200°C. The first stage was conducted at atmospheric pressure under nitrogen atmosphere and the mixture was allowed to react for 120 min under stirring with continuous removal of water. The second stage was started by gradually reducing the pressure to 0.2 mbar while the temperature was raised to the final value of 220°C. These conditions were reached within 60 min, using a linear gradient of temperature and pressure, and maintained for 120 min.

The feed 14HA/DMCD molar ratios used are 20/80, 40/60, 60/40 and 80/20 in order to obtain copolyesters with different compositions. They are here named P14HA-co-PBCHD<sub>zz</sub>-a/b, where a/b is the feed molar ratio of the 14HA/DMCD. The final molar composition of the copolymers is reported in Table 3.7.

The synthesis of the copolymers derived from BD, 14HA, and DMT is analogous to the one described before with the exception of the temperature of the second stage: it increases to 230°C (because of the higher melting point of PBT compare to PBCHD).

The feed 14HA/DMT molar ratios used are 20/80, 40/60, 60/40 and 80/20. They are named P14HA-*co*-PBT-a/b, where a/b is the feed molar ratio of the 14HA/DMT. The final molar composition of the copolymers is reported in Table 3.7.

Ecoflex is the commercial name of the random copolyesters poly(butylene adipate)-*co*-(terephthalate), 54 mol% of PBA and 46 mol% of PBT. It is a commercial sample from BASF®.

### 3.3.3. Molecular characterization of the copolyesters

It is evident, from the data of Table 3.7 that the molecular weights of all the synthesized samples are very high and comparable.

The chemical structure was determined by <sup>1</sup>H-NMR spectroscopy

#### *Aliphatic-Aromatic copolyesters*

As an example, Figure 3.19 shows the <sup>1</sup>H-NMR spectrum for the P14HA-*co*-PBT-40/60 sample and the signal assignments are reported. In all cases the spectra were found to be consistent with the expected structures.

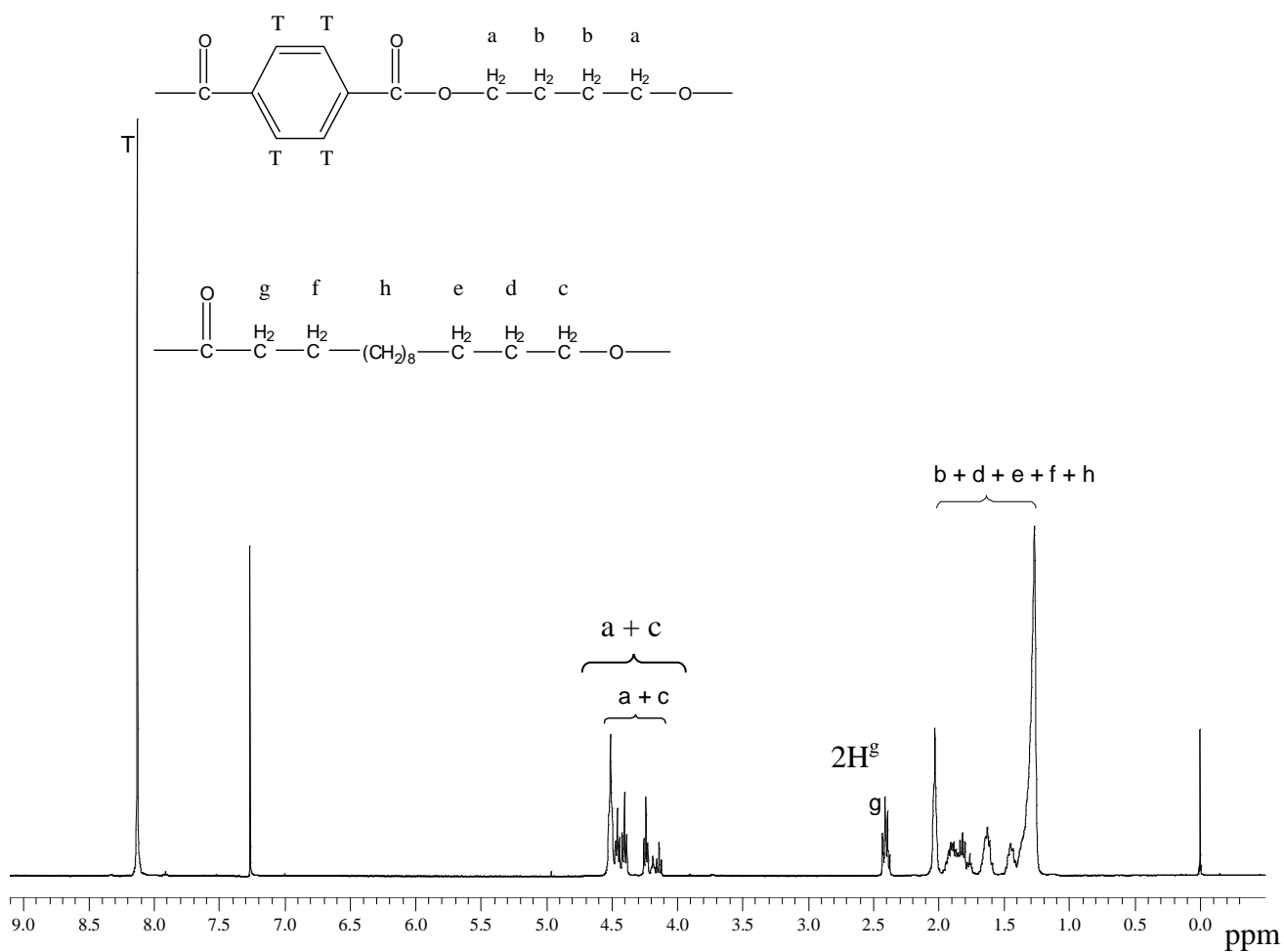


**Figure 3.19** NMR spectra of P14HA-co-PBT-40/60 sample

In order to better understand the molecular structure of the novel copolymers, a more in depth study on the NMR spectrum has been carried out. Fig 3.20 and 3.21 report the expansions of the NMR spectrum of Fig 3.19

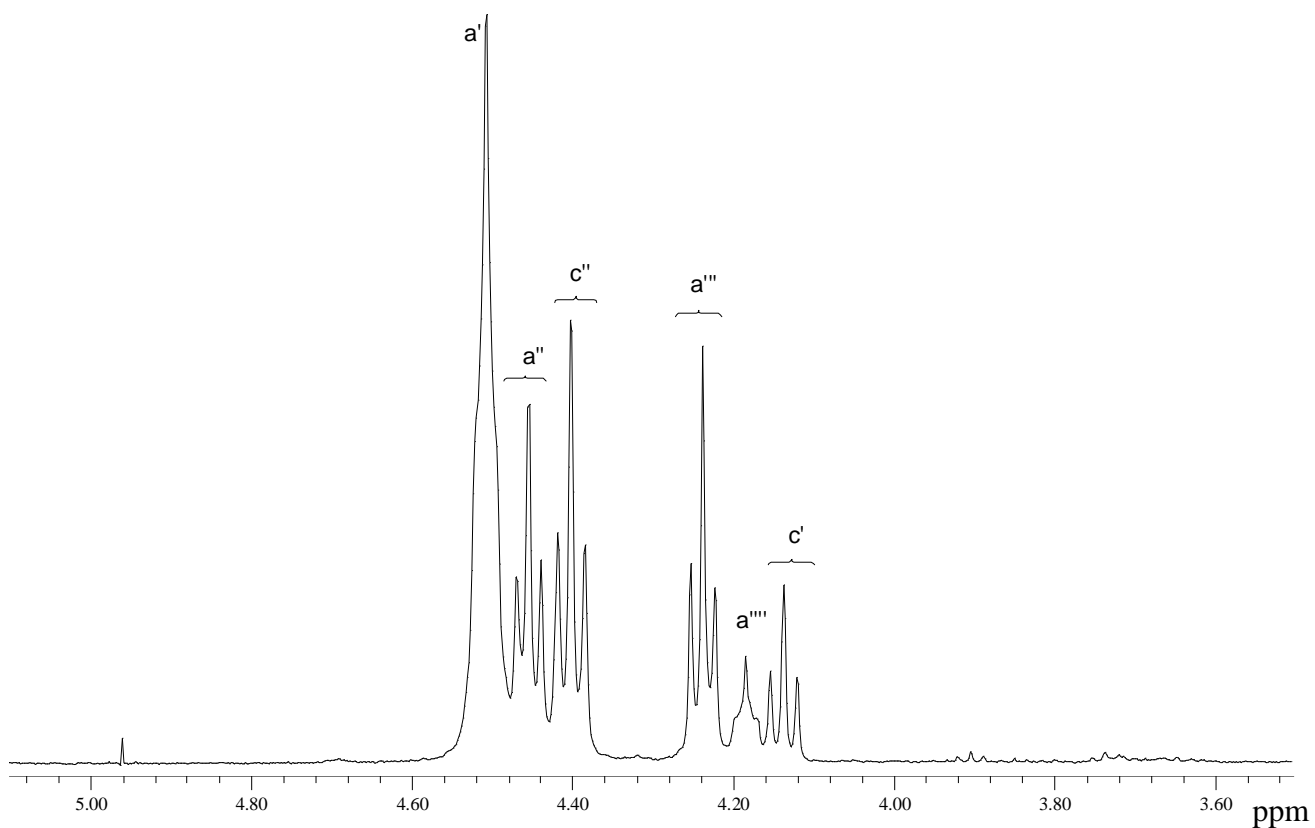


**Figure 3.20** Expansion (3.50 – 5.00 ppm) of the NMR spectrum of P14HA-*co*-PBT-40/60 sample

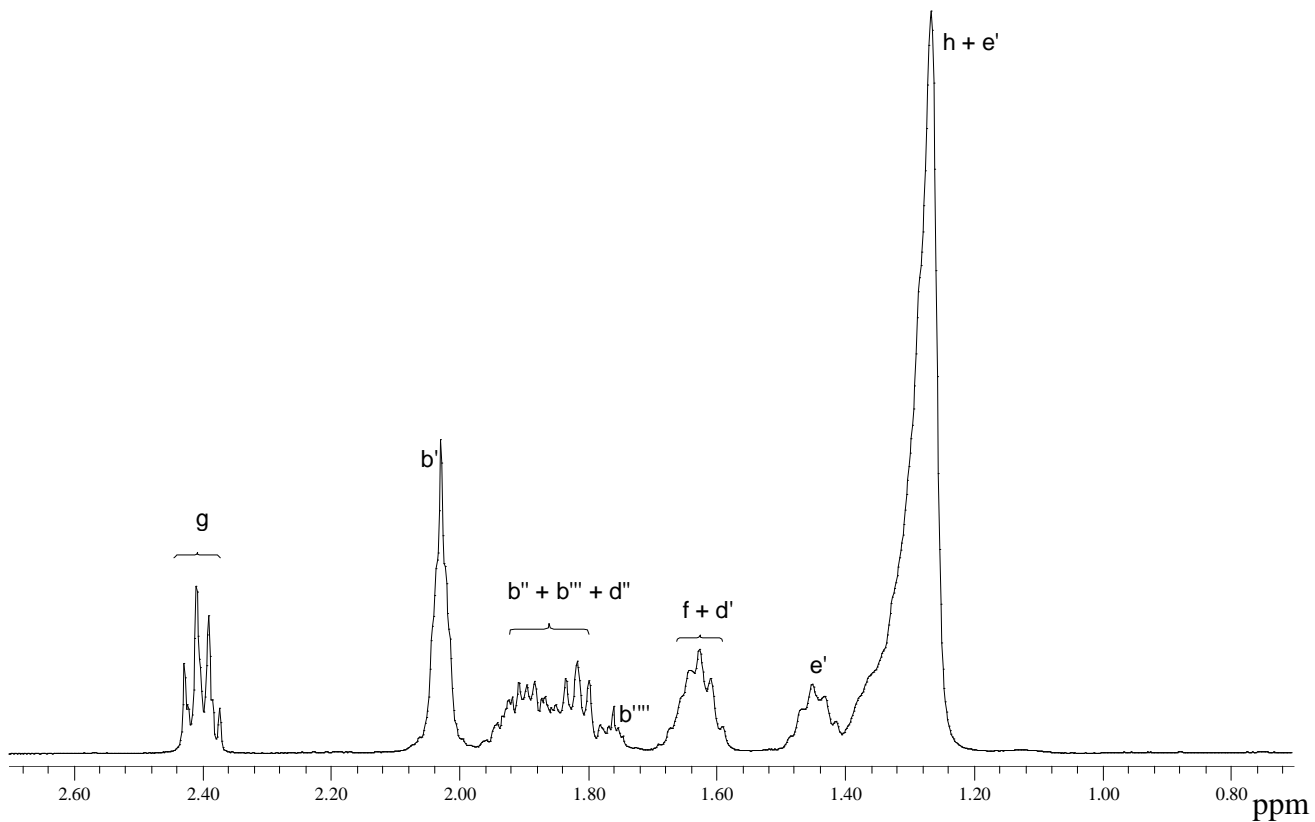
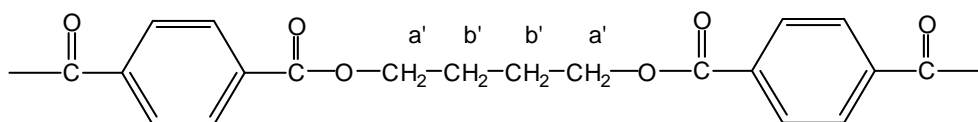


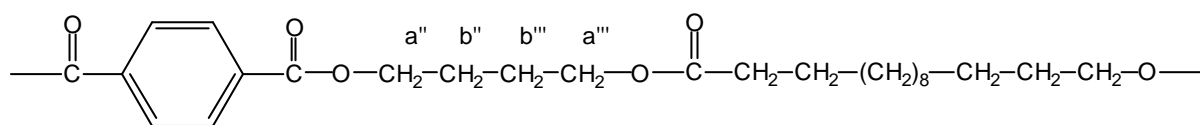
**Figure 3.21** Expansion (0.80 – 2.60 ppm) of the NMR spectrum of P14HA-*co*-PBT-40/60 sample

By considering the different units present in the system, Scheme 3.3 reports the triads, centered to butandiol (B unit), terephthalate (T unit) and hydroxyacid (H unit) groups, that can be obtained during the polymerization reactions.

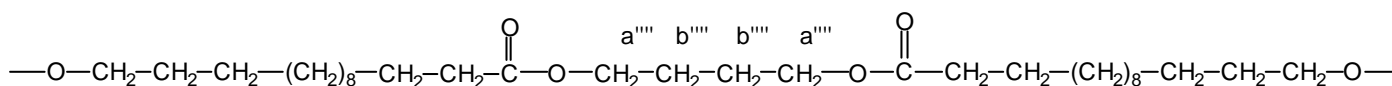
**Scheme 3.3: Possible triads, centered on butanediol (B), terephthalate (T) and hidroxyacid (H) units, obtainable from the polycondensation reactions.**



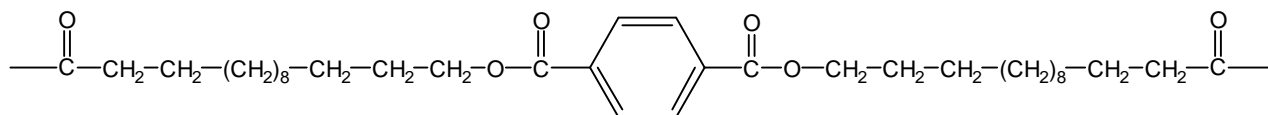
TBT



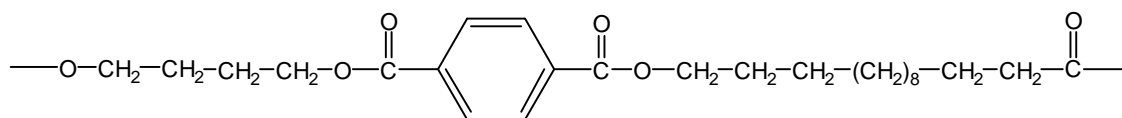
TBH



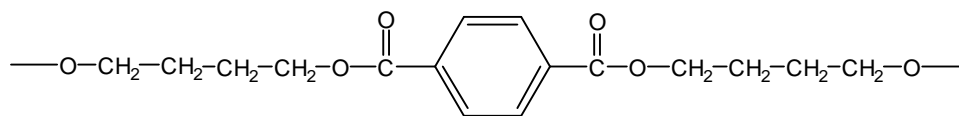
HBH



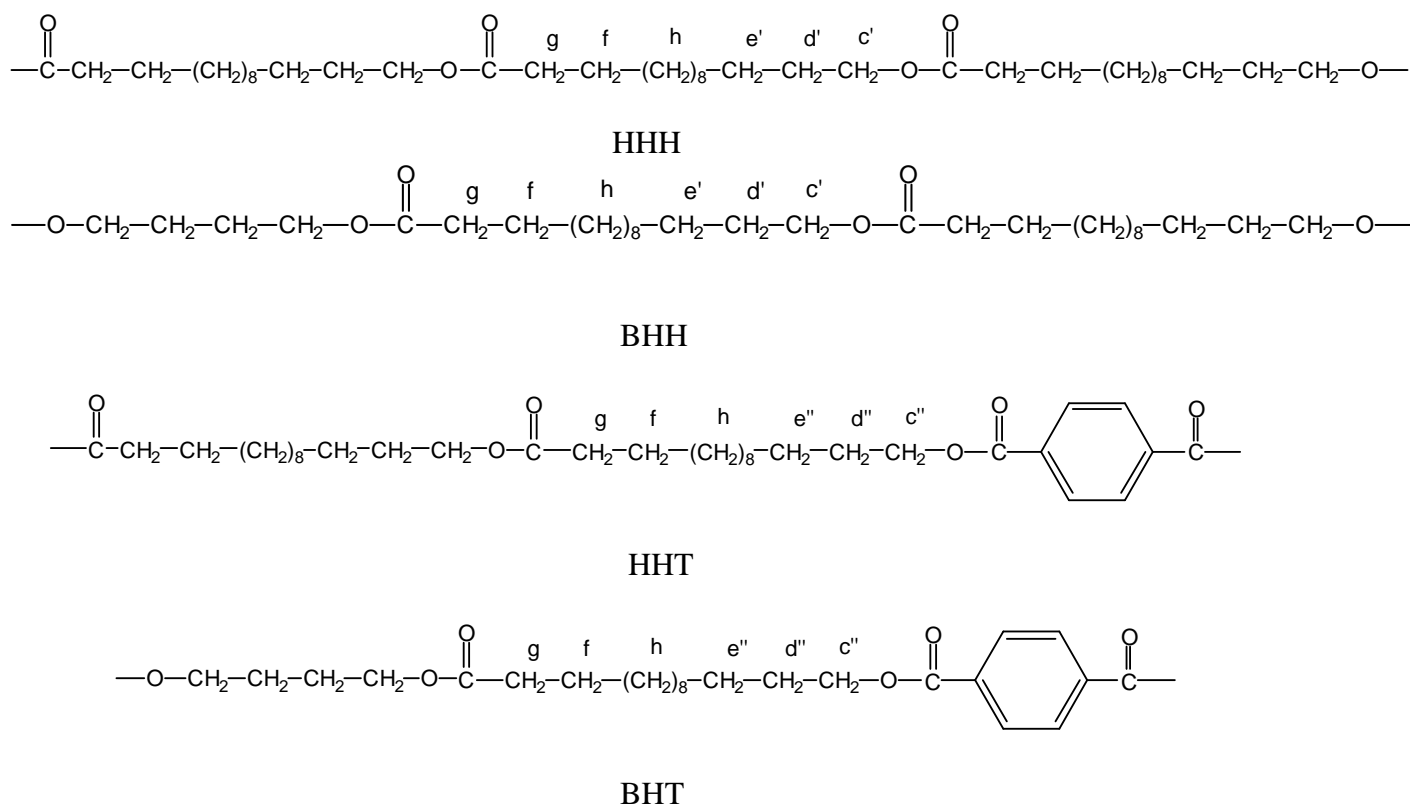
HTH



BTH



BTB



In Fig 3.20, where the expansion of the 3.0-5.0 ppm region of Figure 3.19 is shown, the signals due to  $H^{a'}$ ,  $H^{a''}$ ,  $H^{a'''}$  and  $H^{a''''}$  protons, present in TBT, TBH and HBH triads, are identified. Moreover, from the expansion of the 0.0-2.6 ppm region (Fig 3.21), it is possible to observe the signals attributed to the  $H^{b'}$ ,  $H^{b''}$ ,  $H^{b'''}$ ,  $H^{b''''}$  protons.

The NMR signal of the terephthalic protons ( $H^T$ ) is a singlet at 8.1 ppm, independently of the groups (H or B) linked to the terephthalic unit. Therefore, the  $H^T$  protons in HBH, BTB and HTB triads are not distinguishable. In any case, it is important to underline that the syntheses are carried out in an excess of butandiol and, then, HTH and HTB sequences should be not very frequent.

Moreover, from Fig 3.20 and 3.21 it is possible to identify also the  $H^{c'}$  and  $H^{c''}$  protons (at 4.14 e 4.40 ppm), the  $H^{d'}$  and  $H^{d''}$  protons (at about 1.65 e 1.82 ppm) and the  $H^{e'}$  and  $H^{e''}$  protons (in the range from 1.2 to 1.5 ppm), the  $H^f$ ,  $H^g$  and  $H^h$  protons, all present in HHH, BHH, HHT and BHT structures of Scheme 3.3.

In order to calculate the final copolymer composition and to check if it corresponds to the monomer feed amount, the H/T ratio has been determined by considering the integration of the signals of the two  $H^g$  protons of the hydroxyacid units at 2.4 ppm and the signals the four  $H^T$  protons of the terephthalate units at 8.15 ppm. The H/B ratio has been calculated by integrating the signals of the two  $H^c$  protons of the hydroxyacid units ( $H^{c'}$  and  $H^{c''}$  signals) and the signals of the four  $H^a$  protons of the butandiol ( $H^{a'}$ ,  $H^{a''}$ ,  $H^{a'''}$  and  $H^{a''''}$  signals). The B/T ratio has been obtained

by integrating the signals of the four H<sup>a</sup> protons of the butandiol units (H<sup>a'</sup>, H<sup>a''</sup>, H<sup>a'''</sup> and H<sup>a''''</sup> signals) and the signals of the four H<sup>T</sup> protons of the terephthale units at 8.15 ppm. The results are reported in Table 3.8, where it is notable a good correspondance between the feed and the final compositions.

**Table 3.8: Molar composition of the copolyesters**

Sample	H/T <sup>a</sup>	H/B <sup>a</sup>	B/T <sup>a</sup>
P14HA-co-PBT-80/20	78/22	77/23	52/48
P14HA-co-PBT-60/40	62/38	61/39	52/48
P14HA-co-PBT-40/60	41/59	40/60	52/48
P14HA-co-PBT-20/80	21/79	21/79	52/48

<sup>a</sup> calculated from the <sup>1</sup>H NMR spectra of the polymers

Finally, the copolymer molecular structure has been evaluated. Devaux et al. (Devaux, 1982) proposed a method for the determination of the probability (f) of finding triads that are centered on the B unit (TBH, HBT, TBT and HBH triads), based on the intensities (I) of the NMR signals. The formula are here summarized:

$$f_{TBH} = I_{a''} / (I_{a'} + I_{a''} + I_{a'''} + I_{a''''})$$

$$f_{HBT} = I_{a'''} / (I_{a'} + I_{a''} + I_{a'''} + I_{a''''})$$

$$f_{TBT} = I_{a'} / (I_{a'} + I_{a''} + I_{a'''} + I_{a''''})$$

$$f_{HBH} = I_{a''''} / (I_{a'} + I_{a''} + I_{a'''} + I_{a''''})$$

From these data, it is possible to calculate the length of the TBT and HBH triads (L<sub>TBT</sub> and L<sub>HBH</sub>, respectively) and the parameter B<sub>B</sub>, which defines the randomness degree around the butandiol unit, by means of the equations:

$$L_{TBT} = (f_{TBT} / f_{TBH}) + 1$$

$$L_{HBH} = (f_{HBH} / f_{HBT}) + 1$$

$$B_B = f_{TBH} / F_T + f_{HBT} / F_H$$

where F<sub>T</sub> and F<sub>H</sub> are the molar fractions of the ester and acid functionalites derived from terephthalate and hydroxy units, respectively. F<sub>H</sub> and F<sub>T</sub> do not correspond to the molar fractions of H and T units in Table 3.8, but they must be calculated by considering that the terephthalate unit contains two ester groups, whereas the H units has only one ester group (Tessier, 2003). Therefore:

$$\text{moles of acid groups} = \text{moles of H units}$$

$$\text{mole of ester groupss} = 2 \text{ T moles}$$

**Table 3.9 Final data of  $F_H$  and  $F_T$** 

Sample	H/T	$F_H$	$F_T$
P14HA- <i>co</i> -PBT-80/20	78/22	0.64	0.36
P14HA- <i>co</i> -PBT-60/40	62/38	0.45	0.55
P14HA- <i>co</i> -PBT-40/60	41/59	0.26	0.74
P14HA- <i>co</i> -PBT-20/80	21/79	0.12	0.88

$B_B$  is equal to zero in a homopolymer or in a copolymer with long homogeneous sequences, and to 1 in a random distribution of H and T units around B unit;  $B_B$  varies between 1 and 2 when H and T are alternated around B. Table 3.10 lists the  $B_B$  values obtained

From the measurements of the relative intensities of the  $H^c$  signals ( $I_{c'}$  and  $I_{c''}$ ), it is also possible to evaluate the average length of the HH sequences ( $L_{HH}$ ). In this case the following equations are used:

$$f_{HT} = I_{c''} / (I_{c'} + I_{c''})$$

$$f_{HH} = I_{c'} / (I_{c'} + I_{c''})$$

$$L_{HH} = (f_{HH} / f_{HT}) + 1$$

where  $f_{HH}$  and  $f_{HT}$  are the molar fractions of the HH and HT sequences. The corresponding  $L_{HH}$  values are shown in Table 3.10.

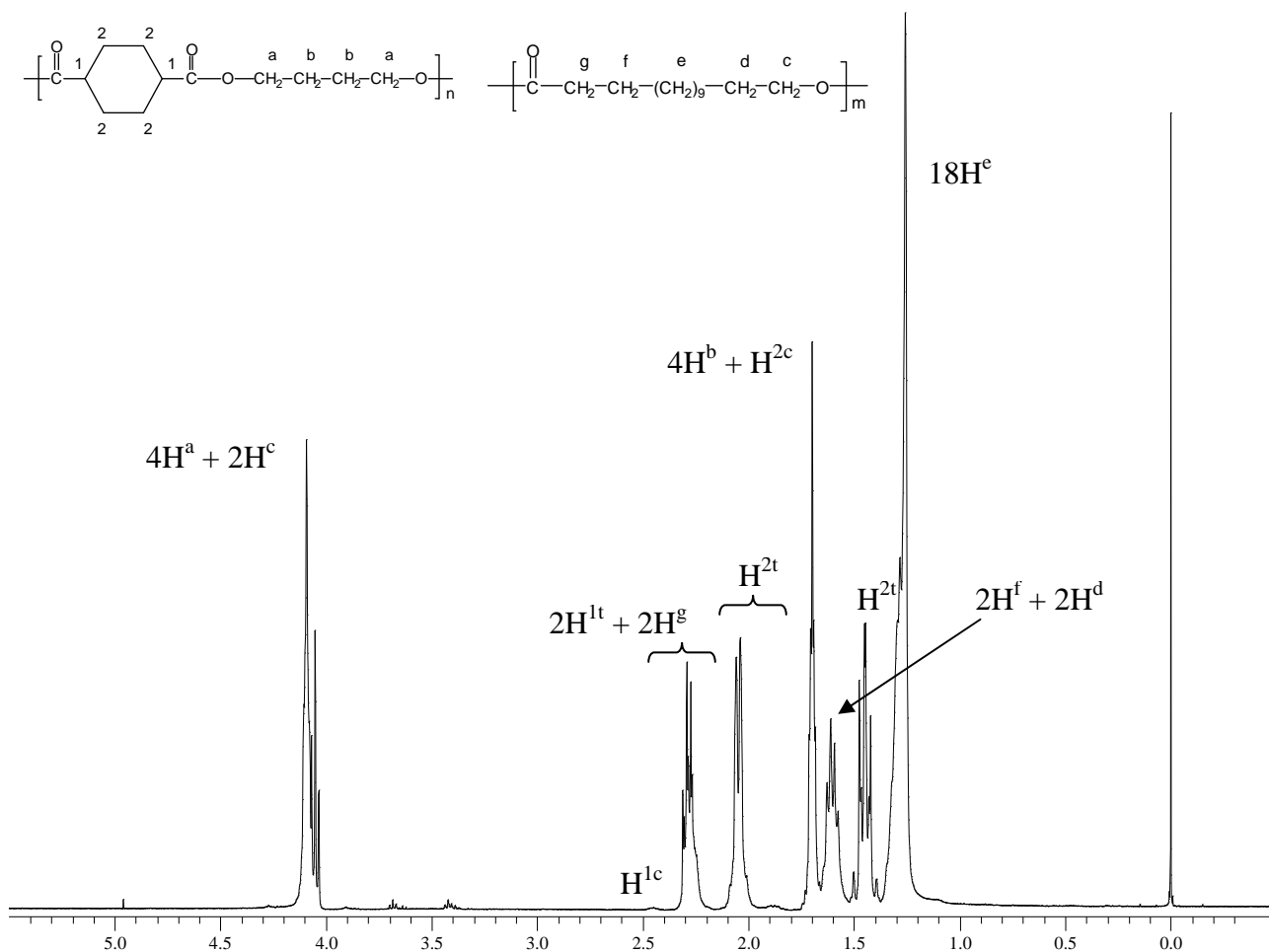
**Table 3.10  $B_B$  values of all the aliphatic-aromatic copolyesters**

Sample	$L_{TBT}$	$L_{HBH}$	$B_B$	$L_{HH}$
P14HA- <i>co</i> -PBT-80/20	1.5	2.7	1.02	2.7
P14HA- <i>co</i> -PBT-60/40	2.2	1.8	1.02	1.8
P14HA- <i>co</i> -PBT-40/60	3.7	1.4	0.99	1.3
P14HA- <i>co</i> -PBT-20/80	7.5	1.2	0.93	1.1

In all cases  $B_B$  was found to be very close to 1, indicating the random nature of the copolymers for all compositions. The sequences of TBT are long in the copolymer rich in PBT (P14HA-*co*-PBT-20/80) and decrease with the decrement of PBT content. Accordingly, the HH unit length is short for the sample rich in PBT and increases with the increment of P14HA amount.

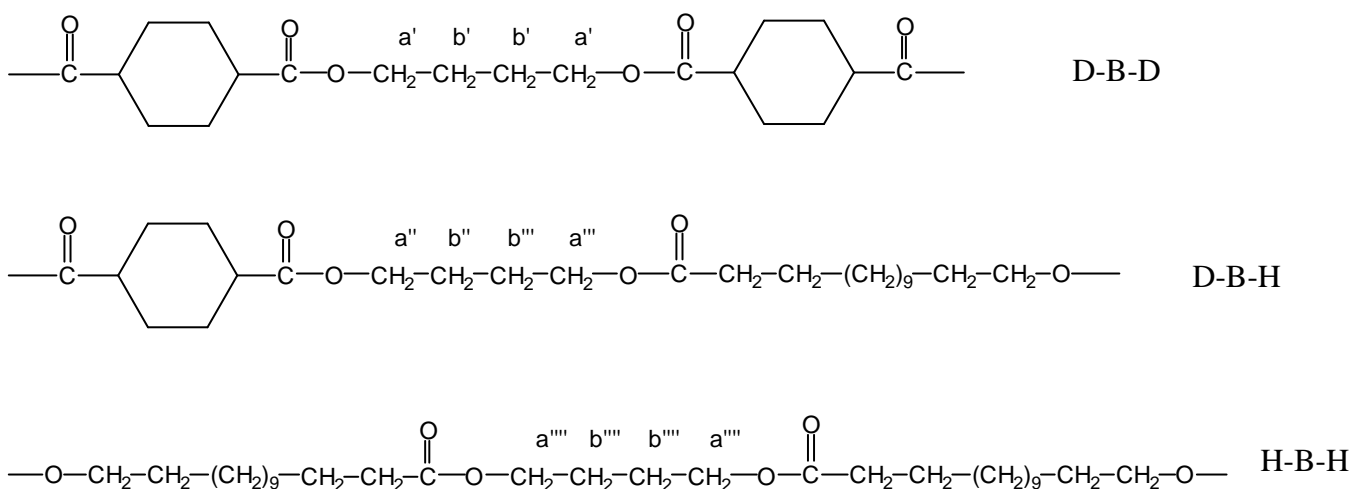
### ***Aliphatic-Aliphatic copolyesters***

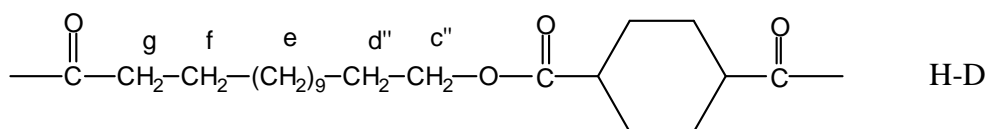
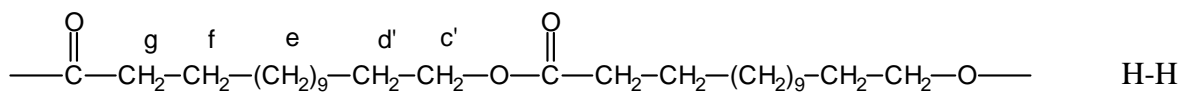
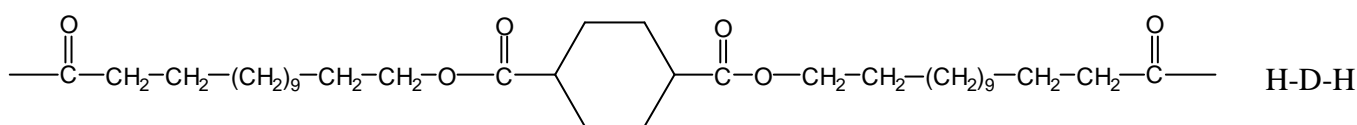
Figure 3.22 shows the  $^1H$ -NMR spectrum for the P14HA-*co*-PBCHD<sub>100</sub>-40/60 sample and the signal assignments are reported. As for the aliphatic-aromatic copolyesters the spectra were found to be consistent with the expected structures.



**Figure 3.22 NMR spectra of P14HA-co-PBCHD<sub>100-40/60</sub> sample**

For the fully aliphatic copolyesters it is not possible (because of the same chemical shift) to identify protons  $H^{a'}$ ,  $H^{a''}$ ,  $H^{a'''}$ ,  $H^{a''''}$  e  $H^{b'}$ ,  $H^{b''}$ ,  $H^{b'''}$ ,  $H^{b''''}$  that are relative to the following sequences:





As discussed for H-T-H sequence in the aliphatic-aromatic copolyesters, the formation of the H-D-H (where D is the cyclohexane dicarboxylate unit) sequence should be less frequent than the others because all the synthesis have been made with an excess of butanediol

Also H<sup>c'</sup>, H<sup>c''</sup> and H<sup>d'</sup>, H<sup>d''</sup> protons that are relatives to the HH and HD, cannot be identified.

For this reason it is not possible for P14HA-*co*-PBCHD copolymers to carry out the same molecular analysis carried out for P14HA-*co*-PBT copolymers. The randomness degree (B) and the sequence length cannot be evaluated for fully aliphatic copolyesters.

The 14HA/DMCD ratio has been calculated considering the signal of the eighteen protons H<sup>e</sup> of the hydroxyacid at 1.25 ppm and the signals of protons H<sup>2t</sup> e H<sup>1c</sup> (4 and 2 protons respectively) of the DMCD ring at 2.05 and 2.45 ppm. The trans percentage in the aliphatic ring has been calculated by considering the signals of protons H<sup>2t</sup> (4 protons) and H<sup>1c</sup> (2 protons). All the results are reported in Table 3.7.

### 3.3.4. DSC analysis

#### *Aliphatic-Aromatic copolyesters*

The P14HA-*co*-PBT are semicrystalline materials whose properties change as a function of the comonomer content. Table 3.11 collects the DSC data of all the samples, homopolymers, copolymers and ECOFLEX as an example of a commercial copolymer

**Table 3.11 DSC data of aliphatic-aromatic copolyesters**

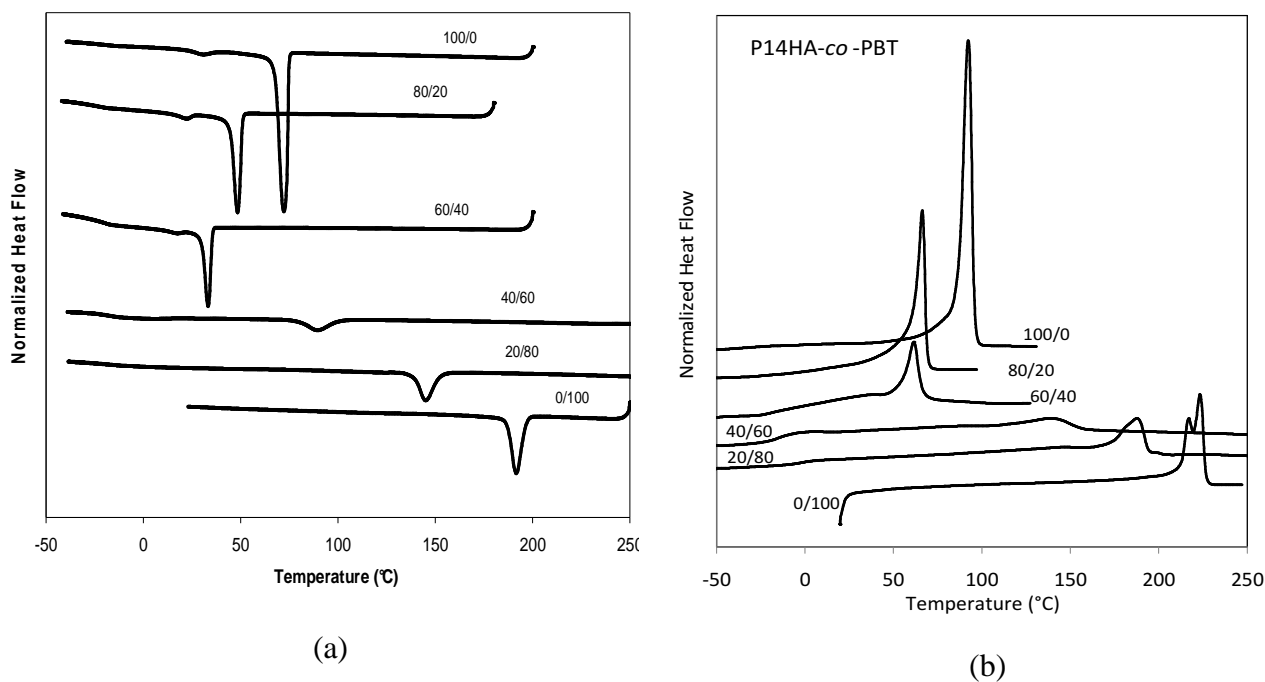
Sample	$T_{cc}$ (°C) <sup>a</sup>	$\Delta H_{cc}$ (J.g <sup>-1</sup> ) <sup>a</sup>	$T_g$ (°C) <sup>b</sup>	$T_m$ (°C) <sup>b</sup>	$\Delta H_m$ (J.g <sup>-1</sup> ) <sup>b</sup>
<i>Homopolymers</i>					
P14HA	72	116	-	92	120
PBT	189	48	-	224	43
<i>Aliphatic aromatic copolymers</i>					
P14HA-co-PBT-80/20	48	62	-	66	68
P14HA-co-PBT-60/40	33	41	-	61	25
P14HA-co-PBT-40/60	90	21	-15	140	15
P14HA-co-PBT-20/80	145	36	-2	188	26
ECOFLEX	80	21	-31	124	11

<sup>a</sup> measured during the cooling scan at 10°C/min

<sup>b</sup> measured during the second heating scan at 10°C/min

Figure 3.23 shows the crystallization and melting curves of these copolymers with different composition.

It is evident that, from pure P14HA, by increasing the content of PBT,  $T_c$  and  $T_m$  decrease from the values of 72 and 92°C of the P14HA to the values of 33 and 61°C of the sample containing 40 mol% of PBT. At higher (>40%) molar content of PBT,  $T_c$  and  $T_m$  notably increase towards the PBT values.

**Figure 3.23 Cooling scan (a) and second heating scan (b) of P14HA-co-PBT copolyesters**

P14HA is characterized by an enthalpy of crystallization of 120 J/g, indicating a very high level of crystallinity, whereas PBT is characterized by a notably lower degree of crystallinity ( $\Delta H_m = 43$  J/g). The copolymers are characterized by a decrement of crystallinity with the increment of PBT content, with a minimum for the sample containing 60 mol% of PBT.

To better understand the crystallization behavior of the copolymers, Figure 3.24 shows the WAXD spectra performed at room temperature.

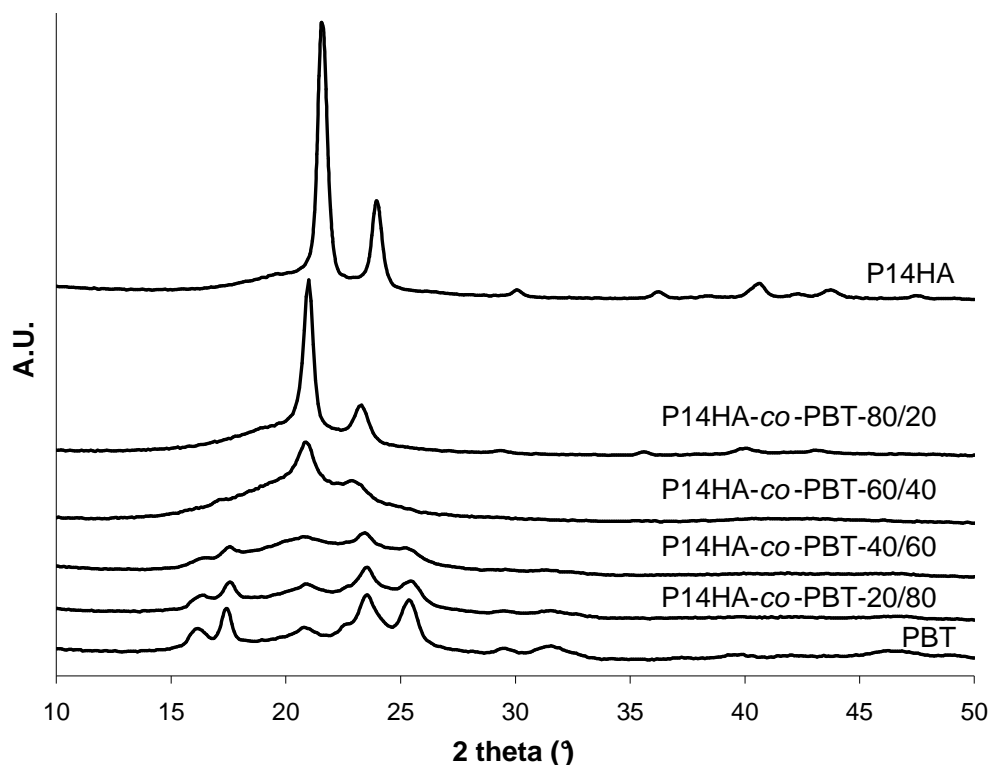


**Figure 3.24 XRD spectra of aliphatic-aromatic copolyesters**

It is evident that the copolymers rich in P14HA unit crystallize in the P14HA crystalline phase and that the degree of crystallinity decreases from P14HA to the P14HA-*co*-PBT-60/40 copolymer.

Increasing the content of PBT (60 mol%), the copolymer starts to crystallize in the crystalline phase of the PBT. Therefore, both P14HA and PBT sequences are able to crystallize even in the presence of a comonomer.

### *Aliphatic-Aliphatic copolyesters*

Table 3.12 shows the DSC results for all the fully aliphatic copolyesters:

**Table 3.12 DSC data for fully aliphatic copolyesters**

Sample	$T_{cc}$ ( $^{\circ}\text{C}$ ) <sup>a</sup>	$\Delta H_{cc}$ ( $\text{J}\cdot\text{g}^{-1}$ ) <sup>a</sup>	$T_g$ ( $^{\circ}\text{C}$ ) <sup>b</sup>	$T_m$ ( $^{\circ}\text{C}$ ) <sup>b</sup>	$\Delta H_m$ ( $\text{J}\cdot\text{g}^{-1}$ ) <sup>b</sup>
<i>Homopolymers</i>					
P14HA	72	116	-	92	120
PBCHD <sub>100</sub> (100% trans)	139	43	18	161-167	42
PBCHD <sub>50</sub> (50% trans)	-	-	-9	-	-
<i>Aliphatic copolymers</i>					
P14HA- <i>co</i> -PBCHD <sub>100</sub> -80/20	51	69	-	68	74
P14HA- <i>co</i> -PBCHD <sub>100</sub> -60/40	37	44	-	60	38
P14HA- <i>co</i> -PBCHD <sub>100</sub> -40/60	59	26	-19	95	18
P14HA- <i>co</i> -PBCHD <sub>100</sub> -20/80	104	36	-27	131 – 138	25
P14HA- <i>co</i> -PBCHD <sub>50</sub> -80/20	58	48	-	66	60
P14HA- <i>co</i> -PBCHD <sub>50</sub> -20/80	-	-	-29	-	-

<sup>a</sup> measured during the cooling scan at 10°C/min, <sup>b</sup> measured during the second heating scan at 10°C/min

Fig. 3.25 represent the crystallization and melting curves of P14HA-*co*-PBCHD<sub>100</sub>

P14HA-*co*-PBCHD<sub>100</sub> are semicrystalline materials with the same behaviour of the aliphatic-aromatic copolyesters: starting from P14HA, by increasing PBCHD<sub>100</sub> content,  $T_c$ , and  $T_m$ , decrease to reach a minimum in the sample with 60% mol of PBCHD<sub>100</sub>. Then, by increasing PBCHD amount,  $T_c$  and  $T_m$  increase towards the values characteristic of PBCHD<sub>100</sub> homopolymer. With high content of cycloaliphatic unit a double melting peak appears and this is attributed to a melting-recrystallization-remelting process occurring during the calorimetric scan (Berti, 2008 A).

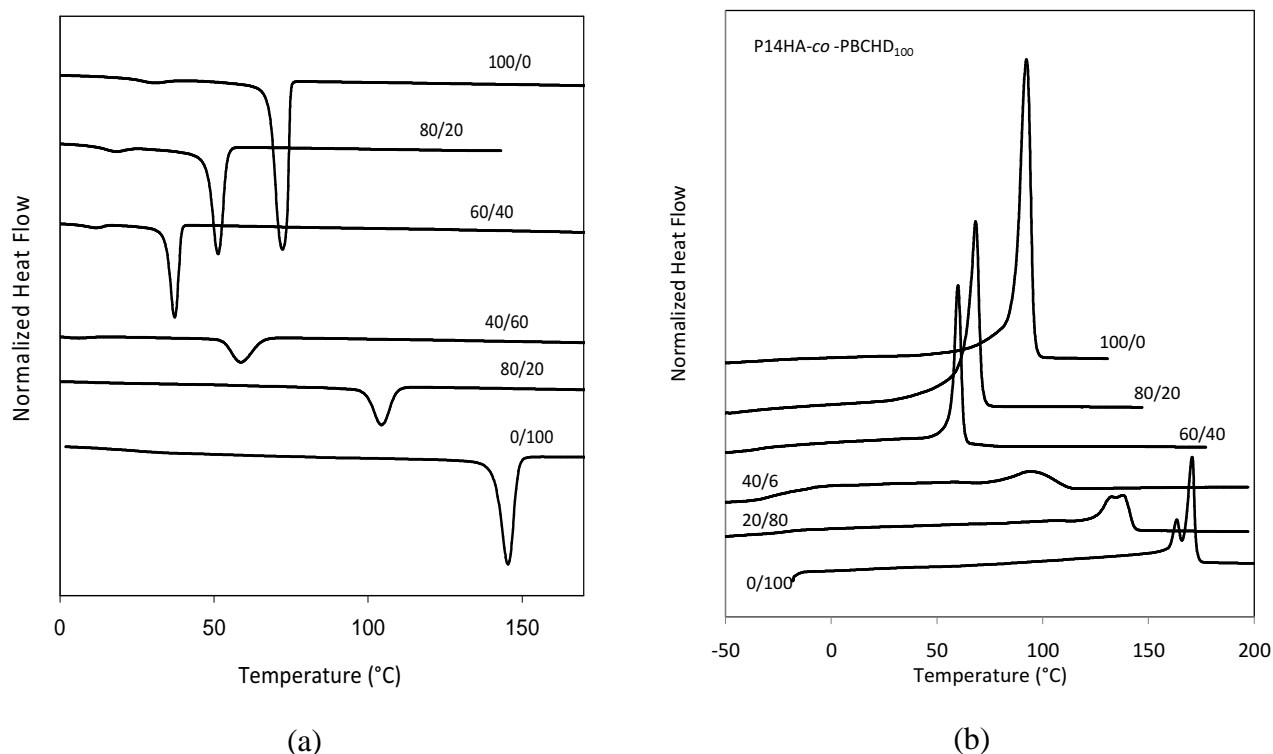


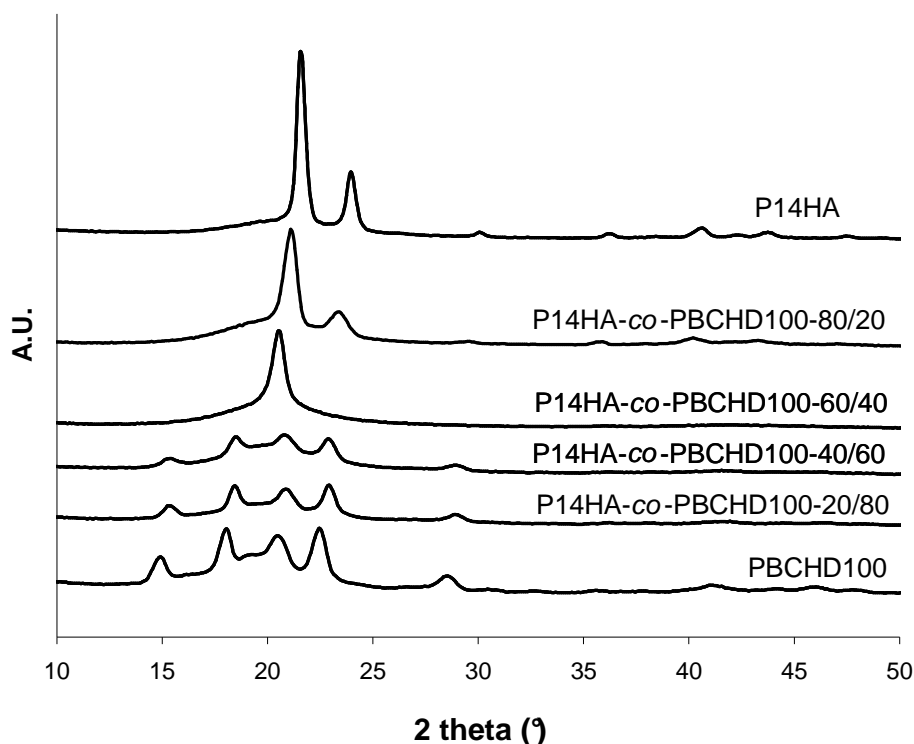
**Figure 3.25 Cooling scan (a) and second heating scan (b) of P14HA-*co*-PBCHD<sub>100</sub> copolyesters**

Starting from P14HA, increasing the PBCHD<sub>100</sub> content, the copolyesters show a decrement of crystallinity with a minimum for the P14HA-*co*-PBCHD<sub>100</sub>-40/60 sample; after that the crystallinity rises again towards the PBCHD<sub>100</sub> values.

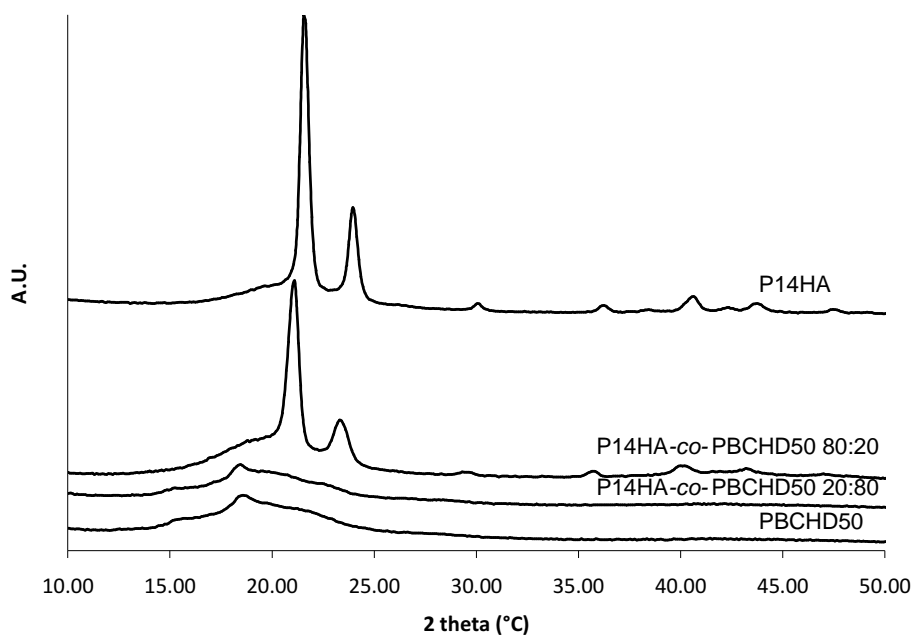
The thermal properties of P14HA-*co*-PBCHD<sub>50</sub> are strongly influenced by the composition: the copolyester rich in P14HA unit is a semicrystalline material, indicating that P14HA is able to crystallize even in presence of PBCHD<sub>50</sub>, that is a well know amorphous unit (Berti, 2008 A), due to the high content of isomer *cis* in the aliphatic ring.

On the contrary, with an high content of PBCHD<sub>50</sub>, the P14HA couldn't crystallize and the material results fully amorphous like the PBCHD<sub>50</sub> homopolymer.

To better understand the DSC results, Figure 3.26 shows the WAXD spectra performed at room temperature of both series of the aliphatic-aliphatic copolyesters.



(a)



(b)

**Figure 3.26 XRD spectra of P14HA-*co*-PBCHD<sub>100</sub> (a) and P14HA-*co*-PBCHD<sub>50</sub> (b) copolyesters**

From Figure 3.26 (a) it is evident that the copolyesters rich in P14HA crystallize in the crystalline phase of the parent homopolymers and that crystallinity decreases with the increment of PBCHD<sub>100</sub> content. The copolyesters rich in PBCHD<sub>100</sub>, instead, crystallize in the crystalline phase of PBCHD<sub>100</sub> homopolymer. This is the same behaviour found in the aliphatic-aromatic copolymers.

In Fig. 3.26 (b) P14HA-*co*-PBCHD<sub>50</sub>-80/20 spectra confirms the capability of this copolymer to crystallize in the P14HA crystalline phase. On the contrary the P14HA-*co*-PBCHD<sub>50</sub>-20/80 specimen shows a WAXS spectrum typical of an amorphous polymer.

### 3.3.5. DMTA analysis

#### *Aliphatic-Aromatic copolyesters*

Fig. 3.27 shows the dynamical mechanical spectra of the two homopolymers (P14HA and PBT) and some aliphatic-aromatic copolymers with different composition

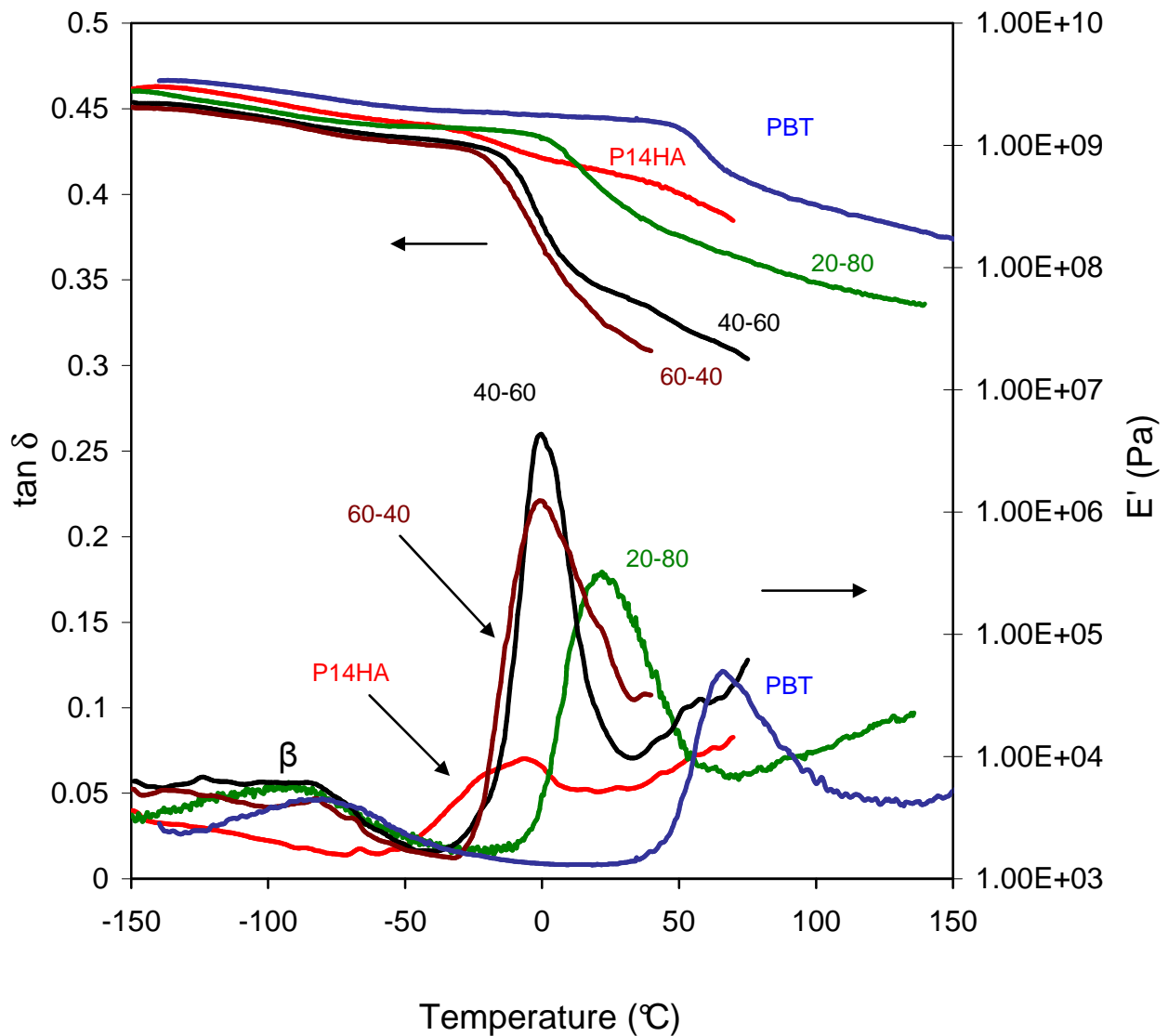


**Figure 3.27 DMTA spectra of P14HA and PBT homopolymers and some of the new copolymers**

Both homopolymers and copolymers, in the temperature range from  $-50^{\circ}\text{C}$  to  $150^{\circ}\text{C}$ , exhibit an intense peak of  $\tan \delta$ , denoted as  $\alpha$  relaxation, which is confidently assigned to the glass-to-rubber transition. The intensity of the peak is proportional to the degree of crystallinity: more crystalline is the sample, less intense is the peak. In the range from  $-150^{\circ}\text{C}$  to  $-50^{\circ}\text{C}$  all the samples (with the exception of P14HA) show a secondary relaxation, denoted as  $\beta$  relaxation, located at about  $-90^{\circ}\text{C}$  and characterized by low intensity. It is worth remembering that the presence of a secondary relaxation, due to the main chain, is beneficial for impact resistance and is often described as a phenomenon which facilitates the macroscopic shear yielding (Chen, 1998).

Considering the elastic modulus ( $E'$ ), Fig. 3.27 shows that P14HA has a lower  $E'$  than PBT in all temperature range: this is due to the higher rigidity of the PBT given by the aromatic ring. In copolymers, when the percentage of P14HA unit increases, the modulus decreases, in agreement

with the thermal results: the crystallinity of the samples become lower and lower and the rigidity of the system decreases.

### *Aliphatic-Aliphatic copolyesters*

Fig. 3.28 shows the dynamical mechanical spectra of the two homopolymers (P14HA and PBCHD) and some aliphatic-aliphatic copolymers with different composition.

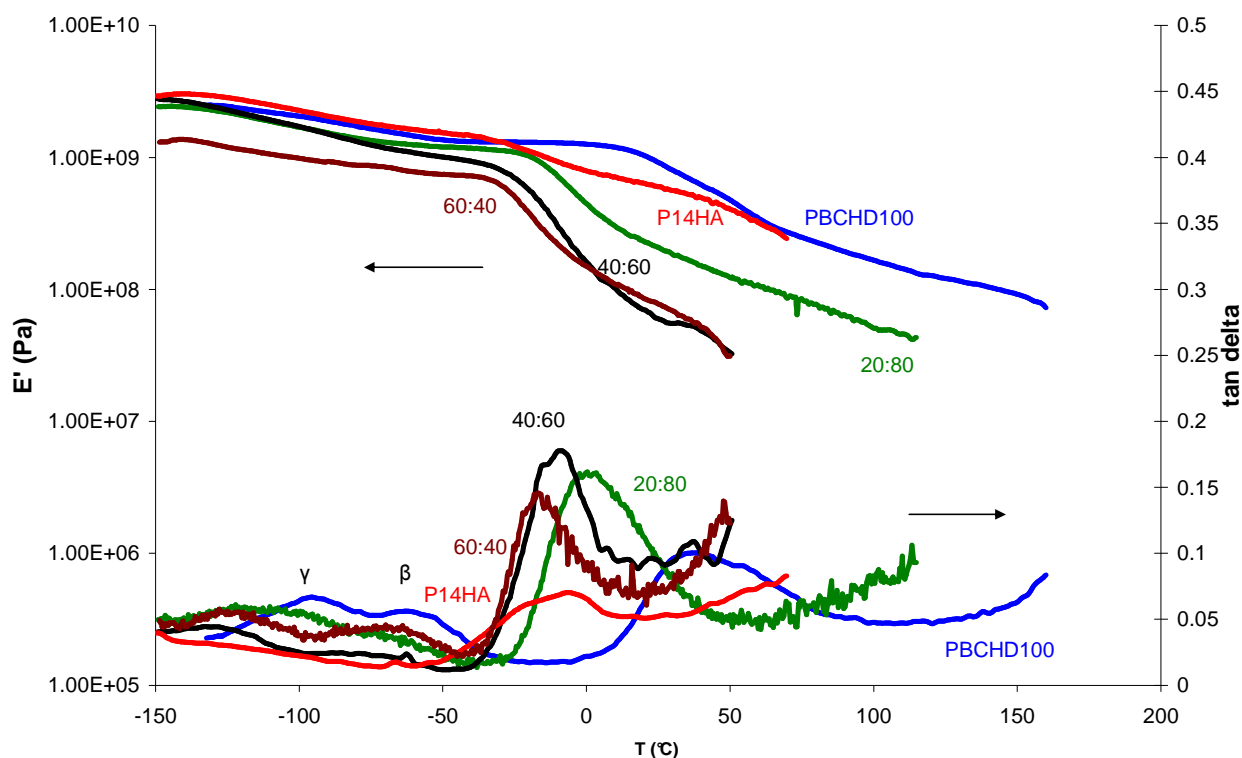


**Figure 3.28 DMTA spectra of P14HA and PBT homopolymers and some of the new fully aliphatic copolymers**

As for the aliphatic-aromatic series, all these samples, in the temperature range from  $-50^{\circ}\text{C}$  to  $150^{\circ}\text{C}$ , exhibit an intense peak of  $\tan \delta$  that is due to the glass transition and, then, strictly related to the crystallinity degree of the material. In the range from  $-150^{\circ}\text{C}$  to  $-50^{\circ}\text{C}$  all the samples show two secondary relaxations (except for P14HA in which they are not detectable) that are more intense in the homopolymers: they are named  $\gamma$  and  $\beta$  relaxations. The  $\gamma$  relaxation has traditionally been associated with restricted motions of the chain in polymers with aliphatic sequences. It is influenced by different factors among which the degree of crystallinity play a significant role (McCrum, 1967): the intensity of the peak increases with the increment of crystallinity. The  $\beta$  relaxation originates from the chair-boat-chair conformational transition of the cyclohexylene ring (Chen, 1998) and, as for  $\gamma$  relaxation, its intensity strictly depends on the flexibility of the chain.

Considering the elastic modulus ( $E'$ ), Fig. 3.28 shows that P14HA has a  $E'$  close to that of PBCHD<sub>100</sub>. In the copolymers, in intermediate compositions, the elastic modulus decreases (as seen for the aliphatic-aromatic series). This behaviour is in agreement with the thermal results: the crystallinity of the samples decreases and the rigidity of the system too.

### 3.3.6. Tensile tests

#### *Aliphatic-Aromatic copolyesters*

Table 3.13 collects the results of the tensile tests of the aliphatic-aromatic copolyesters together with those of Ecoflex as a reference material:

**Table 3.13 Tensile data of P14HA-co-PBT samples**

Sample	Young's Modulus (Mpa)	Elongation at break, %	stress at break (MPa)	stress at yield (MPa)	strain at yield %
P14HA	414.1±50.9	638.0±128	13.5±2.4	17.2±2.3	12.2±0.9
P14HA-co-PBT-80/20	61.0±17.8	613.0±34.9	5.9±0.6	5.7±0.6	60.5±4.0
P14HA-co-PBT-60/40	43.3±9.8	1284.0*	7.9±1.2	4.4±0.7	21.8±2.0
P14HA-co-PBT-40/60	66.3±10.4	757.0±223.5	12.2±3.7	7.8±1.4	30.0±2.4
P14HA-co-PBT-20/80	249.1±36.0	455.8±30.7	23.2±1.0	20.4±0.4	27.7±3.6
PBT	950.3±104.2	271.9±70.7	37.6±2.5	48.3±1.5	15.0±1.1
Ecoflex	67.8±7.9	1204.0±264.0	17.9±2.6	8.4±0.9	36.4±2.9

\*no breakage

P14HA homopolymer is characterized by quite high elongation at break (638%) and Young's modulus (414 MPa) due to the long aliphatic chains and the very high crystallinity, whereas PBT, that has a rigid aromatic aromatic ring in the structure, shows a very high modulus (950MPa) but low elongation at break (271%).

In all the copolymers there is a strong decrement of Young's Modulus due to the lower crystallinity of the samples compared to that of the homopolymer: for example by adding only 20% mol of PBT unit to P14HA the values go from 414MPa to 61MPa. Moreover, the decrement in crystallinity leads to a general increment in the elongation at break.

In particular a very interesting copolymer is the P14HA-co-PBT-40/60: due to its very low crystallinity, it is characterized by the lowest Young's modulus (43MPa) and the highest elongation at break (1284% with no breakage) among all the samples of this series. These results are very similar to those obtained from Ecoflex that is one of the most important polymer currently used in packaging industry.

### *Aliphatic-Aliphatic copolyesters*

Table 3.14 collects the results of the tensile tests of all aliphatic-aliphatic copolyesters together with those of Ecoflex as a reference material:

**Table 3.14 Tensile data of aliphatic-aliphatic samples**

Sample	Young's Modulus (Mpa)	Elongation at break, %	stress at break (MPa)	stress at yield (MPa)	strain at yield %
P14HA	414.1±50.9	638.0±128	13.5±2.4	17.2±2.3	12.2±0.9
P14HA- <i>co</i> -PBCHD <sub>100</sub> -80/20	68.9±7.2	22.9±5.0	5.2±0.5	--	--
P14HA- <i>co</i> -PBCHD <sub>100</sub> -60/40	47.6±6.4	944.6±100.3	3.9±0.2	3.8±0.6	22.8±2.9
P14HA- <i>co</i> -PBCHD <sub>100</sub> -40/60	83.3±6.6	152.2±43.7	6.3±0.4	7.2±0.3	22.5±3.8
P14HA- <i>co</i> -PBCHD <sub>100</sub> -20/80	201.9±20.5	448.8±20.5	18.9±0.7	16.3±0.9	24.8±1.3
PBCHD <sub>100</sub>	727±89	18.0±3.8	40.9±3.6	--	--
P14HA- <i>co</i> -PBCHD <sub>50</sub> -80/20	67.1±11.0	17.8±7.8	4.8±0.5	-	-
P14HA- <i>co</i> -PBCHD <sub>50</sub> -20/80	22.5±6.1	703.9±74.7	4.3±0.6	2.9±0.3	33.9±12.1
PBCHD <sub>50</sub>	157.7±15.4	494.3±52.1	10.6±0.6	10.3±0.7	23.2±1.5
Ecoflex	67.8±7.9	1204.0±264.0	17.9±2.6	8.4±0.9	36.4±2.9

The two PBCHD homopolymers have a very different behaviour: because of the high trans percentage in the aliphatic ring, PBCHD<sub>100</sub> is semicrystalline material and it is characterized by high rigidity (high modulus) and very low elongation at break. PBCHD<sub>50</sub> has a high percentage of cis isomer and this leads to an amorphous material with low modulus and good elongation at break. As reported for the aliphatic-aromatic copolyesters, the aliphatic-aliphatic samples low values of the modulus and high values in the elongation at break at intermediate compositions. The two samples with a content of P14HA of 80 mol% present poor mechanical properties concerning both Young's modulus and elongation at break.

The mechanical properties of P14HA-*co*-PBCHD<sub>100</sub>-60/40 are very close to those of Ecoflex: this is a very interesting result because the novel copolymer is fully aliphatic and is very promising for biodegradability tests.

### **3.3.7. Conclusions**

Novel copolyesters starting from renewable sources were successfully synthesized by combining a biotechnological route to obtain the  $\omega$ -hydroxy acid from fatty acids and chemical syntheses to produce copolyesters from potentially biobased monomers.

The novel bio-based polymers contain long aliphatic chains, which impart flexibility and high crystallizability, as well as aliphatic or aromatic rings, which give to the macromolecules rigidity and, then, high melting temperatures and good mechanical performances. By changing the molar

composition of these copolyesters a wide range of thermal and mechanical properties can be achieved.

All the samples (except P14HA-*co*-PBCHD<sub>50</sub>-20/80) are semicrystalline materials with the crystalline phase of the homopolymers whose units have the highest molar content. The copolyesters are characterized by a lower level of crystallinity than the homopolymer and this strongly influence their mechanical properties.

Another interesting aspect of these new materials is that the presence of 14HA units could improve the biodegradability of PBT (the fully aliphatic copolyesters should be completely biodegradable).

### **3.4. TiO<sub>2</sub> Composites Based on Aliphatic Polyesters**

#### **3.4.1. Introduction**

Degradability or, on the contrary, durability of polymers are very important features affecting the performances of all plastics in daily life. The degradation of polymers, due to different environmental factors, including light exposure, involves several physical and/or chemical processes, accompanied by structural changes, which lead to deterioration of the quality of the polymer properties (mechanical, electrical, aesthetic properties).

For the purpose of increasing durability of polymeric materials, substances, named stabilizers, are often incorporated into the polymer matrix. The study of stabilizers, their characteristics and effects is a growing field of research for developing materials with improved properties. In particular, recently, large interest has been devoted to nanoscale particles and, thus, to the polymer nanocomposite systems (Kumar, 2009).

Among all the particles and nanoparticles which can be used in a polymer matrix to improve its durability, titanium dioxide (TiO<sub>2</sub>) is known for the capability of absorbing UV radiation, producing electron-hole pairs. The photosensitivity of TiO<sub>2</sub> has been thoroughly studied (Carp, 2004). There are three different common crystalline phases of TiO<sub>2</sub>, rutile, anatase, and brookite.

TiO<sub>2</sub> nanoparticles conferred significant protection from UV to polypropylene, prolonging survived life of the outdoor products. Epoxy polymer films filled with TiO<sub>2</sub> nanoparticles increase elastic modulus upon UV irradiation (Kumar, 2009). Photo-stable polyethylene terephthalate films were prepared by a bilayer coating, consisting of a TiO<sub>2</sub> layer on top (Awitor, 2008).

However, the interaction between UV radiation and the TiO<sub>2</sub> surface would generate free radicals that might degrade polymers. For example, in literature it is reported the solid-phase photocatalytic degradation of poly(vinyl chloride) (PVC) – TiO<sub>2</sub> composites (Cho, 2001).

Polystyrene films, where nano-TiO<sub>2</sub> particles grafted the polymer onto the surface, were photocatalytically degraded under UV illumination in air (Zan, 2004).

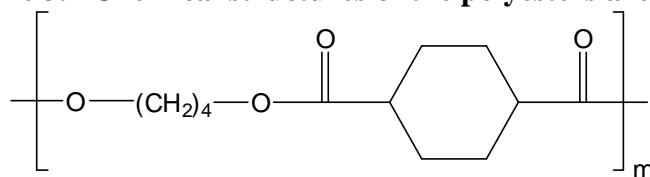
TiO<sub>2</sub> is also an attractive filler for biodegradable polymer matrices (Kokubo, 2008; Lu, 2008). For example, TiO<sub>2</sub> nanoparticles were mixed in a high-shear extruder to poly(butylene succinate), an aliphatic, degradable polyester, to enhance photocatalytic decomposition and biodegradation rates (Miyachi, 2008).

In front of all these new developments, the effect of TiO<sub>2</sub> on some polyesters, recently synthesized and analyzed by the Polymer Science group of the Department of Civil, Environmental and Materials Engineering of University of Bologna, seemed really interesting. New composites, based on poly(butylene 1,4-cyclohexanedicarboxylate) (PBCHD) and poly(1,4-cyclohexylenedimethylene 1,4-cyclohexanedicarboxylate) (PCCD), have been prepared. TiO<sub>2</sub> particles, with size larger than 5 μm, have been mixed with polymer in the molten state. With respect to the nanoparticles, which are characterized by a high surface area and, then, high efficiency, also particles with dimensions of the order of microns can be successful used to improve polymer performance, with the advantage that a good particulate dispersion is often obtained in a easier way in composites than in nanocomposites. The effect of the TiO<sub>2</sub> particles, in forms of anatase and rutile crystals separately, has been analyzed.

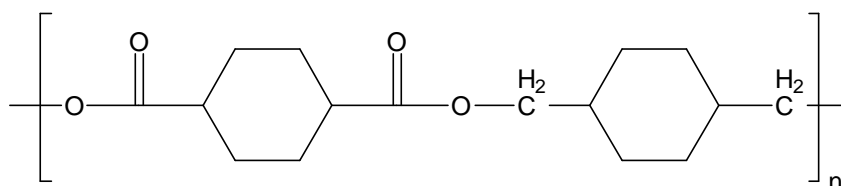
### 3.4.2. Materials

Polyesters, whose chemical formula are reported in Scheme 3.4, were obtained by a two-stage polycondensation, using titanium tetrabutoxide (TBT) as catalyst.

**Scheme 3.4 Chemical structures of the polyesters analyzed.**



PBCHD



PCCD

The poly(butylene 1,4-cyclohexanedicarboxylate) sample is named PBCHD<sub>100</sub>, where 100 indicates the content of the *trans* isomer of the cycloaliphatic unit. PBCHD<sub>100</sub> was prepared from 1,4-butanediol and dimethyl-1,4-cyclohexane dicarboxylate, containing 100% of *trans* isomer (Berti, 2008 A). The  $M_w$  is equal to 33000 and  $M_w/M_n$  is 2.6, determined by gel permeation chromatography (GPC) in chloroform.

The poly(1,4-cyclohexylenedimethylene 1,4-cyclohexanedicarboxylate) sample (PCCD<sub>97</sub>) has been prepared starting from 1,4-cyclohexanedimethanol and dimethyl-1,4-cyclohexane dicarboxylate, as described in (Berti, 2008 B). This sample is characterized by a 66% of *trans* isomer derived from the diol and 97% of *trans* isomer derived from the diester.  $M_w$  is equal to 55,100 and  $M_w/M_n$  is 2.2, determined by GPC in chloroform.

For the polyesters the molecular structure and *trans* content were determined by <sup>1</sup>H NMR analysis, recorded on samples dissolved in CDCl<sub>3</sub>.

TiO<sub>2</sub> particles (from Aldrich Chemicals), crystallized in anatase and rutile crystals separately, are characterized by a size of particles major than 5 μm.

### 3.4.3. Sample preparation

The composites were prepared in a Brabender (Plasti-Corder PL 2000). PBCHD<sub>100</sub> was mixed with TiO<sub>2</sub>, in anatase and rutile crystalline forms separately, at 250° for 10 minutes. PCCD<sub>100</sub> was mixed with anatase and rutile at 180°C for 10 minutes. The composition of the materials is described in Table 3.15.

**Table 3.15 Composition of the TiO<sub>2</sub>-polyester composites**

Polymer matrix	TiO <sub>2</sub> crystalline form	amount of TiO <sub>2</sub> (wt%)	Code name
PBCHD <sub>100</sub>	anatase	1.0	PBCHD <sub>100</sub> 1% ana
		2.0	PBCHD <sub>100</sub> 2% ana
		5.0	PBCHD <sub>100</sub> 5% ana
	rutile	1.0	PBCHD <sub>100</sub> 1% rut
		2.0	PBCHD <sub>100</sub> 2% rut
		5.0	PBCHD <sub>100</sub> 5% rut
PCCD <sub>97</sub>	anatase	2.0	PCCD <sub>97</sub> 2% ana
		5.0	PCCD <sub>97</sub> 5% ana
	rutile	2.0	PCCD <sub>97</sub> 2% rut

### 3.4.4. Thermal properties

Table 3.16 collects all the thermal data of the composites obtained by DSC analysis.

The differences between the two matrixes are related to structure of the polyesters shown in Scheme 3.4: PBCHD<sub>100</sub> and PCCD<sub>97</sub> are both semicrystalline because they have an high content of trans isomer in the aliphatic rings. PCCD<sub>97</sub> has a melting temperature point about 60 degrees higher than the PBCHD<sub>100</sub>: the substitution of the aliphatic –CH<sub>2</sub>– moieties with a cycloaliphatic unit gives a considerable rigidity to the macromolecular chain.

**Table 3.16 Thermal data of all the composites**

Sample	T <sub>CC</sub> <sup>a)</sup> °C	ΔH <sub>CC</sub> <sup>a)</sup> J.g <sup>-1</sup>	T <sub>m</sub> <sup>b)</sup> °C	ΔH <sub>m</sub> <sup>b)</sup> J.g <sup>-1</sup>
PBCHD <sub>100</sub>	146	50	163-170	46
PBCHD <sub>100</sub> 1% ana	148	49	161-169	42
PBCHD <sub>100</sub> 2% ana	148	47	162-169	41
PBCHD <sub>100</sub> 5% ana	148	50	161-168	43
PBCHD <sub>100</sub> 1% rut	148	46	161-169	43
PBCHD <sub>100</sub> 2% rut	147	47	162-169	43
PBCHD <sub>100</sub> 5% rut	147	48	162-169	44
PCCD <sub>97</sub>	198	31	233	30
PCCD <sub>97</sub> 2% ana	222	34	229	26
PCCD <sub>97</sub> 5% ana	228	32	202	36
PCCD <sub>97</sub> 2% rut	201	32	228	28

<sup>a)</sup>Measured in DSC (cooling scan at 10°C.min<sup>-1</sup>)    <sup>b)</sup>Measured in DSC (2<sup>nd</sup> heating scan at 10°C.min<sup>-1</sup>)

PCCD<sub>97</sub> shows only one melting peak while PBCHD<sub>100</sub> has a double melting peak: this is attributed to melting-recrystallization-remelting process occurring during the calorimetric scan. The low endotherm is attributed to the superimposition of the melting endotherm of the pre-existing crystals and the recrystallization exotherm of the material which has just melted. The high endotherm, located at temperatures where the recrystallization can no longer occur, is due to the melting of the crystals formed during the heating scan as a dominant process.

The addition of TiO<sub>2</sub> particles does not affect the thermal properties of the samples: all the composites reflect the same properties of the corresponding matrix.

### 3.4.5. Photodegradation of virgin matrixes (PBCHD<sub>100</sub> and PCCD<sub>97</sub>)

The photodegradability study was performed on films (about 100 μm) prepared by compression molding between two teflon sheets at temperature slightly above the melting temperature, previously determined by DSC measurement.

After having exposed PBCHD<sub>100</sub> and PCCD<sub>97</sub> to UV irradiation at 60°C for different exposure times in an accelerated photo-ageing device (SEPAP 14-24), the films were analyzed by an FTIR instrument.

As shown in Figures 3.29 and 3.30, the photodegradation results in significant changes in the IR spectra in the hydroxyl absorption region of the infrared spectra (3800 – 3200 cm<sup>-1</sup>): in particular there is an increase in absorbance in the band centered near 3430 cm<sup>-1</sup> with the increment of the exposure times. This band has been attributed to the formation of alcohols, acids and hydroperoxydes, which are expected degradation products for polyesters under UV irradiation. Typically, degradation rates in films can be characterized by looking at stable products produced during irradiation, as revealed by the changes in the IR spectra. Here, the photo-oxidation reactions in aliphatic polyesters are shown by the absorbance increase at 3430 cm<sup>-1</sup>; this has the direct consequence that even the effect of photo-oxidation of the composites can be directly monitored by measuring this change in absorbance.

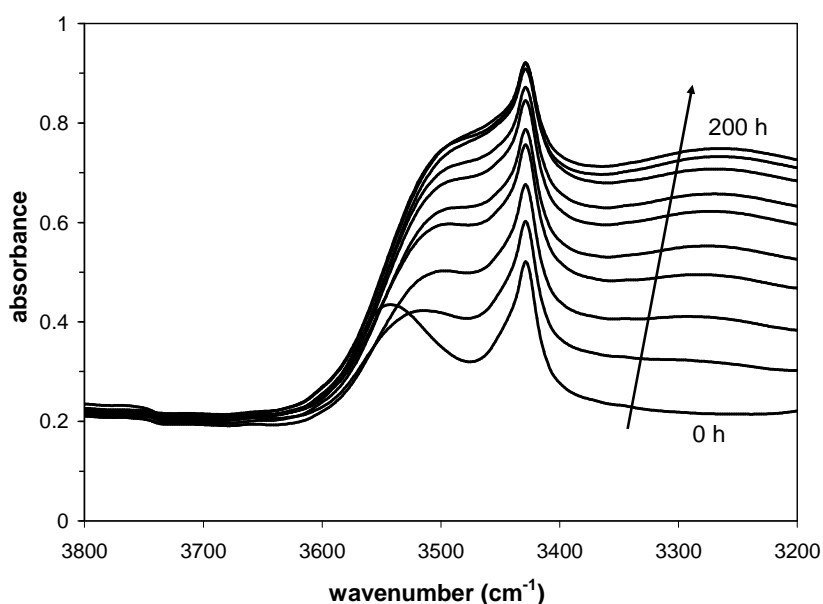


**Figure 3.29** IR spectra for PBCHD<sub>100</sub> – zoom OH region for different exposure times

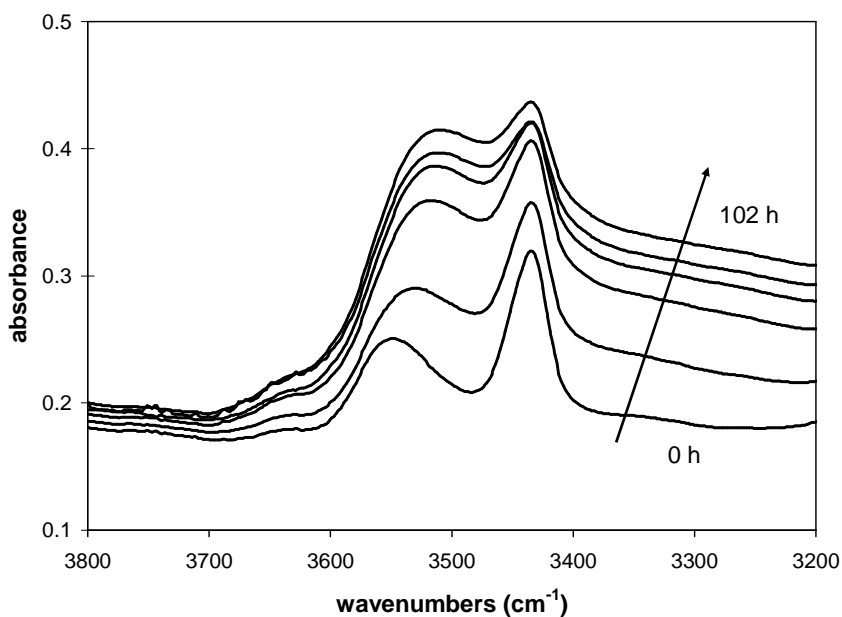


**Figure 3.30** IR spectra for PCCD<sub>97</sub> – zoom OH region for different exposure times

Figure 3.31 shows the change in the absorbance at 3430 cm<sup>-1</sup> versus irradiation time for both PBCHD<sub>100</sub> and PCCD<sub>97</sub>:

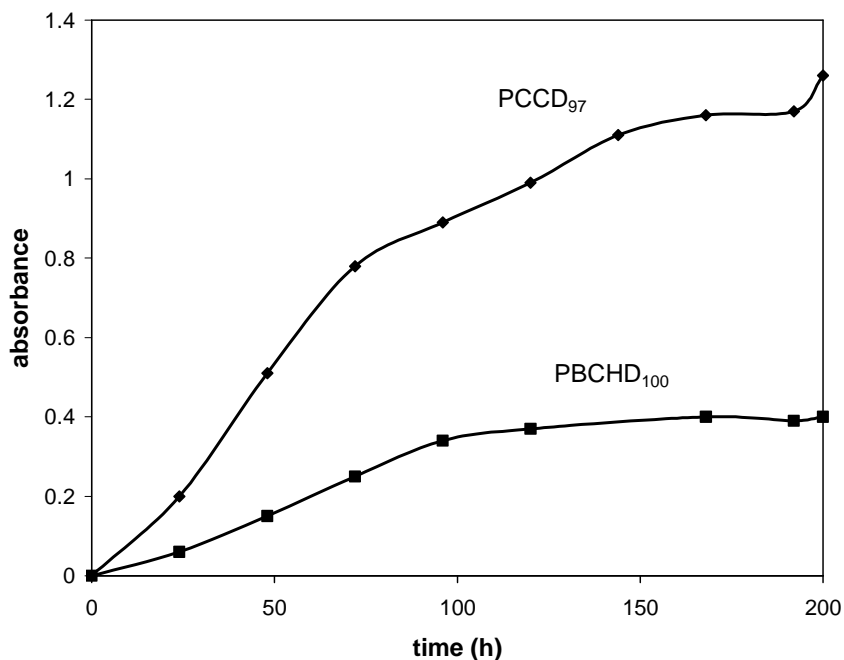


**Figure 3.31** Comparison of the evolution of the OH signal as a function of the ageing time in IR spectra for PBCHD<sub>100</sub> and PCCD<sub>97</sub>

The photodurability of PBCHD<sub>100</sub> is greater than the one of PCCD<sub>97</sub> and this can be related to the molecular structure of the two polymers: a single aliphatic ring is more stable towards UV exposure with respect to two aliphatic rings.

### 3.4.6. Photodegradation of composites

The UV exposure of all the composites has been conducted under the same conditions used for the matrix. UV-vis analysis has been used together with the FTIR analysis to investigate the impact of the TiO<sub>2</sub> on PBCHD<sub>100</sub> and PCCD<sub>97</sub>.

#### *Impact of TiO<sub>2</sub> on PBCHD<sub>100</sub> durability*

Fig. 3.32 shows the evolution of the OH signal versus irradiation time in FTIR spectra. As discussed above, this directly indicates the effectiveness of TiO<sub>2</sub> in protecting the matrix from photo-oxidation.

The addition of TiO<sub>2</sub> in the matrix provides some protection to PBCHD<sub>100</sub> photo degradation and the effect is proportional to the amount of TiO<sub>2</sub> present in the sample. This behavior has been found for both the TiO<sub>2</sub> crystalline forms, rutile and anatase. Comparing the samples with the same percentage of TiO<sub>2</sub> it is clear that anatase is much more effective than the rutile form in protecting from UV radiation the polymeric matrix.

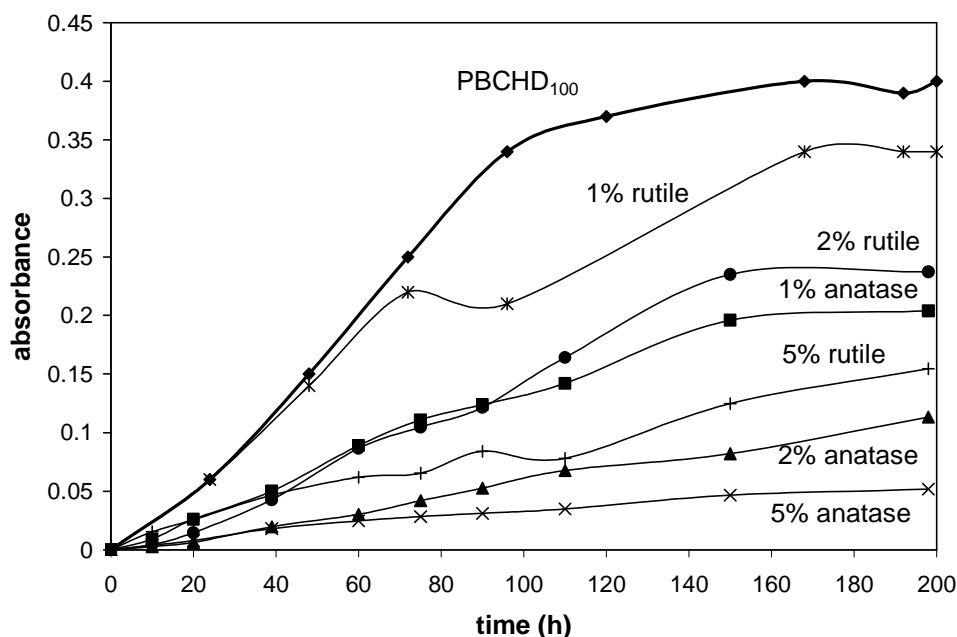


**Figure 3.32** Evolution of OH signal as a function of ageing time in IR spectra for PBCHD<sub>100</sub> and for its composites

To better understand this behavior we performed UV-vis analysis on all the samples has been performed, as shown in Fig. 3.33. The curve of PBCHD<sub>100</sub> shows considerable absorption for wavelengths below 300 nm: this is the UV absorption that leads to the degradation of this polymer. All the composites show strong UV absorptions extending up to wavelengths above 300 nm and this absorption increases with higher percentages of TiO<sub>2</sub>.

These results are in agreement with the FTIR analysis: comparing the samples with the same percentage of TiO<sub>2</sub> but in a different crystalline form it is evident that the absorption of anatase is greater than the one of rutile and this leads to a better protection of the matrix.

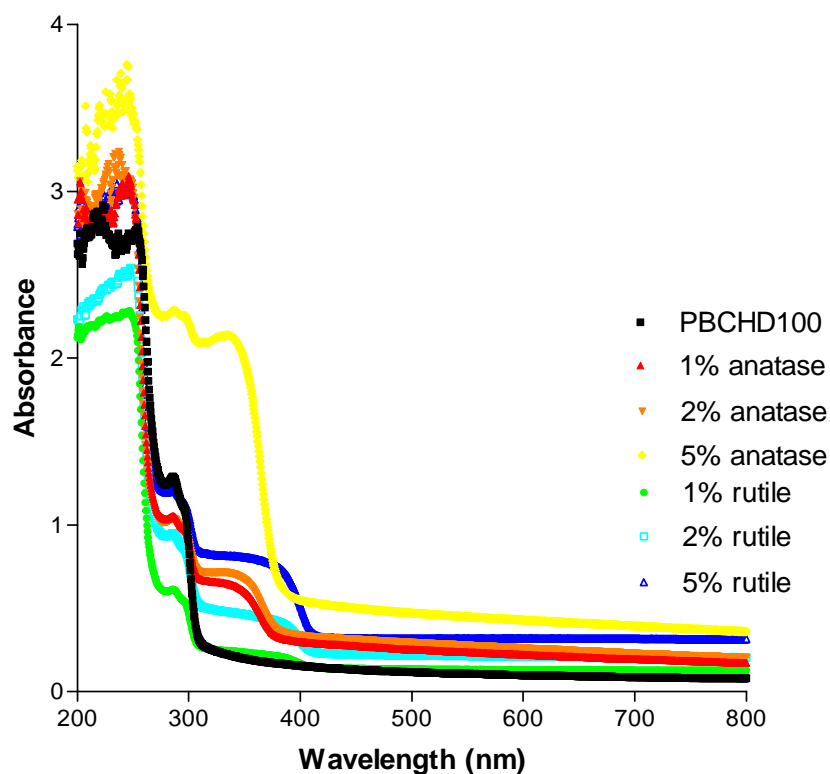


**Figure 3.33 UV spectra for PBCHD<sub>100</sub> samples**

### ***Impact of TiO<sub>2</sub> on PCCD<sub>97</sub> durability***

The same considerations made on PBCHD<sub>100</sub> composites can be extended to PCCD<sub>97</sub> samples. Fig. 3.34 shows the evolution of the OH signal versus irradiation time in FTIR spectra.

The protection of the matrix performed by TiO<sub>2</sub> is clearly evident: the absorbance of the OH signal decrease dramatically in all the composites. As seen for PBCHD the protection effect is directly proportional to the percentage of TiO<sub>2</sub> added.

By comparing the results of the two samples with the same percentage of TiO<sub>2</sub> (2%), but with different forms, it is confirmed that the anatase is more effective than rutile.

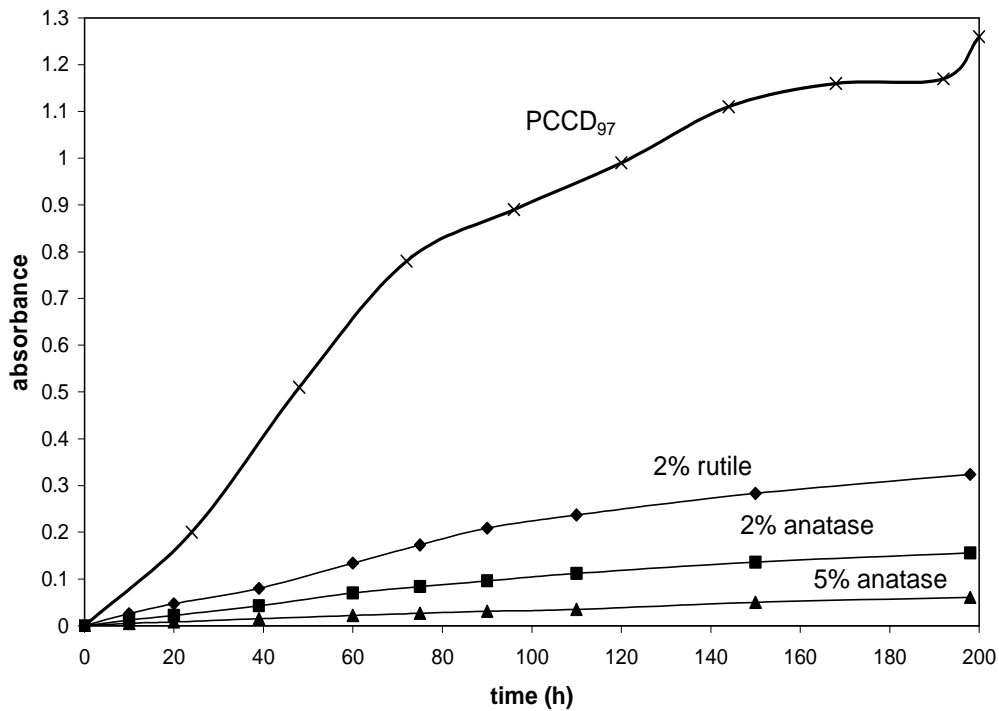


**Figure 3.34 Evolution of OH signal as a function of ageing time in IR spectra for PCCD<sub>97</sub> and for its composites.**

The effect of the two TiO<sub>2</sub> form is clearly explained by the UV-vis data, shown in Fig.3.35. The UV absorptions for wavelengths above 300 nm strongly increase by increasing the percentage of TiO<sub>2</sub> present in the composites and by changing the form from rutile to anatase. All the UV-vis data are in agreement with the results obtained by FTIR.

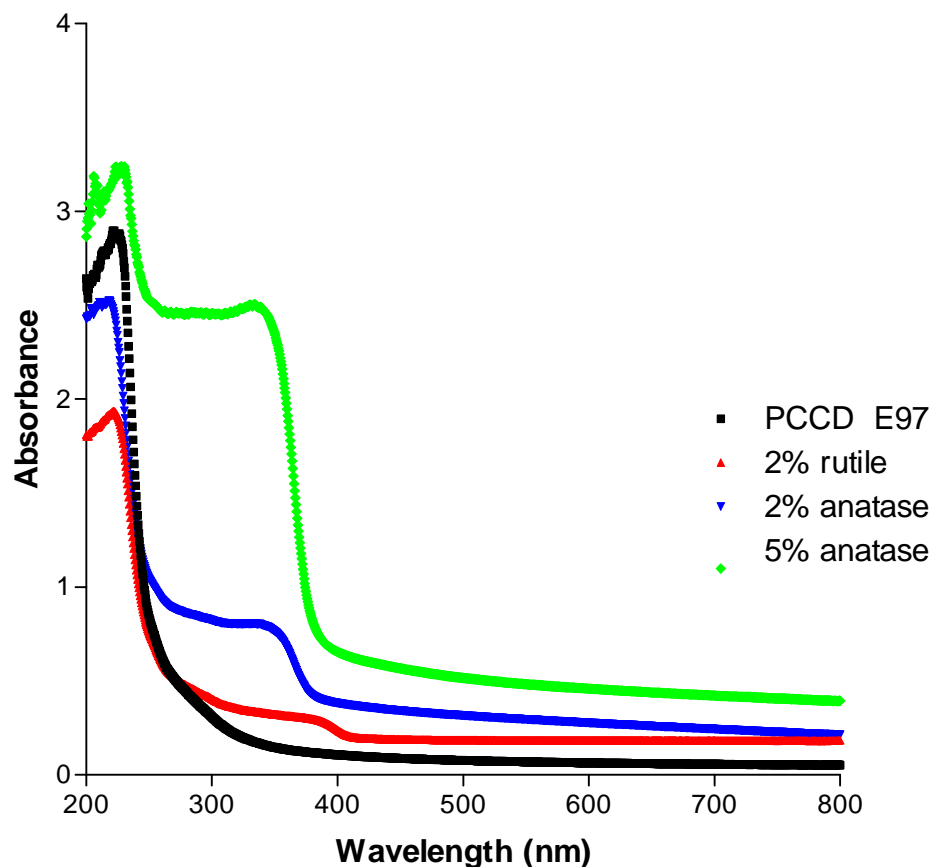


Figure 3.35 UV spectra for all PCCD<sub>97</sub> samples

### 3.4.7. SEM analysis

To better understand the behavior of the two different TiO<sub>2</sub> forms, SEM analysis has been performed. We have chosen two PCCD<sub>97</sub> composites with rutile and anatase at the same percentage (2%) and the SEM images are reported in figures 3.36 and 3.37 respectively.

The pictures indicates that the TiO<sub>2</sub> particles are well dispersed in polymer matrix, especially anatase: indeed rutile with a magnification of 10 μm shows bigger domains compared to those found in the presence of anatase. To see the anatase particles it was necessary a higher magnification.

The adhesion between particles and polymer results good for both anatase and rutile.

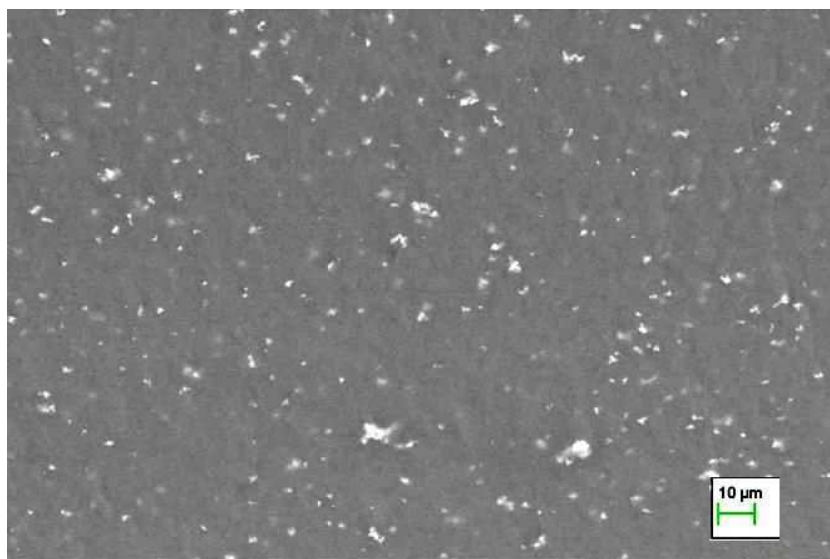


**Figure 3.36 SEM image of the PCCD<sub>97</sub> containing 2% wt of rutile**

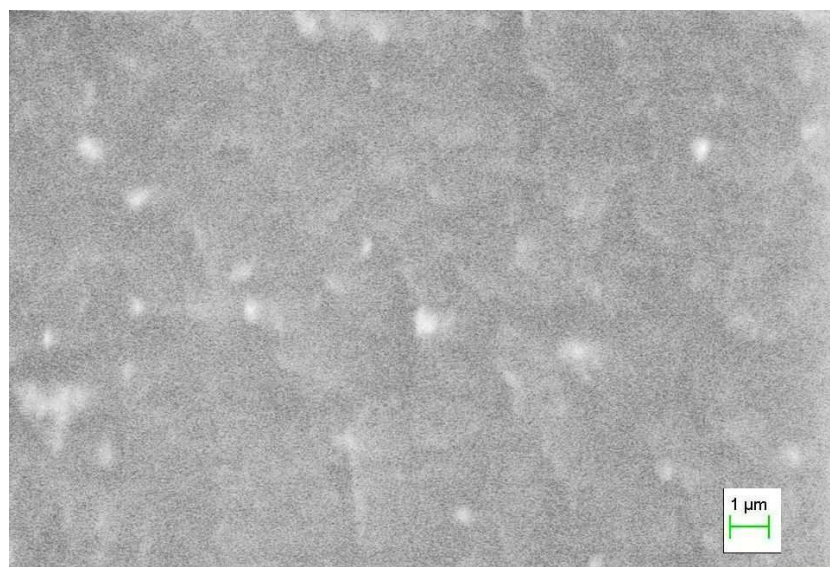


**Figure 3.37 SEM image of PCCD<sub>97</sub> containing 2% wt of anatase**

### **3.4.8. Conclusions**

During this work we have investigated the photodurability of two aliphatic polyesters (PBCHD<sub>100</sub> and PCCD<sub>97</sub>) and their composites with TiO<sub>2</sub>.

The photodurability of PBCHD is higher than those of PCCD: a single aliphatic ring in the monomeric unit results more stable towards UV exposure with respect to two aliphatic rings.

The percentage of TiO<sub>2</sub> in the composites is directly proportional to the protection provided to the matrix. In particular, between the two TiO<sub>2</sub> forms, anatase is more efficient than rutile in both matrixes and this could be related to the better dispersion of anatase particles in the matrix or directly to the different crystalline phase between the two TiO<sub>2</sub> forms.

### 3.5. Aliphatic Polyesters Containing Glycerol

Part of this research has already been published: Annamaria Celli, Paola Marchese, Simone Sullalti, Corrado Berti, Giancarlo Barbiroli, Sophie Commereuc, Vincent Verney, "Preparation of new biobased polyesters containing glycerol and their photodurability for outdoor applications", *Green Chemistry*, **2012**, 14, 182-187

#### 3.5.1. Introduction

Glycerol is a basic component of lipids and a by-product of biodiesel production. Due to its three –OH functional groups, it is often used as monomer together with a diacid for the synthesis of polyesters characterized by a complex three-dimensional structure, and, thus, by elasticity. Glycerol was polymerized with sebacic acid to prepare polyglycerol sebacate (PGS), an elastomeric biodegradable material developed for use in soft tissue engineering (Wang, 2003), in regenerative medical approaches (Sundback, 2005), and for applications in blood vessels in vivo (Metlagh, 2006). Other polyesters based on glycerol with sebacic acid and glycol (Tang, 2006; Liu, 2009), with adipic acid (Stumbé, 2004), with dodecanedioic acid (Migneco, 2009) were mainly developed for medical applications. All the examples describe the use of glycerol to form elastomers with cross-linked structures.

Glycerol can also be used as a monomer to modify the chemical structure of polyester-based thermoplastics, to form branched or cross-linked networks. In this case, only a small amount of glycerol is needed in order to maintain the thermoplastic properties of the starting material. In this research we modified a linear polyester, the poly(butylene dodecanoate) (called 4-12, from the number of carbon atoms of diol and diester, respectively), by adding small amounts of glycerol during the synthesis. The focus was the preparation of a polyester with a low level of branching, in order to improve mechanical properties and to adapt durability toward UV exposure. Indeed, photostability is a very important property for aliphatic polyesters, in that it differentiates them from aromatic polyesters in outdoor applications.

The basic idea is that 4-12, modified with glycerol, changes its structure during the exposition to UV irradiation and these changes influence the resistance to biodegradation. Such a behavior, still to be tested, should be significant for outdoor uses.

#### 3.5.2. Synthesis

The synthesis of the 4-12 homopolymer is described in literature (Barbiroli, 2003). The synthesis of the samples containing glycerol is here reported, in particular for the sample

containing 1.0 mol% of glycerol called (4-12)-GL1.0:

DA (34.55 g, 0.150 mol), GL (0.14 g, 0.0015 mol), BD (16.00 g, 0.18 mol), TBT (0.15 g, 0.44 mmol) were placed inside a round bottom wide-neck glass reactor (250 ml capacity). The reactor was closed with a three-necked flat flange lid equipped with a mechanical stirrer and a torque meter which gives an indication of the viscosity of the reaction melt. The reactor was immersed into a salt bath preheated to 200°C. The first stage was conducted at atmospheric pressure under nitrogen atmosphere and the mixture was allowed to react for 90 min under stirring with continuous removal of water. The reaction was stopped and the reactor was taken out of the silicone bath and cooled to room temperature, new TBT was added (0.15 g, 0.44 mmol). The reactor was again put into the salt bath preheated to 200°C until all products had melted. The second stage was started by gradually reducing the pressure to 0.2 mbar while the temperature was raised to the final value of 240°C. Such conditions were reached within 90 min, using a linear gradient of temperature and pressure, and maintained for 120 min.

The molar glycerol contents used are 0.5, 1.0, and 2.0 mol% in order to obtain polyesters with different compositions. They are named (4-12)-GL<sub>x</sub>, where x is the glycerol feed amount (mol%). The final molar composition of the polymers is reported in Table 3.17.

**Table 3.17: Molecular characteristics of the samples.**

Sample	Feed amount of glycerol (mol%)	Final amount of glycerol in polymers (mol%) <sup>a)</sup>	$M_w * 10^{-3}$ <sup>b)</sup>	$M_w/M_n$ <sup>b)</sup>
4-12	-	-	78	2.5
(4-12)-GL0.5	0.5	0.4 <sup>c)</sup>	92	2.5
(4-12)-GL1.0	1.0	0.8	129	3.4
(4-12)-GL2.0	2.0	0.9 <sup>d)</sup>	224 <sup>d)</sup>	4.1 <sup>d)</sup>

<sup>a)</sup>Calculated by <sup>1</sup>H NMR, <sup>b)</sup>Calculated by GPC, <sup>c)</sup>Limit of detectability, <sup>d)</sup>Calculated in the soluble fraction

### 3.5.3. Molecular characterization

Figure 3.38 shows a comparison between the regions from 3.6 to 5.6 ppm of the <sup>1</sup>H NMR spectra of 4-12 and two of the novel polyesters containing 1.0 and 2.0 mol% of glycerol:

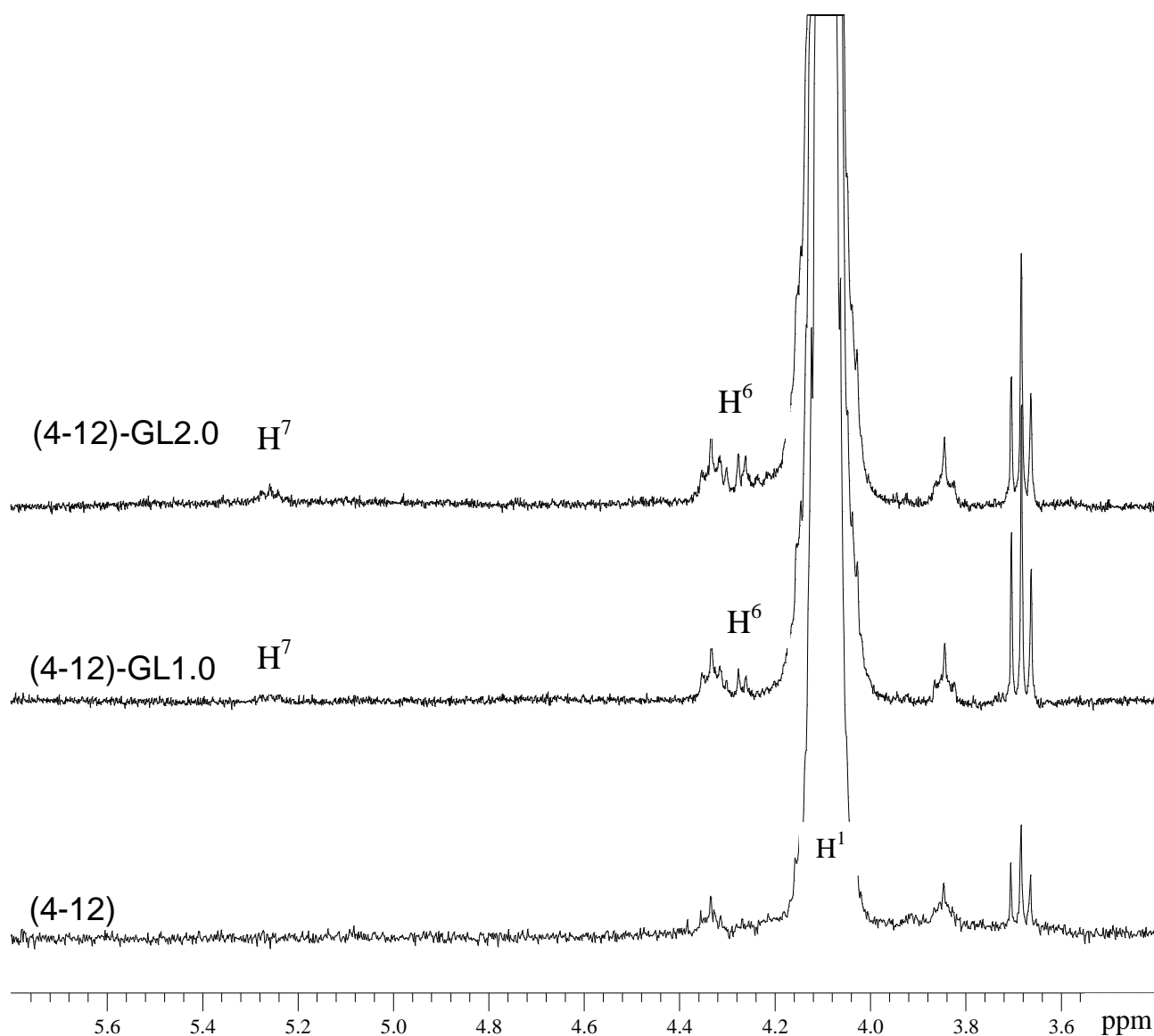


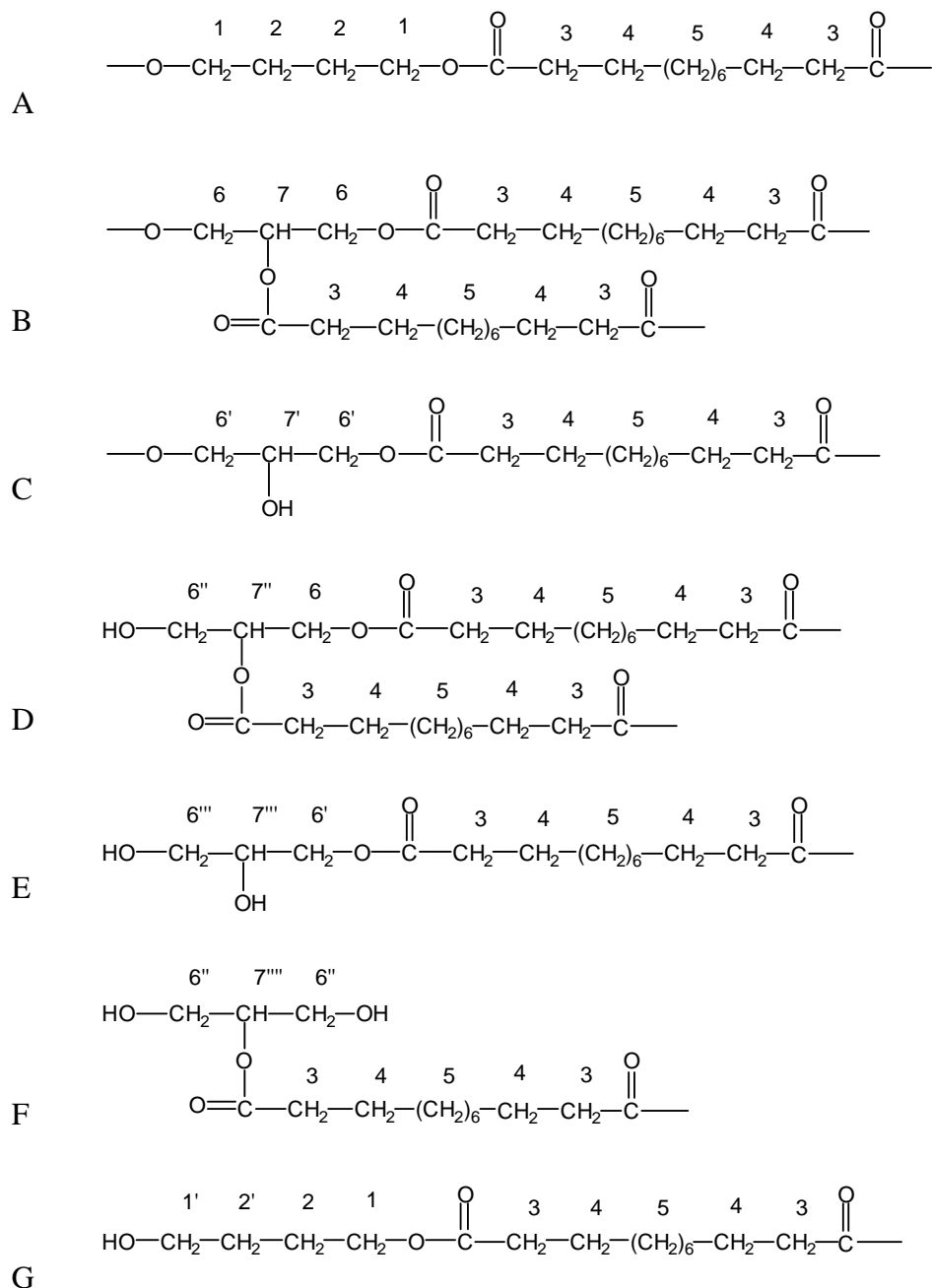
**Figure 3.38**  $^1\text{H}$  NMR spectra of 4-12 and novel polyesters containing 1.0 and 2.0 mol%

The signals at 5.25 ppm were attributed to the proton of the  $-\text{CH}-$  group of the glycerol units ( $\text{H}^7$ ), when all  $-\text{OH}$  react, according to the signal attributions reported for triacetine. Therefore, by comparing the relative intensity of the signals at 5.25 ppm with the one at 4.10 ppm ( $\text{H}^1$ ) it is possible to evaluate the feed amount of glycerol in the final polymers. The results are reported in Table 1 and indicate that all glycerol reacts when present in a low percentage (0.5 and 1.0 mol%). The sample (4-12)-GL2.0 is not fully soluble in chloroform; therefore, the content of glycerol has been evaluated only in the soluble fraction and, for this reason, appears very low. In the solid sample, obtained in the reactor and not precipitated, it is reasonable to assume that all feed glycerol is present.

To better understand the molecular structure of these new polyesters, it is necessary to investigate whether or not all three hydroxyl groups of glycerol react with the 1,12-dodecanedioic acid. Indeed, the secondary hydroxyl group in glycerol (see Scheme 3.5) is characterized by a

higher steric inhibition compared to the other ones and should be less reactive. All the possible dyads derived by the combination of BD, GL, and DA are shown in Scheme 3.5.

**Scheme 3.5: Possible dyads derived from the reactions between BD, DA, and GL.**



- structure A corresponds to the sequence obtained from the reaction between DA and BD to form 4-12 homopolymer;
- structure B corresponds to the sequence obtained from DA and GL, where all three –OH groups react;
- structures C and D correspond to the sequences obtained when only two –OH groups of GL react;
- structures E and F correspond to the sequences obtained when only one –OH of GL reacts with the

formation of a chain end;

- structure G corresponds to the sequence obtained when only one –OH group of BD react with the formation of a chain end.

The signals at 3.7 ppm can be attributed to H<sup>1'</sup> protons. Moreover, the signals at 4.3 and 5.25 ppm were attributed to H<sup>6</sup> and H<sup>7</sup> protons, respectively, according to the signal attributions reported for triacetine. Signals due to other protons are not distinguishable. H<sup>6'</sup>, H<sup>6''</sup>, and H<sup>6'''</sup> should give signals in the 3.7-4.2 ppm region but could also be partially hidden by other, more intense, signals. H<sup>7'</sup> and H<sup>7''</sup> should be evident in the 4.4-4.6 ppm region: their absence indicates that the C and D structures of Scheme 2 are not very probable. H<sup>7'''</sup> and H<sup>7''''</sup>, which should give signals at 3.9-4.1 ppm, do not show a clear evidence of their presence. Therefore, E and F structures, too, probably are not present.

We can conclude that the most probable molecular structures for the 4-12/glycerol polyesters are A and B, corresponding to the 4-12 homopolymer and to a branched system, where glycerol units act as branching agent with its three functional groups. Moreover, starting from B, it is possible to also advance the hypothesis of the formation of some more complex, cross-linked structures. Indeed, the (4-12)-GL2.0 sample is characterized by very high viscosity, which becomes more and more evident as the polymerization time rises. The solubility of this sample in chloroform is not complete: for this reason, NMR and GPC characterizations were only performed on the soluble fraction. Finally, polymerizations performed with starting amounts of glycerol higher than 2.0 mol% are not possible in the conditions described above, given the extremely high viscosity of the medium.

#### **3.5.4. Thermal characterization**

Fig 3.39 shows both the cooling and heating curves of the samples.

All the polymers are semicrystalline: in fact both the homopolymer and the samples with glycerol are characterized by very sharp and intense crystallization and melting peaks, indicating a high level of crystallinity and crystal perfection.

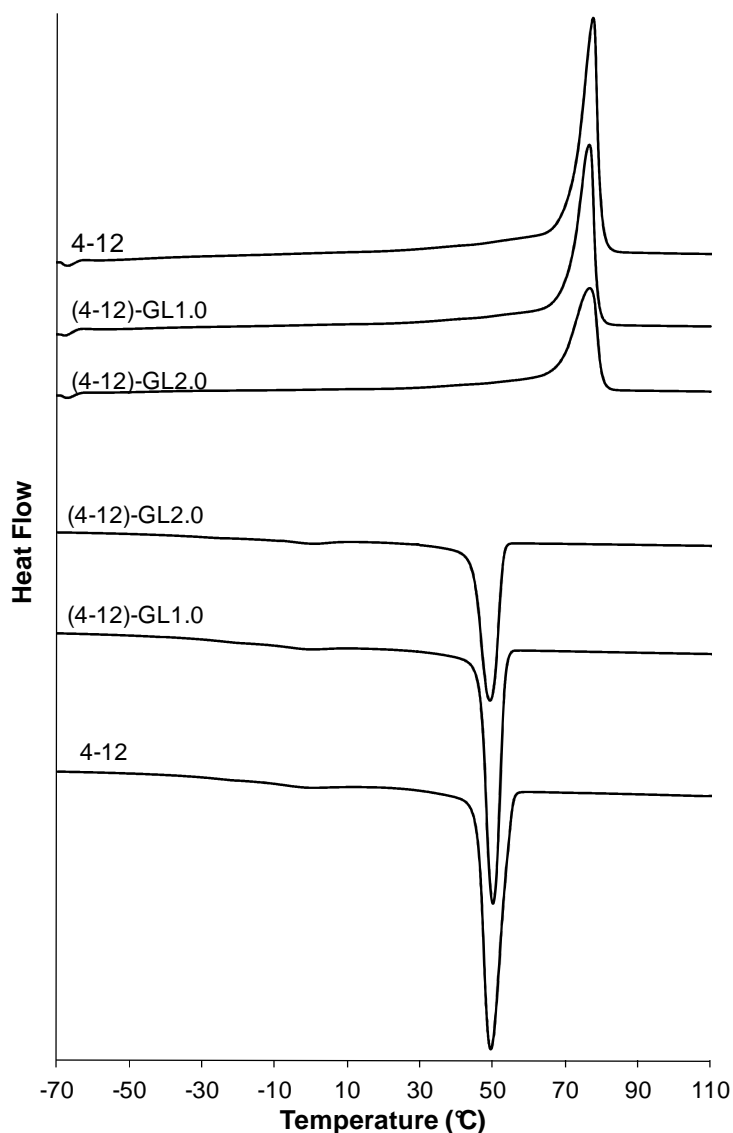


**Figure 3.39 DSC cooling and 2nd heating scans of (4-12)/glycerol samples**

Table 3.18 collects all the thermal data the samples analyzed:

**Table 3.18 Thermal data of the synthesized samples**

Sample	$T_{CC}^a$ (°C)	$\Delta H_{CC}^a$ (J g <sup>-1</sup> )	$T_m^b$ (°C)	$\Delta H_m^b$ (J g <sup>-1</sup> )
4-12	53	87	75	96
(4-12)-GL0.5	55	83	75	96
(4-12)-GL1.0	53	94	74	94
(4-12)-GL2.0	52	92	74	106

a) measured during the cooling scan at 10°C/min

b) measured during the second heating scan at 10°C/min

Melting and crystalline temperatures don't change after adding glycerol and so the enthalpies. In conclusion we can assume that the addition of glycerol does not affect the thermal properties, in spite of changes in molecular structure.

### 3.5.5. DMTA analysis

Figure 3.40 shows the dynamic mechanical spectra of the 4-12 and 4-12/glycerol samples. Looking at  $\tan\delta$  curves, the 4-12 homopolymer shows an intense peak at  $-32^\circ\text{C}$ , due to the glass-to-rubber transition. Another peak is centred at about  $-80^\circ\text{C}$  and can be associated, by analogy with other similar macromolecules, to the motions of the  $-(\text{CH}_2)-$  units of butanediol and/or dodecanedioic acid (Berti, 2008 C).

The glass transition temperatures of all the samples containing glycerol are very similar, in the range from  $-24$  to  $-22^\circ\text{C}$ , thus about  $10^\circ\text{C}$  higher than that of 4-12. This increment can be ascribed to the less flexible chains due to the presence of ramifications occurred after the addition of glycerol.

Even the elastic modulus is affected by the addition of glycerol. Indeed, (4-12)-GL0.5 and (4-12)-GL1.0 show an increment in  $E'$  compared to the (4-12) itself even there is no differences between them two. This increment becomes more important in the presence of 2.0 mol% of glycerol. Ramifications, and partial crosslinking in case of (4-12)-GL2.0, of the novel structures are the main reasons for these good mechanical properties. However, the characteristics of thermoplastic materials are maintained.

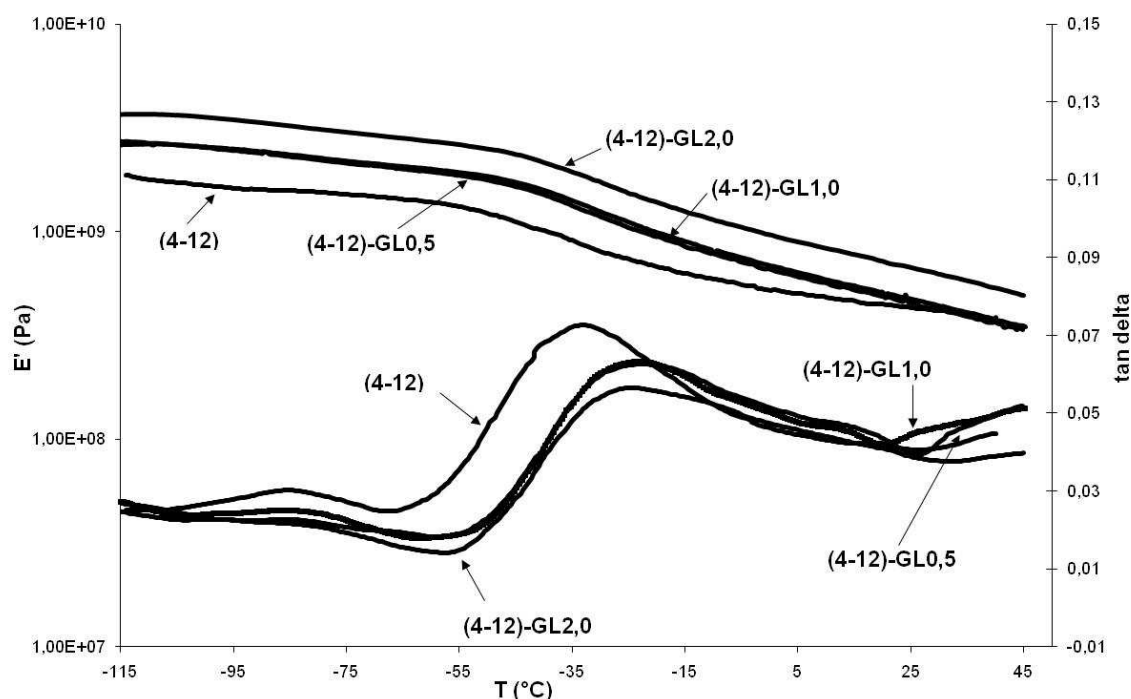
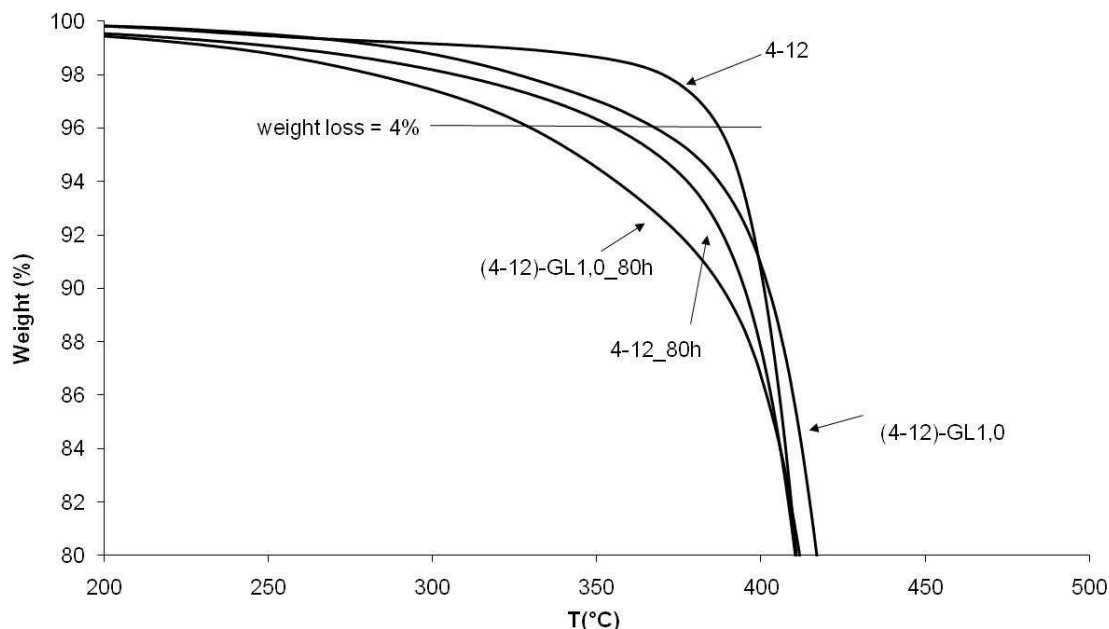


Figure 3.40 DMTA curves of (4-12)-GL samples

### 3.5.6. Photostability

It is notable to understand how the thermal stability of the new samples changes after UV exposure. As an example, in Figure 3.41 are reported TGA curves of 4-12 and (4-12)-GL1.0 before and after UV exposure of 80 hours at 60°C.



**Figure 3.41** TGA curves of 4-12 and (4-12)-GL1.0 before and after UV exposure (4-12\_80h and (4-12)-GL1.0\_80h)

UV exposure leads to a decrement in thermal stability both for the 4-12 and (4-12)-GL1.0: indeed, choosing a 4% weight decrement as reference, the aged samples degrade almost 40°C before the non-irradiated samples. This phenomena is connected to the reactions that occur during UV irradiations and that will be discussed in the next paragraph.

### 3.5.7. Photodegradation

Figure 3.42 shows the evolution of Cole-Cole plots of the 4-12 homopolymer through accelerated photoageing. At short exposure times the Cole-Cole plot looks like a standard circle. It could be noticed a slight deviation at lower frequencies (higher  $\eta'$ ) exhibiting a double distribution of the molecular weights due to very long macromolecular chains.

As photoageing proceeds, the curves clearly put in evidence double phases: one is described as a standard Cole-Cole plot. The zero shear viscosity  $\eta_0$  has a strong decrement as a consequence of UV exposure (from 20 to 60 hours).  $\eta_0$  value falls down about one decade, which means that molecular weight  $M_w$  is divided by about 2. Thus, mass-average molecular weight decreasing points out that scission reactions prevail in this phase. Elsewhere, a second phase is

characterized by a strong deviation of the Cole-Cole curve leading to a linear relationship between  $\eta'$  and  $\eta''$ . It is a typical feature of a crosslinked system (Winter, 1989).

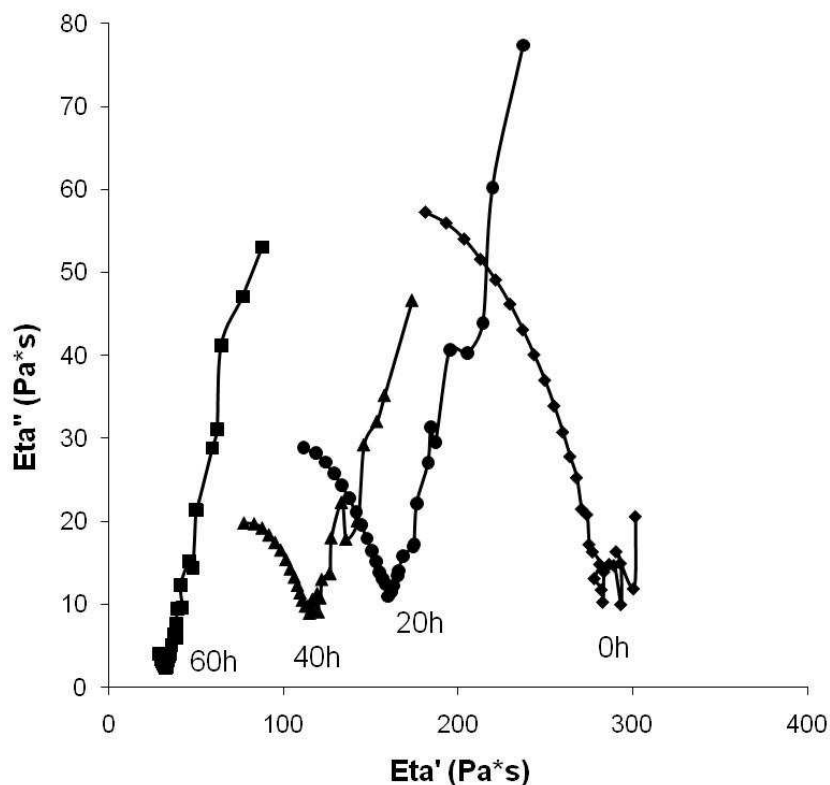


**Figure 3.42** Cole-Cole plots of 4-12 before and after UV exposure. The exposure times are indicated for each curves (h)

Hence, the photodegradation of 4-12 homopolymer exhibits a dual process under our experimental conditions: chain scissions and chain recombinations simultaneously occur, leading to two phases, a crosslinked one and another not crosslinked. It could be considered that, as the photodegradation takes place, the extend of crosslinked phase increases.

Figure 3.43 shows the Cole-Cole plots of (4-12)-GL0.5 before and after UV exposure.

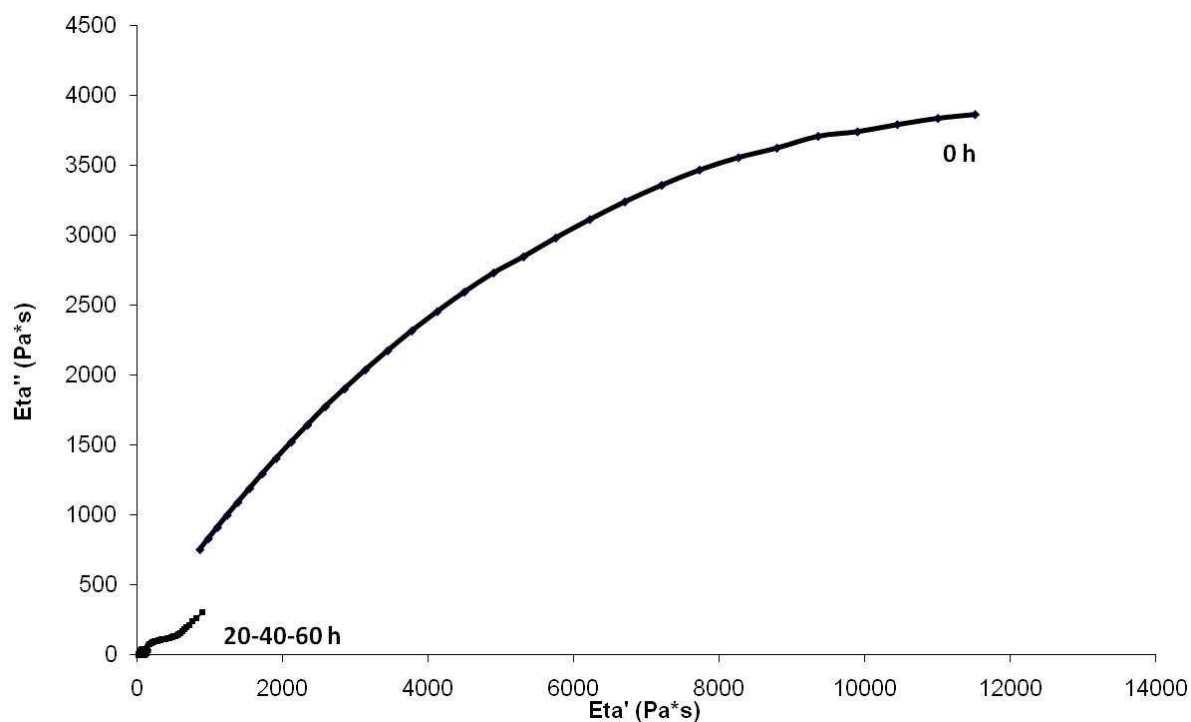


**Figure 3.43 Cole-Cole plots of (4-12)-GL0.5 before and after UV exposure**

The addition of 0.5 mol% of glycerol induces a strong increment in the zero shear viscosity, due to the branching. The viscosity of (4-12)-GL0.5 decreases during UV irradiation. We assume that glycerol introduction in the polymeric backbone impacts the photodegradation mechanism and leads to chains scissions.

Figures 3.44 shows the Cole-Cole plots of a sample modified with 1.0 of glycerol. It is obvious that at  $t=0$  the extrapolated  $\eta$  value is very high, as expected. After 20 h of photoageing at  $60^{\circ}\text{C}$ ,  $\eta$  increases further, thus suggesting that chain recombinations occur. At 40h or longer exposure times, instead, drastic chain scissions prevail.

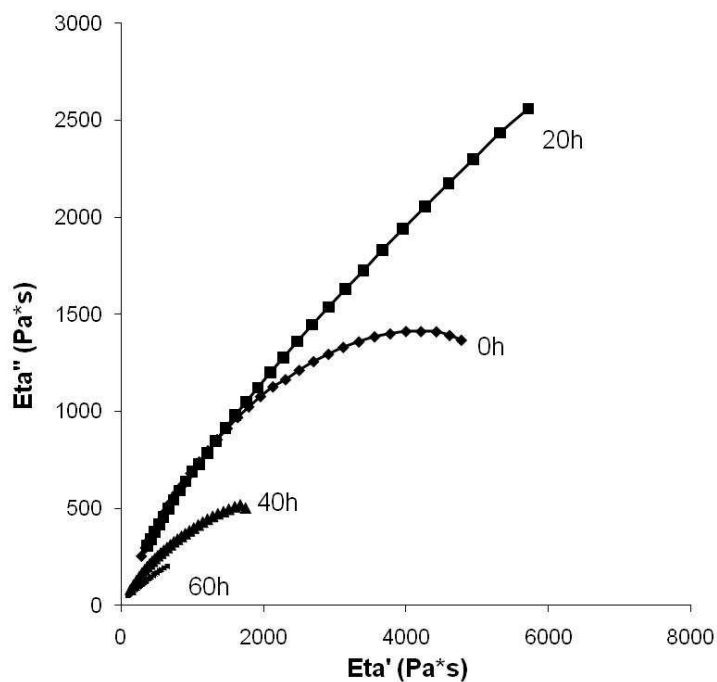


**Figure 3.44** Cole-Cole plots of (4-12)-GL1.0 after different exposure times (h)

To confirm the presence of the unexpected recombination of chains at short exposure times, the accelerated photoaging was also carried out in a similar device (SEPAP 14-24), operating at 45°C, for times varying from 2 to 20 h. The results are shown in Figure 3.45: it must be remarked that an increment of viscosity again occurs at times shorter than 20h and also that chain recombinations are detected.

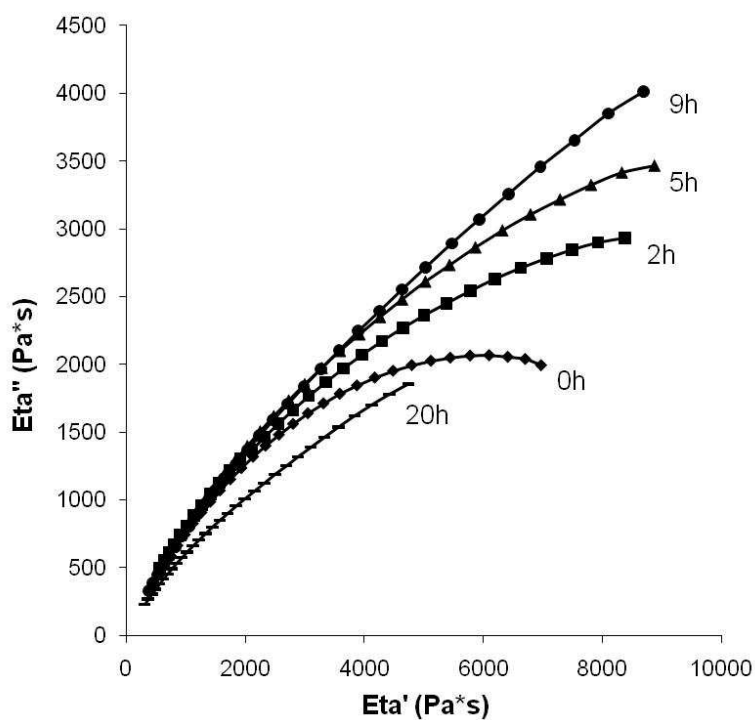


**Figure 3.45** Cole-Cole plots of (4-12)-GL1.0 at 45°C in SEPAP 14-24

Therefore, the behavior of (4-12)-GL1.0 sample shows a strong competition between chain scissions and chain recombinations during photoageing. As the photooxidation proceeds, chain scissions drastically prevail. This means that a small amount of glycerol inserted along the chains of 4-12 is able to strongly modify the behavior of polyester toward photoageing. This can be a significant result for outdoor applications of the polymer.

On the other hand, the (4-12)-GL2.0 (see Figure 3.46) is partially crosslinked already at  $t = 0h$ : the Cole-Cole curve is typically those of a tridimensional network polymer system and could be drawn as a line with a very high slope. In this case, the amount of glycerol is high enough to favor the formation of a very complex molecular structure in the starting material.

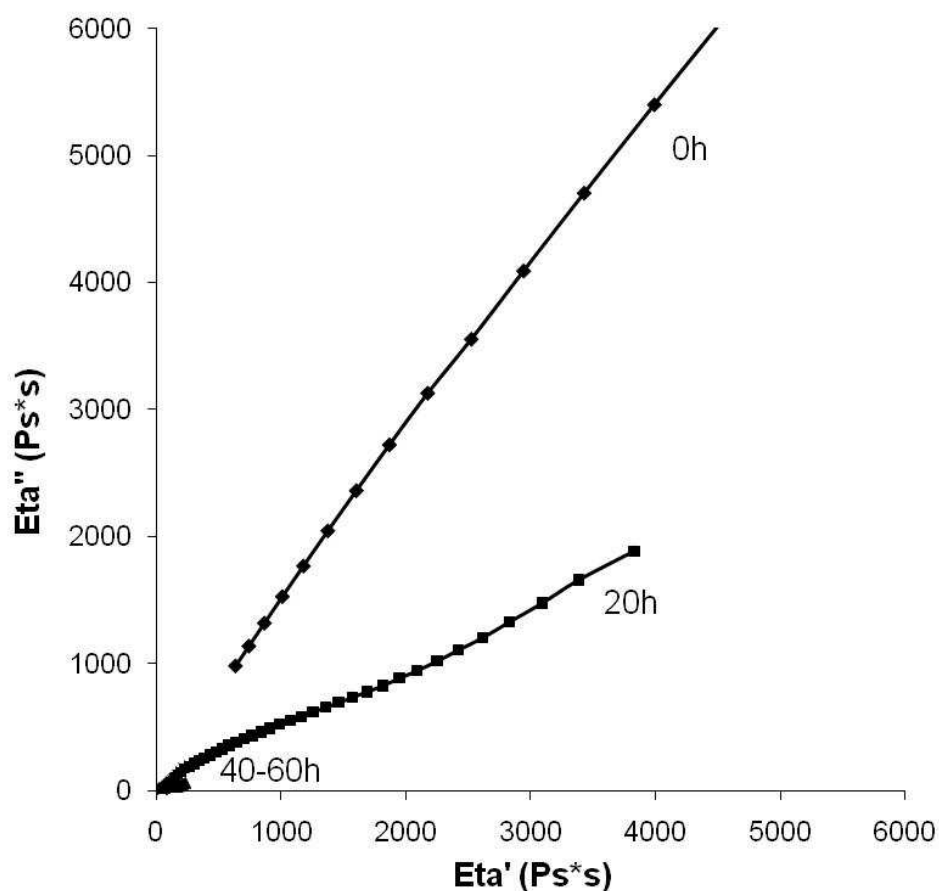


**Figure 3.46** Cole-Cole plots of (4-12)-GL2.0

After UV irradiation, the slope of the line drastically decays upon exposure. It is interesting to remark that a double distribution appears after 20 hours of irradiation. The Cole-Cole curve could be considered as the convolution of an standard arc of circle (corresponding to not crosslinked phase) and a straight-line (ascribed to a network). Consequently, photodegradation mechanism mainly proceeds by chain scissions.

### 3.5.8. Biodegradation

After preliminary biodegradation tests of in an aqueous mineral nutrient liquid medium inoculated with micro-organisms resulting from activated sludge 4-12 homopolymer has been assumed as biodegradable (Berti, 2008 C; Berti, 2009). Repeating the same test on the new synthesized polymers no influence of the glycerol addition has been founded in the biodegradation properties as shown in Figure 3.47:

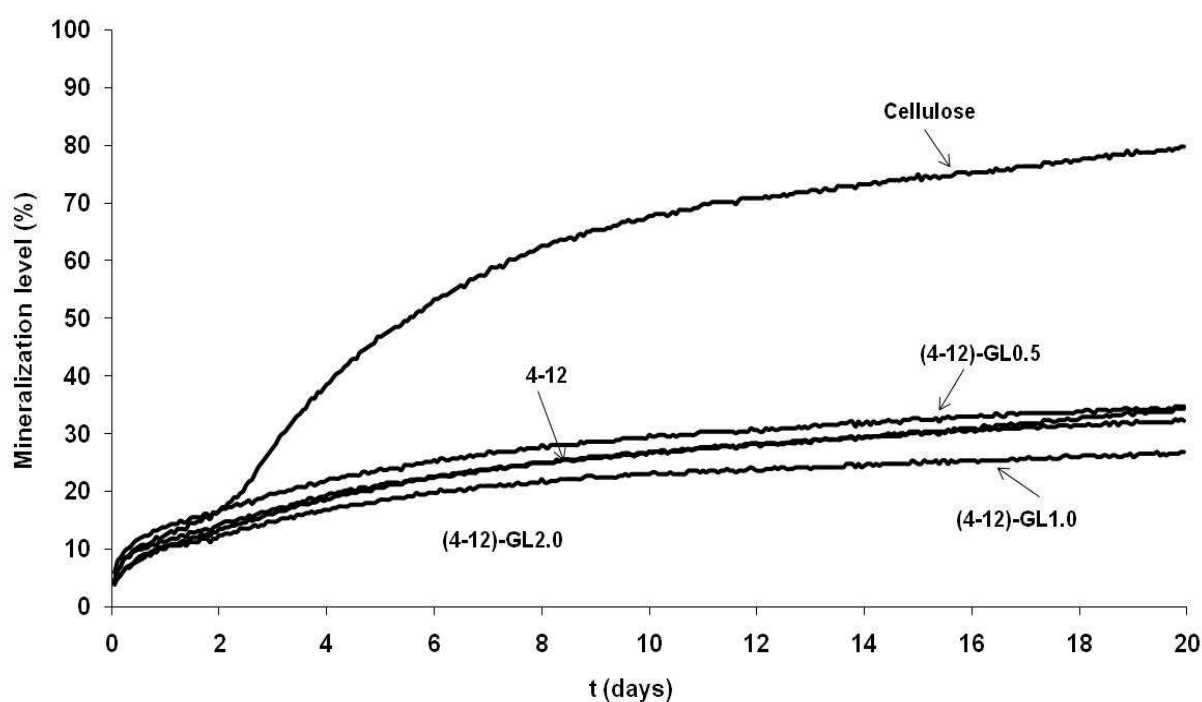


**Figure 3.47 Mineralization level as function of time for all the samples and cellulose as reference**

From these preliminary results it seems that all the new samples present a certain biodegradability. However, some new measurements are in progress to confirm this trend.

Biodegradation of the irradiated samples will also be investigated in order to see the influence of the photodegradation behavior of the different samples.

### 3.5.9. Conclusions

Glycerol was used to modify the properties of a biopolyester, the poly(butylene dodecanoate) (4-12). The monomers used, described in Scheme 1, can all be obtained from renewable feedstock, through chemical or biochemical pathways (Bechthold et al., 2008; Wenhua et al., 2010). A small amount of glycerol, 1.0 mol%, is enough to create a branched structure, and to improve mechanical properties, without modifying the level of crystallinity and melting temperature. In the same time,

small amount of glycerol strongly modifies the behavior of polymer upon photoageing and the photodegradation process. Anyway, chain scissions and chain recombinations (leading to crosslinking) strongly compete. Moreover, under accelerated photoageing, mechanism of chain scissions prevails upon exposure, even in case of previously crosslinked systems. This could act as a significant result for outdoor applications of the materials and could have strong consequences regarding biodegradability upon use. A correlation between photoageing and biodegradability needs further study.



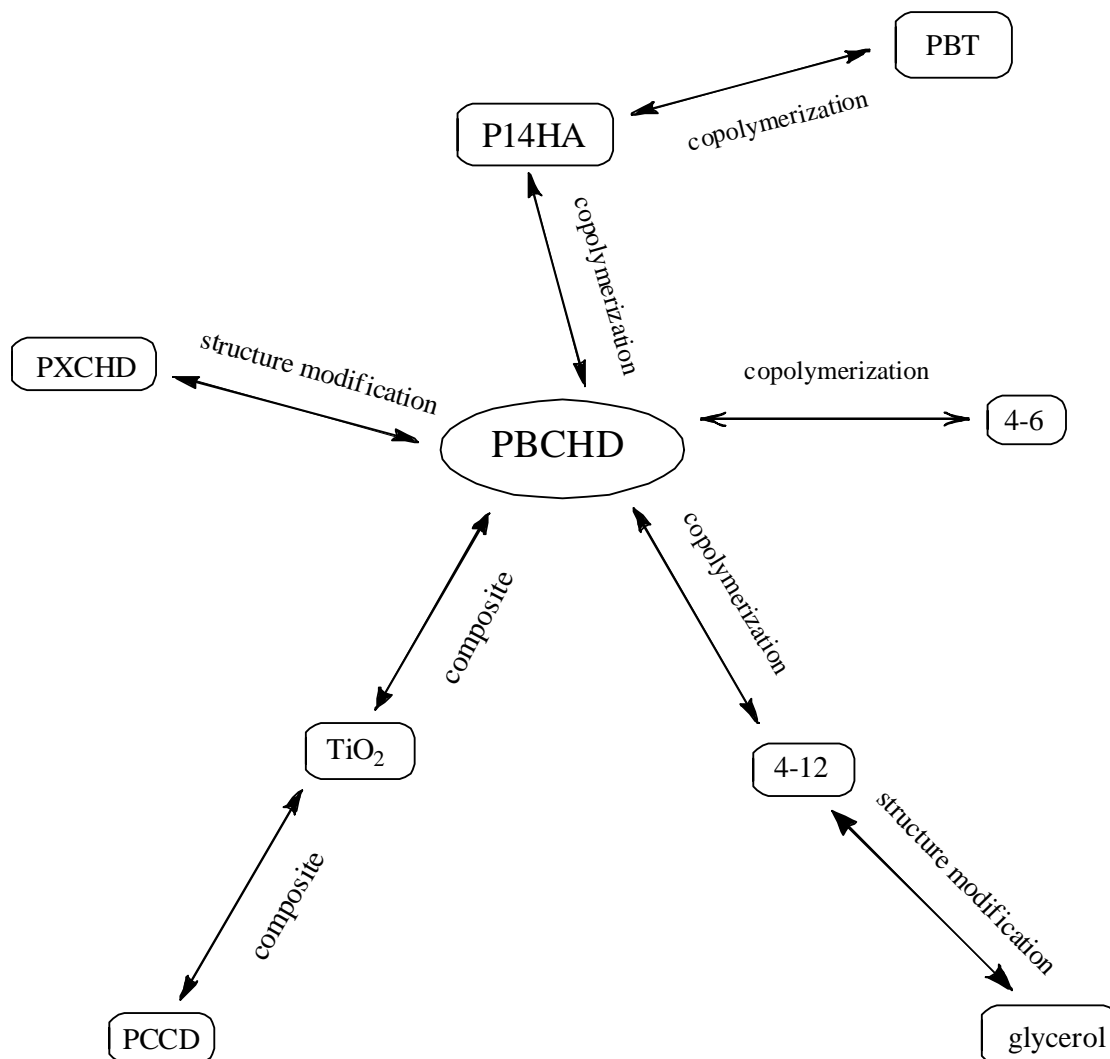
## Chapter 4 : Conclusions

This thesis was focused on the synthesis and characterization of new biobased polyesters, whose monomers can be obtained from renewable resources. A wide family of novel polyesters, copolymers and composites has been prepared and correlation between their molecular structure and final properties have been deeply studied.

The research work started from a homopolymer that was synthesized and fully characterized in our laboratory, the poly(butylene-1,4-cyclohexanedicarboxylate) (PBCHD), obtained from the polycondensation of 1-4 butanediol and DMCD. It is a potentially biobased polymer since its monomers can be both obtained from sugars and limonene (Burk, 2010; Berti, 2010). Moreover, PBCHD is an aliphatic polyester characterized by the presence of 1,4-cyclohexylene units: the ring improves the rigidity to the macromolecules inducing good mechanical and thermal performances. PBCHD can be considered the aliphatic counterpart of Poly(butylenes terephthalate) with the advantage of having a certain degree of biodegradability, according to its amorphous content, and higher resistance to UV irradiation thanks to the absence of aromatic rings (property important for outdoor applications).

PBCHD has been modified in order to obtain new eco-friendly polymers with a wide range of properties (see Scheme 4.1). Copolymers with other “green” polymers (P14HA, 4-6 and 4-12) and composites with TiO<sub>2</sub> has been prepared to achieve specific properties in terms of mechanical, thermal behaviour and durability (specifically, for TiO<sub>2</sub> based blends). Similar copolymers starting from commercial polymers (PBT and PCCD) have been prepared too, with the aim of comparing their final properties with those of the PBCH-based copolymers.

**Scheme 4.1 Resume of all the thesis research**



It results that in copolyesters not only the molar composition, but also the cis/trans ratio of the 1-4-cyclohexylene ring strongly influence the properties of the new materials: by changing the isomeric ratio of the aliphatic ring both semicrystalline (for high trans content) and fully amorphous (for low trans content) polymers can be obtained.

Moreover, the effect of the aliphatic chain length on material performances has been evaluated by synthesizing new polyesters (PXCHD) starting from diols with different  $-\text{CH}_2-$  sequence length. The final properties of the PXCHD polymers fully change by passing from 1,2-ethanediol to 1,8-octanediol as monomers.

Finally, more complex structures have been obtained by adding a small percentage of a three-functional molecule (glycerol) during the synthesis of the 4-12 homopolymer. The presence of branching causes an improvement of elastic modulus and changes the mechanisms of photodegradation, which can be very significant consequences for outdoor applications

It is notable all the new materials are potentially bio-based and biodegradable, as reported in some preliminary tests, and can be candidates for substituting some traditional petroleum-based polymers in specific applications.



## Chapter 5 : References

- Agilent Technology, *Fundamentals of UV-visible spectroscopy*, (2003)
- Aoyagi Y., Yamashita K., Doi Y., Thermal degradation of poly[(R)-3-hydroxybutyrate], poly[ $\epsilon$ -caprolactone], and poly[(S)-lactide], *Polymer Degradation and Stability* (2002), 76, 53-59
- Auras R., Harte B., Selke S., An overview of polylactides as packaging materials, *Macromol. Biosci.* (2004), Vol. 4(9): 835-864.
- Averous L., Boquillon N., Biocomposites based on plasticized starch: thermal and mechanical behaviours, *Carbohydrate Polymers*, (2004), Vol. 56(2): 111-122.
- Awitor KO, Rivaton A, Gardette J-L, Down AJ, Johnson MB. Photo-protection and photocatalytic activity of crystalline anatase titanium dioxide sputter-coated on polymer films. *Thin solid films*, (2008), 516, 2286-2391.
- Barbiroli, G., Lorenzetti, C., Berti, C., Fiorini, M., Manaresi, P, Polyethylene like polymers. Aliphatic polyesters of dodecanedioic acid 1.Synthesis and properties. *European Polymer Journal* (2003), 39, 655-661.
- Bechthold, I. K., Bretz, S., Kabasci, R., Kopitzky, A. Succinic Acid: A New Platform Chemical for Biobased Polymers from Renewable Resources. *Chem. Eng. Technol.* (2008)31, 647-654.
- Berti, C.; Binassi, E.; Colonna, M.; Fiorini, M.; Kannan, G.; Kanaram, S.; Mazzacurati, M. US 20100168461, (2010)
- Berti C., Celli A., Marchese P., Di Credico F., Barbiroli G., Verney V., Commereuc S., Novel copolyesters based on poly(alkylene dicarboxylate)s: 2. Thermal behavior and biodegradation of fully aliphatic random copolymers containing 1,4-cyclohexylene rings, *European Polymer Journal* , (2009), Vol. 45(8): 2402–2412.
- Berti C., Celli A., Marchese P., Marianucci E., Barbiroli G., Di Credico F., Influence of Molecular Structure and Stereochemistry of the 1,4-Cyclohexylene Ring on Thermal and Mechanical Behavior of Poly(butylene 1,4-cyclohexanedicarboxylate), *Macromolecular Chemistry and Physics* (2008), Vol 209(13): 1333–1344. A

- Berti C, Binassi E, Celli A, Colonna M, Fiorini M, Marchese P, Marianucci E, Gazzano M, Di Credico F, Brunelle DJ. Poly(1,4-cyclohexylenedimethylene 1,4-cyclohexanedicarboxylate): influence of stereochemistry of 1,4-cyclohexylene units on the thermal properties. *J. Polym. Sci. Part B: Polym Phys.* (2008); 46: 619-630. B
- Berti, C., Celli, A., Marchese, P., Barbiroli, G., Di Credico, F., Verney, V., Commereuc, S., Novel copolyesters based on poly(alkylene dicarboxylate)s: 1. Thermal behavior and biodegradation of aliphatic-aromatic copolymers. *European Polymer Journal* (2008), 44, 3650-3661. C
- Berti C., Celli A., Marchese P., Marianucci E., Barbiroli G., Di Credico F., The effect of aliphatic chain length on thermal properties of poly(alkylene dicarboxylate)s, *E-POLYMERS*, (2007), 057, 1 – 18
- Biermann, U.; Bornscheuer, U.; Meier, M.A.R.; Metzger, J.O.; Schäfer, H.J. New developments for the chemical utilization of oils and fats as renewable raw materials, *Angew. Chem. Int. Ed.* (2011), 50, 3854 – 3871
- Burk J.M., Sustainable production of industrial chemicals from sugars , *Int. Sugar J.* (2010), 112, 30
- Carp O, Huisman C L, Reller A. Photoinduced reactivity of titanium dioxide. *Progress in Solid State Chemistry*, (2004), 32, 33-177.
- Celli A., Barbiroli G., Berti C., Di Credico F., Lorenzetti C., Marchese P., Marianucci E., Thermal properties of poly(alkylene dicarboxylate)s derived from 1,12-dodecanedioic acid and even aliphatic diols, *Journal of Polymer Science, Part B: Polymer Physics*, (2007), 45, 1053-1067
- Ceresana Research, (2009): <http://www.ceresana.com/en/>
- Chan P., Yu V., Wai L., Yu H., Production of medium-chain-length polyhydroxyalkanoates by *Pseudomonas aeruginosa* with fatty acids and alternative carbon sources, *Applied Biochemistry and Biotechnology*, (2006), Vol.129-132: 933-941.
- Chen LP, Yee AF, Goetz JM, Schaefer J. Molecular structure effects on the secondary relaxation and impact strength of a series of polyester copolymer glasses. *Macromolecules* (1998), 31, 5371–82.
- Cheremisinoff N.P., *Polymer Characterization: Laboratory techniques and analysis*, Noyes Publications, (1996)
- Cho S, Choi W. Solid-phase photocatalytic degradation of PVC-TiO<sub>2</sub> polymer composites. *J. Photochem. Photobiol. A*, (2001), 143, 221-228.

- Colonna M., Berti C., Binassi E., Celli A., Fiorini M., Marchese P., Messori M., Brunelle D. J., Poly(1,4-cyclohexylenedimethylene-1,4-cyclohexanedicarboxylate): analysis of parameters affecting polymerization and cis-trans isomerisation. *Polymer International* (2011), 60, 1607-1613
- Commereuc S., Askanian H., Verney V., Celli A., Marchese P., About durability of biodegradable polymers: structure/degradability relationship, *Macromol. Symp.*, (2010), 296, 378-387
- Desroches M., Caillol S., Lapinte V., Auvergne R. and Boutevin B., Synthesis of biobased polyols by thiol-ene coupling from vegetable oils, *Macromolecules*, (2011), 44, 2489–2500.
- Devaux J, Godard P, Mercier JP., Bisphenol-A polycarbonate–poly(butylene terephthalate) transesterification. I. Theoretical study of the structure and of the degree of randomness in four-component copolycondensates, *J Polym Sci: Polym Phys*, (1982), 20, 1875–80
- European Bioplastics (<http://en.european-bioplastics.org/>)
- Gan Z., Kuwabara K., Abe H., Iwata T., Doi Y., Metastability and Transformation of Polymorphic Crystals in Biodegradable Poly(butylene adipate), *Biomacromolecules*, (2004), 5, 371-378
- Gandini A., The irruption of polymers from renewable resources on the scene of macromolecular science and technology, *Green Chem.*,(2011), Vol. 13(5): 1061-1083.
- Gorenflo V., Schmack G., Vogel R., Steinbuchel A., Development of a process for the biotechnological large-scale production of 4-hydroxyvalerate-containing polyesters and characterization of their physical and mechanical properties, *Biomacromol.*, (2001), Vol. 2(1): 45-57.
- Haveren J. van, Scott E.L. , Sanders J., Bulk chemicals from biomass. *Biofuels, Bioproducts and Biorefining*, (2008), Vol. 2: 41-57.
- ISO 14852. Evaluation of the ultimate aerobic biodegradation of plastics in liquid medium - Method by analysis of carbon dioxide, Genève, (1999).
- Iwata T, Doi Y. Crystal structure and biodegradation of aliphatic polyester crystals. *Macromol Chem Phys*, (1999); 200, 2429–2442
- Keenan T. M., Nakas J. P., Tanenbaum S. W., Polyhydroxyalkanoate copolymers from forest biomass, *J. Ind. Microbiol. Bioetchnol.*, (2006), Vol. 33(7): 616-26.
- Kim D. Y., Dordick J. S., Combinatorial array-based enzymatic polyester synthesis, *Biotechnol. Bioeng.*, (2001), Vol. 76(3): 200-206.
- Kobayashi S., Makino A. Enzymatic Polymer Synthesis: an opportunity for green polymer chemistry., *Chem. Rev.*, (2009), Vol. 109: 5288-5353.

- Kobayashi S., Shoda S., Uyama H., Enzymic polymerization and oligomerization, *Adv. Polym. Sci.*, (1995), Vol. 121: 1-30.
- Kokubo T, Ueda T, Kawashita M, Ikuhara Y, Takaoka GH, Nakamura T. PET fiber fabrics with bioactive titanium oxide for bone substitutes. *J Mater Sci: Mater Med.*, (2008), 19, 695-702.
- Kopinke F. D., Remmler M., Mackenzie K., Thermal decomposition of biodegradable polyesters. I: poly( $\epsilon$ -hydroxybutyric acid), *Polym. Degrad. Stab.*, (1996), Vol. 52(1): 25-38.
- Korupp C., Weberskirch R., Mueller J. J., Liese A., Hilterhaus L., Scaleup of Lipase-Catalyzed Polyester Synthesis, *Organic Process Research & Development*, (2010), Vol. 14(5): 1118-1124
- Kricheldorf H.R., Schwarz G.. New polymer syntheses, 17. Cis/trans isomerism of 1,4-cyclohexanedicarboxylic acid in crystalline, liquid-crystalline and amorphous polyesters *Die Makromolekulare Chemie* (1987), 188, 1281-1294
- Kumar A P, Depan D, Tomer NS, Singh RP. Nanoscale particles for polymer degradation and stabilization – Trends and future perspectives. *Progress in Polymer Science*, (2009), 34, 474-515.
- Kumar R., Gao W., Gross R. A, Functionalized Polylactides: Preparation and Characterization of [L]-Lactide-co-Pentofuranose, *Macromolecules*, (2002), Vol. 35(18): 6835-6844.
- Lee S.Y., Park S.J., Park J.P., Lee Y., Lee S.H., Economic aspects of biopolymer production. In: Steinbüchel A (ed). *Biopolymers - General Aspects and Special Applications*. Pub. Weinheim: Wiley, (2003)
- Lee S.W., Oh D. H., Ahn W. S., Lee Y., Choi J. I., Lee S. Y., Production of poly(3-hydroxybutyrate-co-3-hydroxyhexanoate) by high-cell-density cultivation of *Aeromonas hydrophila*, *Biotechnol. Bioeng.*, (2000), Vol. 67(2): 240-244.
- Lemaire J., Gardette J-L., Lacoste J., Delprat P., Vaillant D., Mechanisms of photooxidation of polyolefins: prediction of lifetime in weathering conditions *Adv. Chem. Ser.*, (1996), 249, 577,
- Linko Y. Y., Seppaelae J., Producing high molecular weight biodegradable polyesters, *CHEMTECH* (1996), Vol. 26(8): 25-31
- Liu C., Liu F., Cai J., Xie W., Long T. E., Turner S. R., Lyons A. Gross R. A., Polymers from Fatty Acids: Poly( $\omega$ -hydroxyl tetradecanoic acid) Synthesis and Physico-Mechanical Studies *Biomacromolecules*, (2011), 12 (9), 3291–98.

- Liu, L., Cai, W., Novel copolyesters for a shape-memory biodegradable material in vivo. *Material Letters*. (2009), 63, 1656-58.
- Liu, Y.; Turner, R. Synthesis and properties of cyclic diester based aliphatic copolyesters, *J Polym Sci, Part A: Polym Chem* (2010), 48, 2162-2169
- Lopez-Cuellar M. R., Alba-Flores J., Rodriguez J. N. Gracida, Perez-Guevara F., Production of polyhydroxyalkanoates (PHAs) with canola oil as carbon source, *Int. J. Biol. Macromol.*, (2011), Vol. 48(1): 74-80.
- Lu W., Ness J.E., Xie W., Zhang X., Minshull J., and Gross R.A. Biosynthesis of Monomers for Plastics from Renewable Oils, *J. Am. Chem. Soc.* (2010), 132, 15451–15455
- Lu X, Lv X, Sun Z, Zheng Y. Nanocomposites of poly(L-lactide) and surface-grafted TiO<sub>2</sub> nanoparticles: synthesis and characterization. *Europ. Polym J.* (2008), 44, 2476-2481.
- McCrum M. G., Read B., Williams G., *Anelastic and Dielectric Effects in Polymeric Solid*, (1967), Wiley, London
- Meier, M.A.R. Metathesis with oleochemicals: New approaches for the utilization of plant oils as renewable resources in polymer science, *Macromol. Chem. Phys.* (2009), 210, 1073–1079
- Metlagh, D., Yang, J., Lui, K.Y., Webb, A.R., Ameer, G.A., Hemocompatibility evaluation of poly(glycerol-sebacate) in vitro for vascular tissue engineering. *Biomaterials*, (2006), 27, 4315-24.
- Migneco, F., Huang, Y.-C., Birla, R.K., Hollister, S.J., Poly(glycerol-dodecanoate), a biodegradable polyester for medical devices and tissue engineering scaffolds. *Biomaterials*. (2009), 30, 6479-84.
- Miyauchi M, Li Y, Shimizu H. Enhanced degradation in nanocomposites of TiO<sub>2</sub> and biodegradable polymer. *Environ. Sci. Technol.* (2008), 42, 4651-4654.
- Mochizuki M, Hirami M. Structural effects on the biodegradation of aliphatic polyesters. *Polym Advan Technol*, (1999), 8, 203–209.
- Montfort J. P., Marin G., Monge P., *Effect of constraint release on the dynamics of entangled linear polymer melts. Macromolecules*, (1984), 17, 1551-1560,
- Muller R. J., Biological degradation of synthetic polyesters—Enzymes as potential catalysts for polyester recycling , *Process Biochemistry*, (2006), Vol. 41(10): 2124-2128.
- Muller R. J., Kleeberg I., Deckwer W.D., *J. Biotech.*, (2001), Vol. 86(2): 87-95

- Muller R. J., Witt U., Rantze E., Deckwer W. D., Architecture of biodegradable copolyesters containing aromatic constituents, *Polym. Degrad. Stab.*, (1998), Vol. 59(1-3): 203-208.
- Othmer K., *Encyclopedia of Chemical Technology*, Wiley, (2005)
- Pagga U., Testing biodegradability with standardized methods. *Chemosphere*, (1997), 35:2953-2972.
- Pan P., Inoue Y., Polymorphism and Isomorphism in Biodegradable Polyesters, *Prog. Polym. Sci.* (2009), 34, 605-640
- Penot G., Arnaud R., Lemaire J., ZnO-photocatalyzed oxidation of isotactic polypropylene. *Die Angewandte Makromolekulare Chemie*, (1983), 117, 71-84,
- Petrović, Z. S.; Milić, J.; Xu, Y.; Cvetković, I. A Chemical Route to High Molecular Weight Vegetable Oil-Based Polyhydroxyalkanoate, *Macromolecules*, (2010), 43, 4120–4125
- Quinzler, D.; Mecking, S. Linear Semicrystalline Polyesters from Fatty Acids by Complete Feedstock Molecule Utilization, *Angew. Chem. Int. Ed.* (2010), 49, 4306–4308
- Rabek J. F., *Polymer Photodegradation: mechanisms and experimental methods*, Chapman & Hall, (1995)
- Rybak A., Fokou P. A. and Meier M. A. R., Metathesis as a versatile tool in oleochemistry *Eur. J. Lipid Sci. Technol.*, (2008), 110, 797–804.
- Scandola M., Ceccorulli G., Doi Y., Viscoelastic relaxations and thermal properties of bacterial poly(3-hydroxybutyrate-co-3-hydroxyvalerate) and poly(3-hydroxybutyrate-co-4-hydroxybutyrate), *Int. J. Biol. Macromol.* (1990), 12, 112-117
- Shen L., Haufe J., Patel M. K., Product overview and market projection of emerging bio-based plastics PRO-BIP 2009, prepared by the Department of Science, Technology and Society (STS) / Copernicus Institute for Sustainable Development and Innovation for the European Polysaccharide Network of Excellence (EPNOE) and European Bioplastics. Utrecht University, Final report, (June 2009).
- Shen Y., Chen X., Gross R. A., Polycarbonates from Sugars: Ring-Opening Polymerization of 1,2-O-Isopropylidene-D-Xylofuranose-3,5- Cyclic Carbonate (IPXTC), *Macromolecules*, (1999), Vol. 32(8): 2799-2802.
- Stumbé, J.-F., Bruckmann, B.. Hyperbranched polyesters based on adipic acid and glycerol. *Macromol. Rapid. Comm.* (2004), 25, 921-24.
- Sturm R N., Biodegradability of nonionic surfac- tants: screening test for predicting rate and ultimate bio- degradation. *J Am Oil Chem Soc*, (1973), 50:159-167

- Sundback, C.A., Shyu, J.Y., Wang, Y., Faquin, W.C., Langer, R.S., Vacanti, J.P., et al. Biocompatibility analysis of poly(glycerol-sebacate as a nerve guide material. *Biomaterials*. (2005), 26, 5454-64.
- Tang, J., Zhang, Z., Song, Z., Chen, L., Hou, X., Yao, K., Synthesis and characterization of elastic aliphatic polyesters from sebacic acid, glycol and glycerol. *Europ. Polym. J.* (2006), 42, 3360-3366.
- Tessier M, Fradet A. Determination of the degree of randomness in condensation copolymers containing both symmetrical and unsymmetrical monomer units: a theoretical study. *e-Polymers*, (2003), 30, 1-16
- Tidjani, R. Arnaud, Formation of treeing figures during the photo-oxidation of polyolefins. *Polymer*, (1995), 36, 2841-2844,
- Trzaskowski J., Quinzler D., Bährle C. and Mecking S., Aliphatic Long-Chain C<sub>20</sub> Polyesters from Olefin Metathesis, *Macromol. Rapid Commun.*, (2011), 1352–1356.
- Turunc O. and Meier M. A. R., Thiol-Ene vs. ADMET: A complementary approach to fatty acid based biodegradable polymers, *Green Chem.*, (2011), 13, 314–320
- Vega J. F., Munoz-Escalona A., Santamaria A., Munoz M. E., Lafuente P., *Comparison of the rheological properties of Metallocene-Catalyzed and conventional high-density polyethylenes. Macromolecules*, (1996), 29, 960-965,
- Verney V., Michel A., Representation of the rheological properties of polymer melts in terms of complex fluidity. *Rheologica Acta*, (1989), 28, 54-60,
- Wang, Y.D., Kim, Y.M., Langer, R., In vivo degradation characteristics of poly(glycerol-sebacate). *J Biomed Mater Res A*. (2003), 66A, 192-197.
- Webb C., Koutinas A. A., Wang R., Developing a Sustainable Bioprocessing Strategy Based on a Generic Feedstock, Springer-Verlag Berlin Heidelberg 2004, Vol. 87, p. 195
- Wenhua, L., Ness, J.E., Xie, W., Zhang, X., Minshull, J., Gross, R.A., Biosynthesis of monomers for plastics from renewable oils. (2010) *J. Am. Chem. Soc.* 132, 15451-15455.
- Winter, H.H., *Gel point in encyclopedia of polymer science and engineering*, (1989), John Wiley & Sons, New York
- Witt U., Einig T., Yamamoto M., Kleeberg I., Deckwer W. D., Muller R. J., Biodegradation of aliphatic-aromatic copolyesters: evaluation of the final biodegradability and ecotoxicological impact of degradation intermediates, *Chemosphere*, (2001), Vol. 44(2): 289-99.

- Wunderlich, B. *Macromolecular Physics: Crystal Nucleation, Growth, Annealing*; (1976), Academic: New York,; Vol. 2.
- Yang F., Qiu Z., Yang W., Miscibility and crystallization of biodegradable poly(butylene succinate-co-butylene adipate)/poly(vinylphenol) blends, *Polymer*, (2009), Vol. 50(10): 2328-2333.
- WO2010078328 Berti C, Binassi E, Colonna M, Fiorini M, Kannan G, Karanam S, Mazzacurati M, Odeh I, Vannini M. (Sabic Innovative Plastics IP B.V., Neth.) Bio-based terephthalate polyesters, *PCT Int. Appl.* (2010)
- Zan L, Tian L, Liu Z, Peng Z. A new polystyrene-TiO<sub>2</sub>-nanocomposite film and its photocatalytic degradation. *Applied Catalysis A: General*, (2004), 264, 237-242.
- Zhao L., Gan Z., Polym. Effect of copolymerized butylene terephthalate chains on polymorphism and enzymatic degradation of poly(butylene adipate), *Degrad. Stab.*, (2006), Vol. 91(10): 2429-2436.

# Complete list of publications

## Publications in international journals

- 1) Annamaria Celli, Paola Marchese, Simone Sullalti, Corrado Berti, Giancarlo Barbiroli, Sophie Commereuc, Vincent Verney, “Preparation of new biobased polyesters containing glycerol and their photodurability for outdoor applications”, *Green Chemistry*, **2012**, 14, 182-187
- 2) Celli, Annamaria; Marchese, Paola; Sullalti, Simone; Berti, Corrado; Barbiroli, Giancarlo. Eco-friendly Poly(butylene 1,4-cyclohexanedicarboxylate): Relationships Between Stereochemistry and Crystallization Behavior”, *Macromol. Chem. Phys.*, **2011**, 212, 1524-1534.
- 3) Berti, A. Celli, P. Marchese, E. Marianucci, S. Sullalti, G. Barbiroli, “Environmentally Friendly Copolyesters Containing 1,4-Cyclohexane Dicarboxylate Units, 1-Relationship Between Chemical Structure and Thermal Properties”, *Macromol. Chem. Phys.*, **2010**, 211, 1559-1571
- 4) Celli, P. Marchese, S. Sullalti, C. Berti, “Eco-friendly (Co)polyesters Containing 1,4-cyclohexylene Units: Correlations between Stereochemistry and Phase Behavior”, *Polymers Research Journals*, **2010**, vol. 4
- 5) Celli, P. Marchese, S. Sullalti, C. Berti, G. Barbiroli, S. Commereuc, “Novel eco-friendly aliphatic copolyesters: structure property relationship and biodegradation behaviour”, *Journal of Biotechnology*, **2010**, 150, 1, 205-206
- 6) Celli, P. Marchese, S. Sullalti, C. Berti, S. Commereuc, V. Verney, “New polymers from renewable resources: synthesis, characterization, and photodurability of aliphatic polyesters containing glycerol”, *Journal of Biotechnology*, **2010**, 150, 1, 206

## Contribution to book chapters

- 7) Celli, P. Marchese, S. Sullalti, C. Berti, “Eco-friendly (Co)polyesters Containing 1,4-cyclohexylene Units: Correlations between Stereochemistry and Phase Behavior” in *Polymer Phase Behavior*, Nova Publisher, **2011**

## Publications in conference proceedings

- 8) S. Sullalti, G. Totaro, H. Askanian, A. Celli, P. Marchese, V. Verney, S. Commereuc, “Photodegradation of aliphatic polyesters and their composites with TiO<sub>2</sub>”, Environmental Microbiology & Biotechnology, 10-12.04.2012 Bologna (Italy)
- 9) Annamaria Celli, Paola Marchese, Simone Sullalti, Corrado Berti, Richard A. Gross, “Unique Fully Aliphatic or Aliphatic/Aromatic Copolyesters Containing Biobased  $\omega$ -Hydroxy Fatty Acids: Molecular Structures and Properties”, book of abstracts EPF’11, 26.06-01.07.2011 Granada (Spain), pag. 213
- 10) Annamaria Celli, Paola Marchese, Simone Sullalti, Justine Boyenval, Sophie Commereuc, “Eco-Friendly Aliphatic Polyesters Containing 1,4-Cyclohexane Dicarboxylate Units: Effect of Diol Chain Length on Thermo-Mechanical Properties”, book of abstracts EPF’11, 26.06-01.07.2011 Granada (Spain), pag. 636
- 11) S. Sullalti, C. Berti, G. Barbiroli, A. Celli, P. Marchese, E. Marianucci, S. Commereuc, V. Verney, “Correlazioni fra struttura chimica, proprietà termiche, meccaniche e biodegradabilità in nuovi poliesteri e copoliesteri completamente alifatici”, book of abstracts XIX Convegno Italiano di Scienza e Tecnologia delle Macromolecole, 13-17.09.2009 Milano (Italy), pag 5.59
- 12) A. Celli, P. Marchese, S. Sullalti, C. Berti, S. Commereuc, V. Verney, “Relationship between chemical structure and thermo-mechanical properties in new aliphatic copolyesters” book of abstracts EPF’09, 12-17.7.2009 Graz (Austria), pag. 169

## Experiences abroad

- Research activity in the laboratories of the Department of Chemical and Biological Sciences, Polytechnic Institute of NYU, Brooklyn, New York from September 2011 to December 2011. The activity was supervised by Prof. Richard A. Gross.
- Research activity in the laboratories of Photochimie Moléculaire et Macromoléculaire, Ecole Nationale Supérieure de Chimie de Clermont Ferrand, Université Blaise Pascal, France from November 2009 to January 2010. The activity was supervised by Prof. Sophie Commereuc.